Relaxation Modulus and Complex Modulus

Chapter · January 2018

DOI: 10.1007/978-3-319-67214-4_3

2 authors:

Boris Radovskiy

21 PUBLICATIONS **95** CITATIONS

SEE PROFILE

Bagdat Teltayev

Kazakhstan Highway Research Institute

72 PUBLICATIONS **272** CITATIONS

SEE PROFILE

Structural Integrity 2
Series Editors: José A. F. O. Correia · Abílio M.P. De Jesus

Boris Radovskiy
Bagdat Teltayev

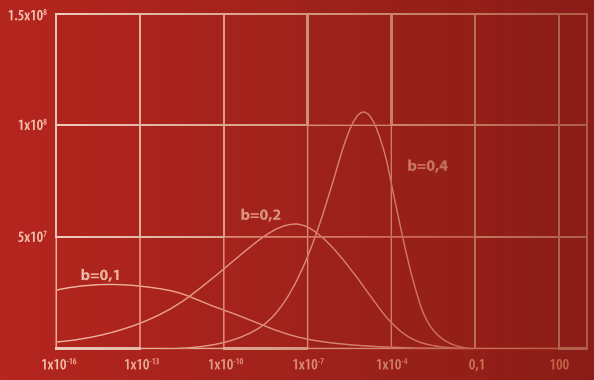

Viscoelastic Properties of Asphalts Based on Penetration and Softening Point

Springer

Structural Integrity

Volume 2

The *Structural Integrity* book series is a high level academic and professional series publishing research on all areas of Structural Integrity. It promotes and expedites the dissemination of new research results and tutorial views in the structural integrity field.
The Series publishes research monographs, professional books, handbooks, edited volumes and textbooks with worldwide distribution to engineers, researchers, educators, professionals and libraries.

Topics of interested include but are not limited to:

- Structural integrity
- Structural durability
- Degradation and conservation of materials and structures
- Dynamic and seismic structural analysis
- Fatigue and fracture of materials and structures
- Risk analysis and safety of materials and structural mechanics
- Fracture Mechanics
- Damage mechanics
- Analytical and numerical simulation of materials and structures
- Computational mechanics
- Structural design methodology
- Experimental methods applied to structural integrity
- Multiaxial fatigue and complex loading effects of materials and structures Fatigue corrosion analysis
- Scale effects in the fatigue analysis of materials and structures
- Fatigue structural integrity
- Structural integrity in railway and highway systems
- Sustainable structural design
- Structural loads characterization
- Structural health monitoring
- Adhesives connections integrity
- Rock and soil structural integrity

More information about this series at http://www.springer.com/series/15775

Boris Radovskiy · Bagdat Teltayev

Viscoelastic Properties of Asphalts Based on Penetration and Softening Point

Springer

Boris Radovskiy
Radnat Consulting
Irvine, CA
USA

Bagdat Teltayev
Kazakhstan Highway Research Institute
Almaty
Kazakhstan

Translated from Russian by N. Kuvshinnikova

ISSN 2522-560X ISSN 2522-5618 (electronic)
Structural Integrity
ISBN 978-3-319-67213-7 ISBN 978-3-319-67214-4 (eBook)
https://doi.org/10.1007/978-3-319-67214-4

Library of Congress Control Number: 2017953781

Reviewers
V.A. Zolotarev, Ph.D., D.Sc., Prof. (Kharkov, Ukraine);
V.V. Mozgovoy, Ph.D., D.Sc., Prof. (Kiev, Ukraine);
A.E. Merzlikin, Ph.D., (Moscow, Russia).

Printed on acid-free paper

This Springer imprint is published by Springer Nature
The registered company is Springer International Publishing AG
The registered company address is: Gewerbestrasse 11, 6330 Cham, Switzerland

Preface

Abstract This book is concentrated mainly with the study of the viscoelastic response of bitumen and asphalt concrete as the functions of time and temperature. It concentrates on the common properties of asphalt concrete, viz., viscoelastic properties of binder, bitumen and air voids content, and stiffness modulus, and does not concern itself with the less common properties. The aim has been to provide the basic parameters of modeling allowing for mix design, pavement design, and analysis. Readers will also note that the relationships outlined are based on materials data commonly available to asphalt concrete producers and users.

Road asphalt is the most important component of the asphalt concrete mixture. Its content in the mixture together with its mechanical properties predetermine the strength, durability, as well as load-bearing and load-distributive capacity of road pavement. Being a composite mixture of hydrocarbons, asphalt typically is a viscous resilient ductile material whose properties depend on temperature and loading conditions. The extent of this dependence differs among different asphalts produced by different methods from different types of crude oil and it varies in the course of aging.

The viscoelastic properties of asphalts and asphalt concretes are ascertained by the way of testing at variable temperature and under load of variable duration or variable rate of application (stress or strain rate), so such testing requires expensive equipment and highly skilled staff. This is required in order to assess, at the designing phase, the asphalt mix design modulus at the given temperature, establish the correct temperature for preparation and compaction of the mixture, verify the pavement resistance to rutting in summer and to thermal cracking in winter, and estimate the asphalt concrete pavement fatigue damage under repeated loading.

In this work, approximate formulas have been developed for prediction of the rheological properties of asphalt based on its standard parameters such as penetration and softening point under different test modes, such as constant stress, constant deformation, or cyclic load.

This monograph consists of four chapters. The first chapter highlights the viscoelastic properties applicable to asphalt and asphalt concretes which are to facilitate further reading. The second chapter determines the dependence of asphalt stiffness modulus on the penetration and softening points. The third chapter

analyzes the interrelationship between various performance criteria: stiffness modulus, relaxation modulus, creep compliance, and complex modulus, and then offers the approximate formulas for defining thereof. The fourth chapter gives examples of practical application of the established dependences for determining the viscoelastic properties of asphalt and asphalt concrete as a function of temperature and loading time.

For many years, the authors' academic interests have been focused mainly on pavement design, analysis, construction, and testing methods (Radovskiy 1973, Radovskiy et al. 1989, Radovskiy 2003; Teltayev and Aytaliev 1999, Teltayev 2006, 2007, 2012). However, in their research work, the authors have had to analyze a moving load effect and time-related processes, so they have had to deal with the viscoelastic properties of many types of construction material, of which asphalt concrete is the most *viscoelastic* material. It is true that reliable information about properties of any material may be obtained through testing. Nonetheless, testing is not always possible, so we need some dependences, which would predict, more or less accurately, the time-related deformation or stress development patterns at different temperatures, based on some simple standard parameters. This is to say that in some cases, it is enough to use such dependences instead of testing. Anyway, the authors have had to use these dependences in their research in the field of pavement strength, so the authors believe that such dependences can be useful for other specialists, too.

Irvine, USA — Boris Radovskiy
Almaty, Kazakhstan — Bagdat Teltayev

References

Radovskiy B (1973) Operating peculiarities of pavement courses from granular materials, pp. 130–134. Impact of dilatancy of the granular materials on strength and distributing ability of the layer, pp. 134–140. Methods of recording of discrete structure for granular materials during pavement design, pp. 140–142. In: Ivanov N (ed) Flexible Pavement Design and Analysis. Transport, Moscow

Radovskiy B, Suprun A, Kazakov I (1989) Pavement design for heavy vehicles. Budivelnyk, Kiev

Radovskiy B (2003) Issues related to mechanics of road materials and pavements. Poligraph Consulting, Kiev

Teltayev B, Aytaliev S (eds) (1999) Deformations and stresses in flexible pavements. M. Tynyshbaev Kazakh Academy of Transport and Communications, Almaty

Teltayev BB (2012) Temperature dependence of stress-strain state of flexible pavements. Sci Tech Road Constr (2): 14–18

Teltayev BB (2006) Stress-Strain State of Flexible Pavements. Sci Tech Road Constr (1): 18–21

Teltayev BB (2007) Influence of the speed of vehicles on the stress and strain state of pavement. Roads & Bridges (17/1): 68–81

Teltayev BB (2007) Theoretical foundation of finite element modeling of temperature induced stress and strain state of pavement with viscoelastic asphalt and concrete layers. In: International scientific and technological conference Erzhanovsk readings II, Actobe, 2007, pp. 307–308

Contents

Chapter 1
Viscoelastic Properties

Abstract This chapter is introductory and discusses aspects related to viscoelastic behavior of bitumen and asphalt mixture. This chapter highlights the viscoelastic properties applicable to asphalt and asphalt concrete which are to facilitate further reading. Some fundamental concepts of linear viscoelasticity are reviewed in order to understand the behavior of bitumen and asphalt concrete. Included in that discussion are the stiffness modulus as introduced by Van der Poel in asphalt technology; the concept of viscoelastic material that was first introduced by Maxwell on the example of bitumen; the concepts of viscosity and relaxation time. This chapter explains how the Boltzmann superposition principle can be applied to predict the evolution of either the deformation or the stress for continuous and discontinuous mechanical histories in linear viscoelasticity. Mathematical relationships between transient compliance functions and transient relaxation moduli are obtained, and interrelations between viscoelastic functions in the time domain are given. Experimental methods to measure the viscoelastic functions in the time and frequency domain are described as applied to asphalt concrete relaxation testing under axial tension and bitumen shear testing under cyclic loading. The first chapter discussed various rheological characteristics of viscoelastic properties of asphalt: creep compliance, relaxation modulus, complex modulus as well as the stiffness modulus, and it was shown that they were interrelated. Last paragraph outlines the time-temperature correspondence principle and gives an example of shift factors obtained based on the test data on asphalt concrete stiffness modulus in the uniaxial tensile testing at different temperatures.

It is quite evident that for many road construction materials, the stress-strain relationship depends significantly on the duration of exposure to load and the temperature. Materials tend to deform in the course of time under constant load, i.e. they demonstrate the so-called creepage. On the other hand, in the course of continuous deforming, the stress in the material decreases, so the material becomes relaxed (of its stress). Such deformation of construction materials depends not only on the magnitude of stress but also on the stress duration. Such properties are inherent in asphalt-concrete and in other mixes of stony materials with organic

B. Radovskiy and B. Teltayev, *Viscoelastic Properties of Asphalts Based on Penetration and Softening Point*, Structural Integrity 2,
https://doi.org/10.1007/978-3-319-67214-4_1

binders, as well as in cement concrete and subgrade soil. As a result, the stress-strain behavior of a road structure depends not only on the magnitude of load but also on the intervals of time between applied loads. In this chapter, we will give a brief summary of basic viscoelastic features of materials.

This work concentrates on viscoelastic properties of asphalt and asphalt concrete. Physical and mechanical properties of asphalts are a subject of many studies. Thanks to the practical importance of this subject, the number of such studies grows rapidly. For instance, the well-known book by Kolbanovskaya and Mikhailov on asphalt physical and mechanical properties, published in 1973, contains 232 references (Kolbanovskaya and Mikhailov 1973); the recent review article (Lesueur 2009) covering the asphalt physical and mechanical properties incorporates 332 references, whereas the references in article (Krishnan and Rajagopal 2003) include 586 items. However, inasmuch as the scope of this work cannot accommodate the analysis of so many sources, we will mention only those required to achieve our main goal, viz. establishing the relationships between the asphalt viscoelastic properties and the standard parameters: penetration and softening point.

1.1 The Concept of Stiffness Modulus

Burmister, Columbia University Professor, developed, in 1943, and published, in 1945, a general solution to calculate stresses and displacements in a layered elastic structure under a constant load with the prospects of application of this solution to the road and airport runway pavements (Burmister 1945). A few years later, a different solution of the same problem was found out at Kharkiv Automobile-Highway University by Professor Kogan (1953). Therefore, there appeared a real opportunity to design a road pavement structure similar to designing other construction projects, such as bridges, buildings, retaining walls, etc., that is to calculate deflection, stresses and deformations in layers and to adjust the thickness of the layers to the extent where such deflection, stresses and deformations do not exceed the ultimate limits prescribed for each material.

To carry out such calculations it was necessary to verify, on experimental basis, the values of the elasticity modulus for the materials and for the soil. However, it has been found out that the elasticity modulus of asphalt concrete and other organic binder materials lowers with the rise of the testing temperature and with the duration of load application. In other words, it has been revealed that asphalt concrete is a viscoelastic material rather than an elastic material, and its rigidity decreases with the rise of the temperature and increases parallel to increasing the speed of the load motion.

The first step in reflection of viscoelastic properties of asphalt and asphalt concrete in the process of designing of pavement structure, as well as in selection of the type of asphalt suitable for the environment on the project site was undertaken in 1954 by Van der Poel (Shell Research Laboratory in Amsterdam) (Van der Poel

1954). He coined the term of asphalt stiffness modulus by analogy with the modulus of elasticity:

$$S(t) = \sigma_c / \varepsilon(t) \tag{1.1}$$

The stiffness modulus is a ratio of constant tensile stress to the strain $\varepsilon(t)$, including both recoverable and irrecoverable strain and depending on the load duration t and, certainly, on the temperature T. Basing on his experimental findings, Van der Poel developed a nomograph for determining the stiffness modulus of bitumen. Soon afterwards, he introduced a similar notion of stiffness modulus for asphalt concrete (Van der Poel 1958). Later, in 1964, Van der Poel's colleagues and followers, Heukelom and Klomp derived an empirical formula to determine the stiffness modulus for asphalt concrete (with air porosity less than 3%) and proposed to apply it in pavement design (Heukolom and Klomp 1964). To find the stiffness of asphalt concrete, it is necessary to find the stiffness of given asphalt via Van der Poel's nomograph and to know the volume fractions of binder and aggregates.

After Van der Poel's suggestion, the stiffness modulus came into use in pavement design manuals as a mechanical property of asphalt concrete. It acts as an elasticity modulus, depending, however, on the temperature T and the time of the load duration t. The SHELL experts (Claessen et al. 1977) suggested determining the S value for asphalt concrete layer, based on the bitumen stiffness found via Van der Poel's nomograph where the load duration $t = 0.02$ s. This is roughly the length of a 0.20 m imprint divided by the speed of a truck equal to 10 m/s (36 km/hr).

The elasticity modulus of a perfectly elastic body does not depend on time and temperature, whereas the asphalt concrete stiffness modulus depends on those factors. Introducing the *T- and -t* dependent modulus E into the theory of elasticity formulas is an attempt to take into account the real viscoelastic nature of material.

The option proposed by Van der Poel together with Heukelom and Klomp as to replacement of the elasticity modulus by the stiffness modulus was first implemented in Shell's Pavement Design Manual (1978), and thereafter in the Asphalt Institute's thickness design manual (1982), and in the British (British Standards, BS EN12697 2001) and French (Design of Pavement Structures, Technical Guide SETRA 1994) manuals.

Parallel to and independently of Heukelom and Klomp (1964), Teliayev (1964) proposed two calculation models for road pavement designing based on the theory of elasticity formulas: one for moving load and the other one for fixed load. In the first model of calculation, a dynamic load factor is introduced and the elasticity modulus is determined for the load duration of 0.1 s. In the fixed load calculation, such dynamic load factor is not involved, and a modulus static value is used. Teliayev's proposal was implemented in 1972 in Russian Pavement Design Manual VSN46-72. Since then, the Russian theory-of-elasticity-based pavement design manuals (Industry-Specific Construction Standard 46–83 1985; Industry Road Code 218.046-01Б 2001), assume in moving vehicle calculations the asphalt concrete modulus corresponding to the load duration of 0.1 s at the temperature of 0 °C

(for bending analysis) or 10 °C (for elastic deflection analysis). This was the step towards considering the viscoelastic properties of materials in pavement design.

However, for reflecting such properties in a theory-of-elasticity solution for a fixed load, it is not enough just to take a modulus corresponding to a certain time of load duration, e.g. 0.1 s Firstly, the deeper the point, the longer the effect of vertical stress caused by a moving load in such point. Secondly, even at the same traffic speed the duration of the state of stress in a given point differs with regard to different stress components or, say, type of displacement: vertical and horizontal. Thirdly, viscoelastic material "memorizes" the previous impacts. For instance, the vertical normal stress and deflection in a point behind a moving wheel will be higher than in a similar point in front of it.

To reflect the real viscoelastic properties, it is necessary to have a solution for a strain-stress behavior problem in a viscoelastic layered structure under a moving load. Such solutions were derived in Privarnikov and Radovskii (1981), Radovskiy (1982), Chen et al. (2011), etc.

1.2 The Concept of Viscoelastic Material

It is noteworthy that the concept of viscoelastic material was first introduced by the Great physicist Maxwell drawing on the example of bitumen:

> Thus a block of pitch may be so hard that you cannot make a dint in it by striking it with your knuckles; and yet it will, in the course of time, flatten itself out by its own weight, and glide downhill like a stream of water.
>
> (Maxwell 2001, p. 276).

In other words, under a momentary load application ("with knuckles"), asphalt behaves as an elastic body, while under constant load ("by its own weight"), it behaves as viscous liquid.

According to R. Hooke's Law, deformation of a perfectly elastic body is proportional to stress:

– under shear:

$$\gamma = \frac{\tau_c}{G}, \tag{1.2}$$

– under tension:

$$\varepsilon = \frac{\sigma_c}{E} \tag{1.3}$$

and such deformation is completely reversible, i.e. this deformation is recoverable after unloading.

Here, γ = a shearing strain (angular deformation), ε = longitudinal strain (deformation), τ_c = tangential stress; σ_c = normal stress; $G = E/2(1 + \nu)$—elasticity shear modulus, E = elasticity modulus (longitudinal modulus or Young modulus); ν = Poisson ratio. Under the load duration of around 1 s, the Poisson ratio ν for asphalt at a low winter temperature (− 25 °C or lower) is equal approximately to $\nu = 0.35$, whereas at summer temperature to $\nu = 0.45-0.50$. For the sake of convenience, the value of $\nu = 0.5$ for asphalt is usually assumed; then the longitudinal modulus is equal to triple shear modulus $E = 3G$, which simplifies the calculations with acceptable accuracy.

According to the Newtonian law, the rate of deformation of perfectly viscous liquid is proportional to the shear stress:

– Rate of deformation under the shear:

$$\frac{d\gamma}{dt} = \frac{\tau_c}{\eta}, \tag{1.4}$$

and the deformation caused by constant shearing stress:

$$\gamma(t) = \frac{\tau_c t}{\eta}, \tag{1.5}$$

– Rate of deformation under tension:

$$\frac{d\varepsilon}{dt} = \frac{\sigma_c}{3\eta}, \tag{1.6}$$

and the deformation caused by constant tensile stress:

$$\varepsilon(t) = \frac{\sigma_c t}{3\eta} \tag{1.7}$$

Viscous flow deformation is irreversible. The external force energy, spent on this deformation turns into a heat. Here, the η is a viscosity factor or simply "viscosity", sometimes called "Newtonian viscosity" or "dynamic viscosity". The factor of three in the two previous expressions appears for the same reason as in the ratio between the longitudinal elastic modulus and the shear elastic modulus $E = 3G$. The water viscosity at 20 °C in the SI system is equal to 0.001 Pa s. The asphalt viscosity at the softening point measured by the ring-and-ball method, lies within the range from 800 to 3000 Pa s.

The viscoelastic material similar to asphalt combines the properties of a perfectly elastic body and those of viscous liquid. Maxwell (1866) proposed the first and the simplest model of viscoelastic body behavior.

If the stress τ_c or σ_c was applied at an initial moment and then remains constant, the deformation of a simplest viscoelastic body, according to Maxwell's proposal, is defined as a sum of perfectly elastic deformation and perfectly viscous deformation:

– Under the shear:

$$\gamma(t) = \frac{\tau_c}{G_g} + \frac{\tau_c t}{\eta}, \tag{1.8}$$

– Under the tension:

$$\varepsilon(t) = \frac{\sigma_c}{E_g} + \frac{\sigma_c t}{3\eta} \tag{1.9}$$

Here, G_g and E_g are instantaneous elastic shear and tension moduli, respectively. They correspond to vanishing load duration and to low temperature, when viscoelastic material behaves like a perfectly elastic body, which is conventionally designated with a "g" (glassy) index. The asphalt instantaneous shear modulus approaches G_g = 1000 MPa, while the instantaneous longitudinal modulus E_g = 3000 MPa. Right after application of the load, the material becomes immediately deformed and thereafter, in the course of time, the deformation increases as the material tend to creep under constant load.

However, if the deformation γ_c or ε_c is applied at an initial moment and then is maintained constant, the stress, according to Maxwell, decreases in the course of time:

– Under the shear:

$$\tau(t) = G_g \gamma_c e^{-(t/\lambda)} \tag{1.10}$$

– Under the tension:

$$\sigma(t) = E_g \varepsilon_c e^{-(t/\lambda)} \tag{1.11}$$

Here $\lambda = \eta/Gg$ is the time of shear relaxation. Where deformation is constant, the stress in the material decreases, as it relaxes the stress. The value λ shows the time of essential loss of the initially applied stress.

The concept of *relaxation time*, which is a fundamental notion in physics and mechanics, was first introduced by Maxwell in this very article ("…which may be called "time of relaxation" of the elastic force"), (Maxwell 1866, p. 53). If the load duration is short, as compared to the time of relaxation ($t/\lambda << 1$), the viscoelastic material behaves almost like elastic material. However, when $t/\lambda \gg 1$, it behaves almost like viscous material. The concept of the relaxation time reflects the idea of spontaneous recovery of equilibrium state after the instance when a physical system

has been somewhat unbalanced. The processes running at the time of deformation of real materials are characterized by a set of relaxation times λi rather than by a single time of relaxation. Such a set corresponds to Maxwell's generalized model consisting of multiple parallel simple Maxwell models, considered above, albeit differing in the time of relaxation.

The formulas (1.1) and (1.9) allow writing an expression for the elasticity modulus introduced by Van der Poel with regard to Maxwell simple liquid:

$$S_m(t) = \frac{E_g}{1 + E_g t/3\eta} \tag{1.12}$$

Considering both instantaneous elastic reversible deformation and the viscous flow irreversible deformation, it should be noted that the above simple Maxwell liquid model does not reflect an essential property of elastic materials, in particular, that of asphalt concrete, namely, their tendency to time-related yet reversible deformation. Later, more sophisticated and more generalized mathematical and empirical models were proposed, which described viscoelastic materials and, besides, reflect their ability to elastic recovery. Some of them will be considered below with regard to asphalt.

1.3 Stress-Strain Relations of Linear Viscoelasticity

Mathematically, viscoelastic materials are those materials where the stress-strain relationship includes time. Such materials are polymers, asphalts, asphalt concrete, cement concrete, soil, rock and many others. The properties of viscoelastic materials, as well as their characteristics and test techniques are described in detail in the works Ferry (1963), Tshoegl (1989).

The equations, that combine stress, strain, and time for a linear viscoelastic body, are provided by Bolzmann-Volterra law. Let us explain the essence of this law in the context of axial tension. According to R. Hooke's Law, when a rod of *elastic* material is extended, its longitudinal strain, at any time, is proportional to the tensile stress acting at the same time $\varepsilon = \sigma/E$.

Unlike this, increment of longitudinal strain $d\varepsilon(t)$ in a viscoelastic rod at a given moment of time t, due to the load action during the period $d\tau$, lying between τ and $\tau + d\tau$ (where $\tau \leq t$), is proportional to the increment of the applied stress $d\sigma(\tau)$ within the preceding period of time τ, and the proportionality factor $D(t - \tau)$ depends on the time interval $(t - \tau)$ between these time points:

$$d\varepsilon(t) = D(t - \tau)d\sigma(\tau) \tag{1.13}$$

If we conceive deformation of a viscoelastic body as a flow, then it becomes clear that $D(t)$ is an increasing function: the longer time has passed since application

of a tensile load, remaining constant thereafter, the higher the creep deformation induced thereby at a time.

Likewise, with regard to viscoelastic material, increment of stress $d\sigma(t)$ at the time t is proportional to the increment in the deformation $d\varepsilon(\tau)$ applied at the preceding point of time τ, with the proportionality factor $E(t - \tau)$ depending on the time interval $(t - \tau)$:

$$d\sigma(t) = E(t - \tau)d\varepsilon(\tau) \tag{1.14}$$

where $E(t)$ is a decreasing function.

In axial tension of a viscoelastic rod, increments (1.13) or (1.14), induced by action at the time points τ during the whole time elapsed t, are summed and the relationship between stresses, strains and time is expressed by Boltzmann relations:

$$\varepsilon(t) = \int_0^t D(t - \tau)\frac{\partial\sigma(\tau)}{\partial\tau}d\tau \tag{1.15}$$

$$\sigma(t) = \int_0^t E(t - \tau)\frac{d\varepsilon(\tau)}{d\tau}d\tau \tag{1.16}$$

According to Boltzmann principle, the magnitude of deformation in any point of a body at a given time t is influenced by the stresses, existing during all preceding moments τ. The shorter the time interval $(t - \tau)$ the higher such influence is, and it is characterized by the function $D(t)$. Likewise, the magnitude of stress in any point of a body at a certain time t is influenced by the strains, existing during all preceding moments τ. The shorter the time interval $(t - \tau)$ the higher such influence is, and it is characterized by the function $E(t)$.

In the theory of viscoelasticity, Boltzmann relations play such important role, as does Hooke's Law in the theory of elasticity. Therein, the functions $E(t)$ and $D(t)$ characterize the stress-strain relationship and time dependence in the same way as this relationship is characterized for elastic material (independent of the time) by the longitudinal elasticity modulus E and elastic compliance $1/E$.

The function $D(t)$ is experimentally determined via tensile testing at constant stress and is called the creep compliance. It is equal to the ratio of measured deformation at a point of time t to the constant stress σ_c, applied at the initial moment:

$$D(t) = \frac{\varepsilon(t)}{\sigma_c} \tag{1.17}$$

Having compared the expressions (1.1) and (1.17), it is evident that Van der Poel's stiffness modulus, in terms of the theory of viscoelasticity, is the value inverse to the uniaxial creep compliance at tension

$$S(t) = 1/D(t) \tag{1.18}$$

The function $E(t)$ is determined via tensile testing under constant strain and is called the modulus of relaxation. It is equal to the ratio of measured stress at a point of time t to the constant strain ε_c:

$$E(t) = \frac{\sigma(t)}{\varepsilon_c} \tag{1.19}$$

In designing a structure made of viscoelastic material, the modulus of relaxation $E(t)$ plays such an important role as does the modulus of elasticity E in the theory of strength of materials.

Having considered the relations (1.15) and (1.16), where stresses and strains appear on the left and right side, we can deduce that the creep compliance $D(t)$ and the modulus of relaxation $E(t)$ must be interrelated. The relationship between them can be ascertained via the combined analysis of the equalities (1.15) and (1.16) and is expressed by the equation:

$$\int_0^t D(t-\tau)E(\tau)d\tau = \int_0^t D(\tau)E(t-\tau)d\tau = t \tag{1.20}$$

Knowing the $D(t)$, we can derive the $E(t)$ from the Eq. (1.20), i.e. we can derive the modulus of relaxation from the creep test results, and vice versa. This is important in terms of practicability, for creep testing is technically easier than relaxation testing. The creep compliance value $D(t)$ and the modulus of relaxation $E(t)$ can also be deduced from the results of sample testing under periodically variable load at different frequencies, which is practically valuable for small t values.

Equalities (1.13)–(1.20) are given for strain. They look almost the same in terms of shearing deformation (shear strain), for instance, when it comes to torsion testing. However, in this case, instead of $D(t)$ and $E(t)$, they contain the shear creep compliance $J(t) = \gamma(t)/\tau_c$ and shear relaxation modulus $G(t) = \tau(t)/\gamma_c$. Likewise Eq. (1.20), they are interrelated by equation:

$$\int_0^t J(t-\tau)G(\tau)d\tau = \int_0^t J(\tau)G(t-\tau)d\tau = t \tag{1.21}$$

If we assume roughly that Poisson ratio $v(t)$ does not depend on the time and temperature, then the viscoelastic properties under axial tension and under shear may be interrelated simply by

$$D(t) = J(t)/3, \quad E(t) = 3G(t) \tag{1.22}$$

We can deduce from (1.18) and (1.22) that the asphalt creep compliance $J(t)$ may be expressed from its stiffness modulus using the formula

$$\mathrm{J}(t) = 3/S(t) \tag{1.23}$$

Here, we confine ourselves to linear viscoelasticity dependences. However, in case of large deformation, asphalts, especially bitumen-polymer binders, display considerable non-linear properties (Krishnan and Rajagopal 2003; Vinogradov et al. 1977). Exploring the approximate boundaries of the domain of asphalt concrete linearity at different temperatures have been carried out since the 1970s (Monismith et al. 1966) until now (Mehta and Christensen 2000; Zolotaryov 2010).

Hereinbefore, we have considered the basic relations in the theory of linear viscoelasticity, which is part of the continuum mechanics, viz. the science that studies the motion and the stress-strain status of such continua albeit without microstructural analysis thereof: the theory of the strength of materials, theory of elasticity, theory of plasticity, theory of linear viscoelasticity, etc. These same relations are also the subject of rheology, which is the science dealing with deformation and flow of material and which is situated at the confluence of mechanics and physical chemistry. Unlike mechanics, rheology studies viscoelastic properties of materials with respect to their composition, which allows adjusting such properties. Hence, with regard to asphalts and asphalt concrete, the terms "viscoelastic properties" and "rheological properties" are often used as interchangeable. For example, the book of Reiner (1965), one of the rheology ancestors, considers the connection between mechanical properties of asphalt and its composition and microstructure.

1.4 Experimental Methods for Viscoelastic Materials

Creep compliances $J(t)$, $D(t)$ and relaxation moduli $E(t)$, $G(t)$ are determined by testing under the stationary or periodic loading mode. The stationary load mode is understood to be a process where one of the parameters, such as stress or strain, remains constant in time, whereas the other parameter is measured as variable in time. The main stationary test methods for viscoelastic materials are relaxation testing and creep testing.

In experimental determining of relaxation moduli $G(t)$ or $E(t)$, a sample, first, is to be deformed up to the preset level of strain ε_c, and decrease in stress is recorded over prolonged period of exposure at constant deformation. The stress-time dependence $\sigma(t)$ is measured under constant strain $\varepsilon_c = \text{const}$ and the relaxation modulus under strain $E(t) = \sigma(t)/\varepsilon_c$ is determined. Likewise, the shear relaxation modulus $G(t) = \tau(t)/\gamma_c$ is determined by way of torsion testing under constant shear deformation $\gamma_c = \text{const}$.

There are certain requirements to the devices used for relaxation modulus measurement. Among them, there are two fundamental requirements: (1) instantaneous achievement of the initial deformation ε_c; and (2) absolute stiffness of the dynamometer used to measure the load in time in order to determine the stress $\sigma(t)$. The first requirement arises because the stress becomes partially relaxed during the time elapsed from the moment of application of initial deformation, thus distorting the resultant relaxation curve. The other requirement is reasoned by the fact that if a force measuring system is supple, then deformation varies in the process of testing. However, the more rigid the dynamometer is the less sensitivity achievable, i.e. the measured accuracy of the load applied to the sample. In fact, both requirements can be fulfilled only partially inasmuch as it is impossible to create any initial deformation at once, while it is not possible to measure load with a rigid dynamometer.

The same problems, although less acute, arise in the course of creep testing. To determine the shear $J(t)$ or longitudinal $D(t)$ creep compliance, a sample, first, is to be quickly loaded up to the preset stress level σ_c, which remains constant, while the deformation therein ε(t) evolves in time; it is measured to find the creep compliance $D(t) = \varepsilon(t)/\sigma_c$. In the same way, shear creep compliance is determined $J(t) = \gamma(t)/\tau_c$.

There are also two fundamental requirements as to creep testing: (1) creation of instantaneous initial stress σ_c; (2) the need to maintain constant stress whereas the cross section of the sample may vary in the process of creeping. The first requirement is caused by the fact that in case of slow load application, part of the deformation will happen by the moment of attaining the initial stress, thus affecting the creepage curve under $\sigma_c = const$. This requirement can be satisfied only in part by way of taking into account the effect of the loading rate on the creepage curve, correcting the test results through calculations. The second requirement entails sophisticated design of the creep measuring devices.

Therefore, the biggest problem in stationary testing is the need for an almost instantaneous non-impact application of stress or deformation. The testing error is especially significant where the observation time t is small enough to be comparable with the duration of the instance of constant stress or deformation creation. For example, if it takes 0.5 s. to apply stress σ_c, remaining thereafter constant in the course of creep testing, then the values of $D(t)$ are acceptable only where $t > 5$ s. Therefore, stationary test modes are better to use for determining the modulus $E(t)$ or creep compliance $D(t)$ where the t is long enough.

Figure 1.1 displays Mozgovoy's results of asphalt concrete relaxation testing under axial tension (Mozgovoy 1986). He used a test sample sized 40 × 40 160 mm of asphalt concrete mix, prepared with asphalt of penetration 70 d mm, softening point of 47.5 °C and Fraas brittle point −12 °C. The mix contained 6% asphalt, 40% crushed stone and 13% of filler [4-A mix composition according to Mozgovoy (1986)]. The asphalt concrete had the air porosity of 3.3%.

Mozgovoy succeeded in designing a simple device, which ensured non-impact application of preset tensile deformation for the time around 0.003–0.006 s. The deformation was maintained constant while reducing the load on the sample. The absence of essential eccentricity under strain was monitored by four longitudinal

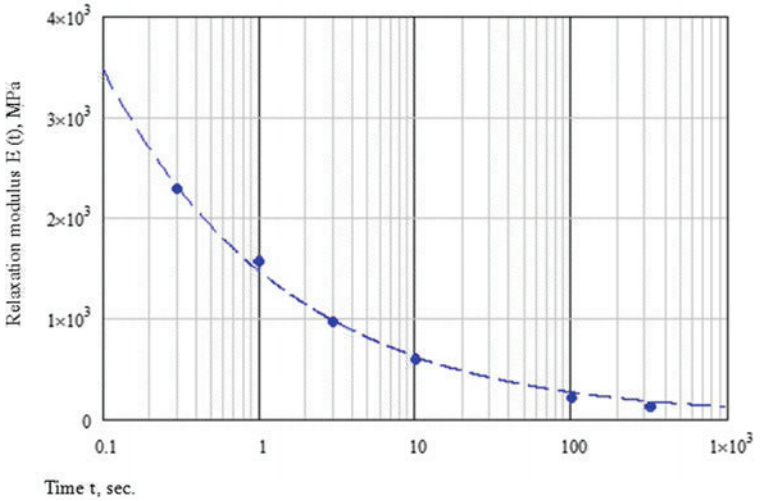

Fig. 1.1 Asphalt-concrete relaxation modulus under axial tension at the temperature of 20 °C (Mozgovoy 1986)

deformation sensors glued on the side edges of the sample. The effect of the sample own weight was excluded due to horizontal positioning of the sample which rested on a horizontal surface with minimum contact friction between the sample and the surface. The sample was placed inside a thermostat. The data points, as shown in Fig. 1.1 below, cover the range of 0.3–320 s.

Nowadays, the most convenient and commonly used method for determining the viscoelastic properties of asphalt and asphalt concrete is the periodical loading testing. In the former USSR, such tests were carried out since the 1970s at Kharkiv Automobile-Highway University by Zolotarev and his team or researchers (Vinogradov et al. 1977; Zolotaryov 1977). They are being conducted now by road laboratories in all US states to determine the grade of organic binders in accordance with standard specification of Superpave, classifying the binders in terms of performance and environmental conditions: the weekly mean maximum temperature of road pavement in summer and the minimum temperature in winter (ASTM D 6373, AASHTO M 320) with regard to the traffic volume.

Periodic loading testing can be performed with a bending load applied to a beam-shaped sample resting on two supports or cantilevers, or with a shear load applied to a disk-shaped sample by way of twisting thereof. A sample is exposed to harmonic time-varying stress or to deformation with constant, throughout the test angular frequency ω.

A bending test under a given sinusoidal-varying stress $\sigma(t) = \sigma_0 \sin(\omega t)$ with the certain constant amplitude of stress σ_0 after a few cycles, ascertains the sinusoidal-varying deformation $\varepsilon(t) = \varepsilon_0(\omega) \sin(\omega t - \delta)$ with the amplitude ε_0, which lags behind the stress by a phase angle δ. The deformation amplitude value ε_0 and the phase angle δ depend on the frequency ω and the testing temperature.

Having measured the ε_0 and δ, it is possible to find the absolute value of the complex longitudinal relaxation modulus

$$E_d(\omega) = |E^*(\omega)| = \sigma_0/\varepsilon_0(\omega) \tag{1.24}$$

In the USA, the standard practice used for determining the rheological properties of asphalt binders (according to ASTM D 7175 Standard) is torsion testing of a disk-shaped sample (Fig. 1.2) with the use of a dynamic shear rheometer (DSR) (Fig. 1.3).

A sample of 25 mm in diameter and 1 mm thick, or 8 mm in diameter and 2 mm thick is confined between a fixed lower metal disk and a moving upper metal disk. The upper disk is connected to a spindle where to torque is applied, rotating the spindle around its vertical axis alternatively clockwise and anticlockwise (Fig. 1.3). There are two types of shear rheometers: rheometers that control the applied shear stress or shear strain. In a rheometer where a controlled torque is applied to a sample, the cyclic varying shear stress is maintained constant, while the angular deformation of a moving plate is being measured. A sample is exposed to sinusoidal variable stress $\tau(\omega) = \tau_0 \sin(\omega t)$ with a certain preset amplitude τ_0 and frequency ω. After a few cycles, the varying deformation $\gamma(t) = \gamma_0(\omega) \sin(\omega t - \delta)$ is determined with the amplitude $\gamma_0(\omega)$ and at the same frequency, such deformation lagging in phase behind the applied stress by the angle δ. The deformation amplitude $\gamma_0(\omega)$ and the phase angle $\delta(\omega)$ are measured (Fig. 1.4).

Fig. 1.2 A 1 mm thick 25 mm-in-diameter sample for shear testing under cyclic twisting with the use of a DSR

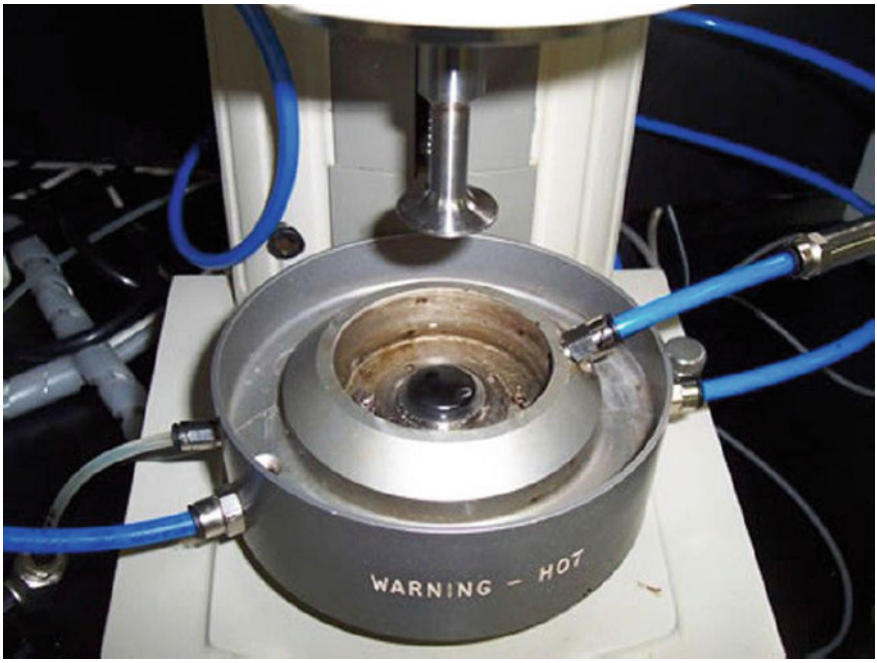

Fig. 1.3 Dynamic shear rheometer (DSR)

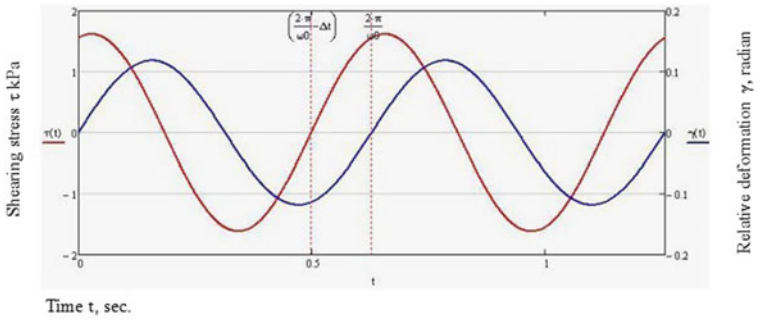

Fig. 1.4 An example of BND 90/130 asphalt test results: testing with a dynamic shear rheometer at T = 46 °C and ω = 10 rad./s: *red curve*—applied stress; *blue curve*—measured angular deformation Testing was carried out at KazDorNII (Kazakhstan Road Research Institute) with the use of a DSRII Air stress-controlled dynamic shear rheometer (Bohlin Instruments)

The ratio of the maximum shear stress τ_0, as applied to the sample, to the generated angular deformation $\gamma_0(\omega)$ is the absolute value of complex shear modulus $|G^*(\omega)|$, or just the shear dynamic modulus G_d.

$$G_d = |G^*(\omega)| = \tau_0/\gamma_0(\omega) \tag{1.25}$$

Strictly speaking, the common practice of replacement of the term "the absolute value of complex shear modulus" with "the dynamic modulus" is not correct because, in mechanics, the term "dynamic" is used to denote momentary loading, where the dead load and the inertial forces play a significant role, while in the asphalt testing, described herein, the said factors are absent.

The higher the frequency and the lower the temperature are, the higher the G_d is. The dynamic shear modulus may be described as a vector having two components: a storage modulus G' and a loss modulus G''. The storage modulus G' characterizes resistance to reversible deformation and the loss modulus G'' describes the resistance to viscous deformation. The dynamic modulus is expressed through these components as the length of a vector is expressed through the lengths of its components.

$$G_d = |G^*| = \sqrt{G'^2 + G''^2} \tag{1.26}$$

where: $G' = G_d \cos(\delta), G' = G_d \sin(\delta)$.

The relation $tg(\delta) = G''/G'$, which is called the mechanical loss tangent, characterizes the ratio of viscous and elastic resistance to deformation of material depending on the temperature and frequency. When phase angle $\delta = 0$ deformation and stress coincide in phase, which is typical for an elastic body (according Hooke's Law—Formula (1.2)). When phase angle $\delta = \pi/2$, the rate of deformation coincides with stress in phase, which is typical for viscous liquid (according to Newton Law—Formula (1.4)). When $\delta = \pi/4$, the share of elastic and viscous resistances in the overall resistance to deformation is the same. Figure 1.4 below gives an example of asphalt testing at the frequency of $\omega = 10$ rad/s, where the full wave period is $2\pi/10 = 0.628$ s.

BND 90/130 asphalt produced by Pavlodar Petrochemical Factory was tested at KazdorNII (Kazakhstan Road Research Institute) at the temperature of 46 °C. Shear stress was applied with the amplitude of $\tau_0 = 1.617$ kPa, which caused deformation with the amplitude of $\gamma_0 = 0.1183$. Hence, the absolute value of the complex shear modulus (dynamic shear modulus) in this example is:

$$G_d(\omega = 10) = |G^*(\omega = 10)| = \tau_0/\gamma_0(\omega = 10) = 1.617/0.1183 = 13.67\kappa\,\Pi\text{a}.$$

The deformation-against-stress lag time is $\Delta t = 0.129$ s (Fig. 1.4). For convenience, the vertical red dashed lines show the time of stress transition through zero (the right straight line). It is clear that the deformation lags behind the stress. The lag time of 0.129 s. at the frequency of 10 rad/s corresponds to the phase angle $\delta = 1.29$ rad or 74°. The storage modulus G′ = 13.67 cos (74°) = 3.77 kPa, the loss modulus G″ = 13.67 sin (74°) = 13.14 kPa, the loss tangent $tg(\delta) = tg(74^\circ) = 3.49$.

It is most practicable to run periodic loading tests at high frequencies. This allows to obtain information about viscoelastic properties of material where the loading time is very short, less than 1 s, and where relaxation testing and/or creep testing is difficult to complete. Stationary and periodic loading test modes supplement each other and used in combination. Such possibility of combined use is based on the existing precise linear viscoelasticity dependences between the moduli under stationary and periodical loading (Ferry 1963; Tshoegl 1989).

For instance, there are precise formulas that express the storage modulus G' and the loss modulus G'' via the shear relaxation modulus $G(t)$:

$$G'(\omega) = \omega \int_0^\infty G(s)\sin(\omega s)ds, \quad G''(\omega) = \omega \int_0^\infty G(s)\cos(\omega s)ds \tag{1.27}$$

It is clear, that these formulas can be used only in case of integral convergence, i.e. for those materials that relax upon stress completely at infinite period of time (when $G(t)$ approaches zero as $t \to \infty$), viz. for liquids. For viscoelastic solid materials $G(t)$ approaches a constant finite as $t \to \infty$, viz. to a long-term modulus and such formulas look somewhat different.

Besides, there are precise formulas that allow finding a shear relaxation modulus $G(t)$ based on the results of determining G' or $G''(\omega)$:

$$G(t) = \frac{2}{\pi}\int_0^\infty \frac{G'(\omega)}{\omega}\sin(\omega t)d\omega, \quad G(t) = \frac{2}{\pi}\int_0^\infty \frac{G''(\omega)}{\omega}\cos(\omega t)d\omega \tag{1.28}$$

It should be noted that the relaxation modulus $G(t)$ is the most useful viscoelastic characteristic. The formulas (1.27) and (1.28) are written for shear moduli $G(t)$; however, they look the same for longitudinal relaxation moduli $E(t)$.

To determine the integral and find the $G(t)$ using the above formulas (1.28), one needs to know the values of the $G'(\omega)$ or $G''(\omega)$ within a wide frequency range, or, conventionally speaking, within an infinite range, which is not practically feasible, because every periodical loading device allows to run tests only within a limited frequency range. Likewise, if we endeavor to determine $G'(\omega)$ or $G''(\omega)$ using the formulas (1.27), we need to know the relaxation modulus for all range of time variation.

In this connection, a significant practical interest lies in the approximations that allow combining the results of stationary loading tests and periodic loading tests. Some approximations of this type will be given below.

The most common tools used to describe the measured values of creep compliances $J(t)$, $D(t)$ and those of the relaxation moduli $G(t), E(t)$ are the expressions containing a sum of exponents Ferry (1963), Tshoegl (1989). For instance, the shear relaxation modulus can be described as a generalized Maxwell model

$$G_M(t) = \sum_{i=1}^{N} g_i \exp(-t/\lambda_i) \tag{1.29}$$

where the moduli g_i are the "spectral forces" reflecting the contribution of the processes having different relaxation times λ_i into the material behavior.

Physicists and chemists associate the characteristic times λ_i and the relevant values g_i with various viscoelastic deformation mechanisms. Under such approach, specters make up a source of information about those mechanisms and a tool for adjusting mechanical properties of material. In particular, some molecular theories have been offered (Rouse; Bueche; Doi-Edwards, Bird-Armstrong, etc.) that correlate the times λ_i with the mobility of various segments of a polymer macromolecule. This approach may be useful for adjusting the properties of bitumen binders too.

The values g_i and λ_i in the formula (1.29) are selected to fit the measurement results of $G_M(t)$. To obtain a smooth curve, it usually takes one or two relaxation times per decade of time variation (Ferry 1963). Therefore, to describe $G_M(t)$, for instance, the asphalt relaxation modulus within 10^{-5} to 10^5 s, we would need about 15 summands in the right part of (1.29), i.e. N = 15. Therefore, we have to estimate the N number of relaxation times λ_i and the same number of spectral forces g_i, i.e., say, the 30 unknowns in order to describe the experimental curve $G_M(t)$. This task is time consuming, even if you have a computer, for the sole reason that it belongs, in terms of mathematics, to the class of ill-posed problems, because a slightest change of the value λ_i corresponds to a very big change in g_i (Friedrich et al. 1996). Besides, an experimentally determined relaxation modulus depends on the properties of the asphalt and on the testing temperature of the same, so, such properties will govern all other chosen parameters λ_i and g_i, whose total number amounts to 2 N (e.g. 30 unknowns).

It is clear that such expressions (1.29) containing around 30 parameters which do not explicitly correlate with the standard properties, are not acceptable for describing viscoelastic properties of asphalt for practical purpose. It is far more convenient to use semi-empirical formulas containing a few parameters, which can be easily correlated with such simple standard parameters as penetration and softening temperature.

1.5 Time–Temperature Analogy

The analogy in the temperature effect and time effect on the behavior of viscoelastic material was first ascertained in the course of polymer testing (Kobeko et al. 1937; Leaderman 1941; Williams et al. 1955). For instance, if we are to increase deformation under constant load, we need to increase either the loading time (duration) t or the testing temperature T. It means that creep compliance $D(t)$ or $J(t)$ increases in line with increasing t or T. Likewise, increasing the $t$or T entails decreasing of the

relaxation modulus $E(t)$ or $G(t)$. It is worth mentioning, however, that the factor of temperature prevails over the load duration. This is to say that, for instance, a rise of T by a few degrees (5–8 °C) only entails decreasing of the asphalt relaxation modulus to the same extent as it is caused by an increase of the load duration tenfold at constant T.

Therefore, the temperature dependence of mechanical properties of many viscoelastic materials can be converted to time dependence (Ferry 1963). To do this, any temperature T_r is selected as reference temperature, and the time of load duration at such temperature t_r is expressed as dependence on the time of load duration t at the arbitrary temperature T:

$$t_r = t/a_T(T) \tag{1.30}$$

where $a_T(T)$ is the time–temperature shift factor, determined on the basis of the test data and being a decreasing function of T; t_r is the reduced time at temperature T_r.

It is important to note that, for a given viscoelastic material, the same function $a_T(T)$ is applicable to various viscoelastic properties: to viscosity η, relaxation modulus $E(t)$, creep compliance $D(t)$, complex modulus $E_d(\omega)$ and even to strength parameters. The principle of the time-temperature analogy (or time–temperature superposition) lies in the fact that all relationships between stresses, deformations and reduced time t_r in the form of (1.30) coincide; the temperature and time produce an interchangeable effect on such relationships, meaning that time and temperature are not individual factors but a combination thereof (1.30).

The $(T - t)$ analogy principle, firstly, simplifies the analysis due to reduction of the number of variables (just t_r instead of T and t), and, secondly, permits to greatly extend the existing test data over to the domain of very short time intervals or, otherwise, very long intervals. For example, instead of trying to measure deformation at 20 °C under the loading duration of 0.001 s., we can simply lower the test temperature by 10–15 °C and measure deformation under the loading duration of 1 s. Knowing the $a_T(T)$, we can ascertain how much such temperature should be lowered.

If we know the viscosity-time dependence $\eta(T)$, the function of time–temperature shift can be found from the relation (Ferry 1963):

$$a_{T_r}(T) = \frac{\eta(T)}{\eta(T_r)} \tag{1.31}$$

where $\eta(T_r)$ is viscosity at reference temperature T_r.

The time–temperature shift factor $a_T(T)$ is usually described by the expression (1.32) or (1.33). The first one was proposed in the form similar to Arrhenius formula (1916) for relationship between the rate of chemical reaction and temperature. This expression is as follows:

$$a_{T_r}(T) = \exp\left[\frac{E_a}{R}\left(\frac{1}{(273+T)} - \frac{1}{(273+T_r)}\right)\right] \tag{1.32}$$

where $a_{T_r}(T)$ is the time–temperature shift factor reduced to the reference temperature T_r; T is the test temperature, °C; E_a is the activation energy, J/mol; R = 8.314 J/(mol K) is the universal gas constant. The *Ea/R* ratio in the formula (1.32) is given by Kelvin scale (K).

The formula (1.32) contains only one "adjustable" parameter E_a, so it can be helpful in describing only part of the curve $a_{T_r}(T)$ within a certain variation interval of T. For instance, Van der Poel (1954) assumed the value of the asphalt activation energy to be E_a = 50 kcal/mol = 2.09 × 10^5 J/mol.

Another commonly used expression for $a_{T_r}(T)$ was proposed by Williams, Landel and Ferry (WLF equation) (Williams et al. 1955):

$$a_{T_r}(T) = \exp\left[\frac{\ln(10)C_1(T-T_r)}{C_2+(T-T_r)}\right] \tag{1.33}$$

Here: ln (10) = 2303 is the natural logarithm of ten; C_1, C_2 are empirical constants; C_1 is a non-dimensional quantity; and C_2 has the temperature dimension (K). If the reference temperature T_r is selected to be 50° above the glass-transition point (vitrifying temperature), then the following "standard" constant values are recommended: C1 = 8.86, C2 = 101.6 (Williams et al. 1955).

The authors of the WLF formula (1.33) have demonstrated its suitability for many polymers (polyisobutylene, polyvinyl acetate, polyurethane, etc.) and their solutions, for India rubber, organic glass-forming liquids (glucose, glycerin, etc.) and for inorganic glass-forming liquids. The WLF formula has two "adjustable" parameters and, therefore, it appears to be applicable within a wider temperature range than Arrhenius formula. Moreover Ferry (1963) suggested using the reference temperature as an "adjustable" parameter where the values of C_1, C_2 are standard values. As to asphalts, Vinogradov and Zolotarev recommend using, as the reference temperature, the asphalt softening point (according to the ring-and-ball method) and assuming that $C_1 = 23$, $C_2 = 218$ for the temperatures below the softening point (Vinogradov et al. 1977).

Let us consider an example of using the temperature-time analogy based on the test data on asphalt concrete stiffness modulus, provided by Mozgovoy, that were obtained in the uniaxial tensile testing of samples sized 40 × 40 × 160 mm. The composition of the mix and the properties of the components thereof are the same as above, in the description of Fig. 1.1 (4-A mix acc. to (Mozgovoy 1986)). Upon application of the load, remaining constant thereafter, the relative longitudinal deformation $\varepsilon(t)$ was measured, where t = 0.1, 1, 10, 32 and 100 s.

The tests ran at the temperature of 20, 15, 0, −5 and −8.5 °C. Figure 1.5 shows the values of the asphalt concrete stiffness modulus $S(t) = \sigma_c/\varepsilon(t)$ at these temperatures. The data points at each T are connected with straight lines. If we take any temperature as a reference temperature, e.g. T_r = 20 °C and make a parallel shift of

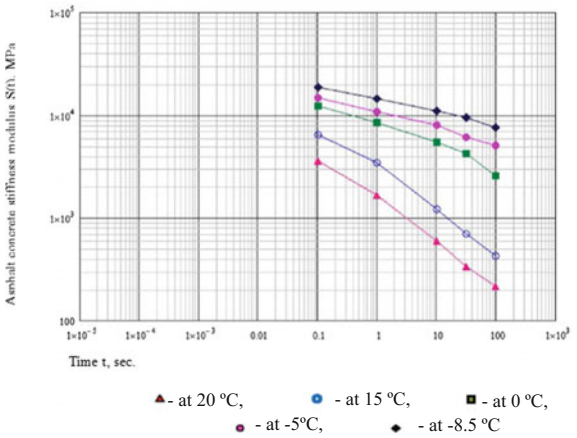

Fig. 1.5 Asphalt concrete stiffness modulus based on creep test results under axial strain (Mozgovoy 1986)

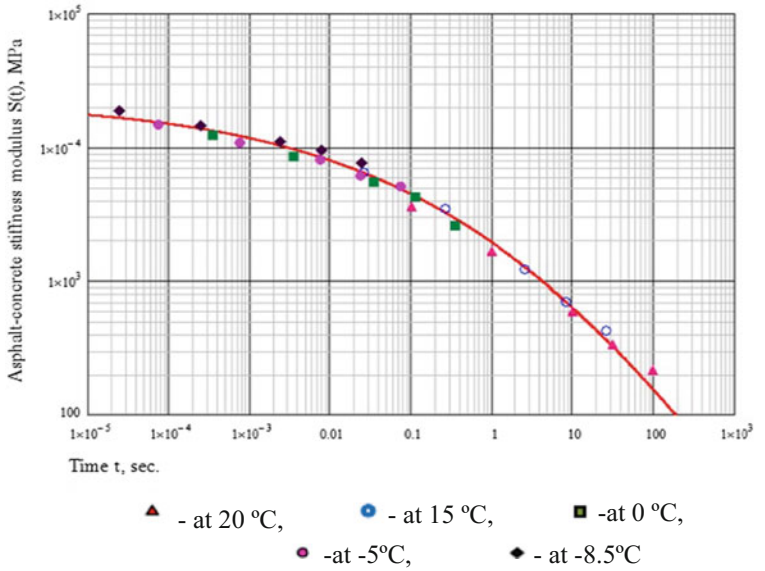

Fig. 1.6 Asphalt concrete stiffness modulus based on creep test results under axial strain—generalized (master) curve at T = 20 °C

the data points, relating to each test temperature, along the logarithmic time axis by the segment $a_{T_r}(T)$, then it appears that they are grouped together around the middle curve, as shown in Fig. 1.6 below. In this case, to determine the $a_{T_r}(T)$, we used the Arrhenius formula (1.32), assuming $E_a = 1.88 \times 10^5$ J/mol.

For instance, for the points belonging to the temperature T = 15 °C, we will have

$$a_{T_r}(T) = \exp\left[\frac{1.88 \cdot 10^5}{8.314}\left(\frac{1}{(273+15)} - \frac{1}{(273+20)}\right)\right] = 3.82,$$

i.e. decreasing the test temperature by 5 °C is equivalent to reducing the load duration 3.82 times at the reference temperature T_r = 20 °C.

Therefore the test data $S(t)$, obtained at 15 °C for t = 0.1, 1, 10, 32 and 100 s. correspond to the reduced time moments t_r = 0.0262, 0.262, 2.62, 8.38 and 26.2 s. at the temperature of 20 °C. The master curve plotted along such resultant points, as shown in Fig. 1.6, passes close to the actual data points for 20 °C.

This example demonstrates that, thanks to application of the time–temperature analogy, we extended the experimental "time window" from 0.1 … 100 s. to seven logarithmic decades, viz. 0.00001 … 100 s. at the reference temperature 20 °C.

The information about the viscoelastic properties, as discussed above, is enough to pass over to ascertaining the relationship between the simple standard parameters of asphalt and the characteristics of its viscoelastic properties.

References

Asphalt Institute (1982), Research and development of the Asphalt Institute's thickness design manual, Manual Series1, Research Report 82–2, Maryland

British Standards (2001), BS EN12697: Bituminous mixtures. Test methods for hot mix asphalt, British Standards Publ., UK, HD23/99 (1999). Design manual for roads and bridges, vol 7, Pavement Design and Maintenance

Burmister D (1945) The general theory of stresses and displacements in layered soil systems. J Appl Phys 6(2):89–96, (3):126–127, (5):296–302

Chen EY, Pan GE, Norfolk TS, Wang O (2011) Surface loading of a multilayered viscoelastic pavement. Road Mat Pav Des 12:849–874

Claessen A, Edwards J, Sommer P, Uge P (1977) Asphalt pavement design—the shell method. In: Arbor A (ed) Proceedings of the 4th international conference on the structural design of asphalt pavements, vol I, pp 39–74

Design of Pavement Structures, Technical Guide (in French). SETRA, Laboratoire Central des Pontset Chaussées, Dec 1994

Ferry JD (1963) The viscoelastic properties of polymers (Translation from English). IL, Moscow

Friedrich C, Honerkamp J, Weese J (1996) New ill-posed problems in rheology. Rheol Acta 35:186–193

Heukelom W, Klomp A (1964) Road design and dynamic loading. In: Proceedings of the association of asphalt paving technologists, vol 33, pp 92–123

Industry Road Code 218.046-01Б (2001) Design of flexible pavement. Moscow

Industry-specific construction standard (1985) Design of flexible pavement. Transport, Moscow, pp 46–83

Kobeko PP, Kuvshinskii EV, Gurevich GI (1937) Analysis of amorphous state. News Acad Sci USSR 3:329–344

Kogan B (1953) Stress and strains in multilayered pavement. In: Works of Kharkov Automobile-Highway University (14), pp 33–46

Kolbanovskaya A, Mikhaylov V (1973) Paving asphalts. Transport, Moscow
Krishnan JM, Rajagopal KR (2003) Review of the uses and modeling of bitumen from ancient to modern times. American society of mechanical engineers. Appl Mech Rev 56(2):149–214
Leaderman H (1941) Textile materials and the time factor: I: mechanical behavior of textile fibers and plastics. Text Res 11:171–193
Lesueur D (2009) The colloidal structure of bitumen: consequences on the rheology and on the mechanisms of bitumen modification. Adv Coll Interface Sci 145(1–2):42–82
Maxwell JC (1866) On the dynamical theory of gases. Philosophical Transactions of the Royal Society (A157) London, pp 26–78
Maxwell J (2001) Theory of heat. Elibron Classics (Reprint of the 1872 edn.)
Mehta YA, Christensen DW (2000) J Assoc Asph Pav Tech 69:281–312
Monismith CL, Alexander RL, Secor KE (1966) Rheological behavior of asphalt concrete. In: Proceedings of the association of asphalt paving technologists, vol 35, pp 400–450
Mozgovoy VV (1986) Assessment of low temperature cracking resistance in asphalt pavements, Ph.D. Thesis, Ukrainian Transport University, Kiev
Privarnikov A, Radovskii B (1981) Action of moving load on viscoelastic multilayer base. Int Appl Mech 17(6):534–540
Radovskiy B (1982) Theoretical foundation of pavement design as viscoelastic layered system subjected to moving load. Synopsis of Thesis, State Automobile and Road Technical University, Moscow
Reiner M (1965) Rheology. NAUKA, Moscow
Shell (1978) Pavement design manual—asphalt pavements and overlays for road traffic. Shell International Petroleum Co Ltd, London
Teliaev P (1964) Stress state of pavement under static and short-term loading. Highways 6:20–21
Tschoegl N (1989) The phenomenological theory of linear viscoelastic behavior. Springer, Heidelberg
Van der Poel C (1954) A general system describing the viscoelastic properties of bitumens and its relation to routine test data. J Appl Chem 4:221–236
Van der Poel C (1958) On the rheology of concentrated dispersions. Rheol Acta 1:198–205
Vinogradov GV, Isayev AI, Zolotaryov VA, Verebskaya EA (1977) Rheological properties of road bitumens. Rheol Acta 16:266–281
Williams ML, Landel RF, Ferry JD (1955) The temperature dependence of relaxation mechanisms in amorphous polymers and other glass-forming liquids. J Amer Chem Soc 77:3701–3707
Standard Specification for Performance Graded Asphalt Binder: ASTM D6373, AASHTOM320
Zolotaryov V (1977) Asphalt concrete durability. Vysshaya Shkola, Kharkov
Zolotaryov VA (2010) Fundamental asphalt concrete linear viscoelastic deformation. Sci Tech Road Ind: 24–27

Chapter 2
Determining of Asphalt Stiffness Modulus

Abstract This chapter deals with the development of equation that expresses the bitumen stiffness modulus as a function of time, temperature and the simple properties of bitumen such as penetration (or penetration index) and softening temperature. As mathematical model for describing the stiffness of bitumen, Christensen and Anderson (CA) equation was used. The parameters of CA model were related to the bitumen properties based on Van der Poel's experimental data. The instantaneous value for longitudinal modulus was obtained by extrapolation of values for stiffness modulus according to Van der Poel at low temperatures and small load durations. With the purpose of extrapolation, the model developed to describe the viscoelastic properties of amorphous glass forming polymers was applied. To express the zero-shear viscosity of bitumen as a function of temperature based on Van der Poel's data, the parameters of time-temperature superposition function were related with the penetration index of binder. The approximate formula was obtained for the exponent of power in CA model as a function of penetration index. Using developed equation, stiffness modulus of bitumen can be easily calculated in a wide range of temperatures and loading time.

In this section, we obtain empiric formula, showing asphalt stiffness modulus as a function of temperature and load duration. As the basic information regarding asphalt, we use only its penetration (i.e., the depth of needle penetration under GOST 11501-78 or ASTMD 5) and softening point (calculated by "ring-and-ball" test under GOST 11506-73 or ASTMD 36)—indexes for asphalt, which are always calculated in all road laboratories of Russia, Ukraine, Kazakhstan, Belorussia and western European countries.

2.1 Test Data on Asphalt Stiffness Modulus

As it was mentioned before, Van der Poel (1954a, b) called asphalt stiffness modulus a ratio of constant tensile stress σ_c to the strain $\varepsilon(t)$

B. Radovskiy and B. Teltayev, *Viscoelastic Properties of Asphalts Based on Penetration and Softening Point*, Structural Integrity 2,
https://doi.org/10.1007/978-3-319-67214-4_2

$$S(t) = \sigma_c/\varepsilon(t) \tag{2.1}$$

To determine $S(t)$, Van der Poel (1954a, b) used two types of loading experiments, namely constant stress experiment—static creep test—and the dynamic test with the alternating stress of constant amplitude and frequency.

Creep test was carried out by steady loading conditions of tension or bending, as well as shear (twisting in rotation viscometer), and $S(t)$ was calculated, which Van der Poel called static asphalt stiffness modulus. During such a test, the load duration exceeded 1 s and reached 10,000 s. Stiffness modulus, obtained by torsion test, was transformed into stiffness modulus under tension by multiplying into 3, as the Poisson's ratio of asphalt was roughly assumed as equal to 0.5 without regard to temperature.

Van der Poel carried out tests by cyclic loading in conditions of bending of the beam on two piers or consoles with frequency ω from 1 to 1000 rad/s. Relation of amplitude of applied stress to amplitude of measured deformation, i.e., absolute value of longitudinal complex modulus $E_d(\omega) = |E^*(\omega)| = \sigma_0/\varepsilon_0(\omega)$ he called dynamic stiffness modulus. Van der Poel mentioned that inaccuracy for repeated test results with cyclic loading was 6%—much less than with steady load, especially for asphalt of low temperature susceptibility.

Having compared test results for steady and cyclic load, Van der Poel made a conclusion that if to replace a cyclic frequency with the value, reciprocal to time of loading, then the dynamic modulus is roughly equal to static stiffness modulus:

$$S(t) \approx E_d(\omega)|_{\omega=1/t} \tag{2.2}$$

He verified transformation (2.2) from tests with cyclic loading to the creep test, using a simple model of Maxwell's visco-elastic liquid Eq. (1.9). Therefore, Van der Poel showed relation of asphalt stiffness modulus with load duration in the diagram $\log S(t) - \log t$, laying off $S(t)$ for small durations of loading as the modulus E_d with similar scale for time t and for value, reciprocal to cyclic frequency $1/\omega$. One curve $S(t)$ slipped into continuation of another at t around one second. It gave the chance to use jointly the test results of constant stress and oscillating loading covering large period of load duration within 10^{-3} до 10^4с on one diagram $\log S(t) - \log t$ for the given asphalt with certain temperature.

Van der Poel joined into single variable impact of temperature and load duration on asphalt stiffness modulus, having used principle of time-temperature analogy, which we described in Sect. 1.5. As the work was performed before publication of the mentioned article of M. Williams, R. Landel and J. Ferry (WLF), he used only the formula like S. Arrhenius (1.32) to determine time–temperature shift function, accepting activation energy for asphalt E_a = 50 kcal/mol = 2.09 × 10^5 J/mol.

Van der Poel tested 47 types of asphalt, obtained from various crude oils by different methods (distillation, temperature cracking, oxidation, precipitation, mixing). These types of asphalt were essentially differed from each other regarding

response of stiffness modulus $S(t)$ to temperature variation. To identify them, Van der Poel used penetration index PI, which was introduced by Pfeifer and Van Doormal in 1936 (Pfeiffer and Van Doormal 1936) as a parameter of the temperature susceptibility of asphalt:

$$PI = \frac{20 - 500A}{1 + 50A} \tag{2.3}$$

where A is temperature susceptibility, characterizing slope of the line log (P) versus T, where P is a penetration of needle into asphalt:

$$A = \frac{\lg(800/P)}{T_{rb} - 25} \tag{2.4}$$

Here P is a penetration depth at 25 °C, T_{rb}—softening point for asphalt, measured by "ring and ball" method (ring and ball temperature), whereas it is assumed that penetration depth for all types of asphalt at softening point is equal to 800, i.e., 800 dmm (decimillimeters).

The cause, why Pfeifer and Van Doormal chose this Eq. (2.3) and proposed to use PI but not A as the characteristics of temperature response, was their aim to characterize Mexican asphalt, which had the penetration 200 at 25 °C, as zero index $PI = 0$. In accordance with the formula (2.3), for asphalt with PI = 20, penetration does not depend on temperature at all (A = 0), and with PI = −10 asphalt, to the contrary, is infinitely susceptible to the temperature variation.

As a rule, penetration index for asphalt does not exceed PI from −3 to +5. In the vast majority of cases, the paving asphalt is characterized by PI from +2 to −2. Asphalt with PI less than −2 is so responsive to temperature variation that the mixes, prepared with it, are subject to forming of cracks during fast cooling in winter. Particularly, GOST 22245-90 for paving asphalt oil restrains penetration index for asphalt of types BND 40/60 −BND 200/300 within $-1 < PI < +1$.

Therefore, Van der Poel used penetration at 25 °C P (according to ASTM D5) and softening point T_{rb} (according to ASTM D36) and penetration index PI, which was calculated on their base to characterize asphalt.

Asphalts, tested by Van der Poel, were of penetration index from −2.6 to +6.3, i.e., performed tests included as the asphalt, very susceptible to temperature variation, as well as asphalts of low temperature susceptibility. Testing temperature was chosen with consideration of temperature susceptibility for asphalt and its softening point. For example, asphalt with PI = −2.3 and T_{rb} = 66 °C was tested at T = 5, 15, 25, 35, and 45 °C, and asphalt with low temperature susceptibility with PI = + 5.3 and T_{rb} = 116 °C—at T = −20, 0, 20, 40 and 60 °C. Experimentally obtained values for stiffness modulus for the given T with different t during tests by constant and cyclic load were included into diagram of relation for stiffness modulus—time in the scale $\log S(t) - \log t$ and smooth curve $S(t)$ was drawn through the experimental points.

Based on experimental data, Van der Poel developed a nomograph for determination of stiffness modulus (Van der Poel 1954a, b). With this nomograph for a given penetration of asphalt P and its softening point T_{rb}, one can determine the stiffness of asphalt cement as a function of T and load duration t or cyclic frequency ω. Depending on penetration index, P difference of temperatures (T_{rb} − T), and load duration t within 10^{-6} and 10^{10} s, Van der Poel's nomograph covers the range of values for bitumen stiffness modulus S from 10^{-4} to 2.5×10^{9} Pa.

Having determined a bitumen stiffness modulus from the nomograph, it is possible to predict the stiffness modulus for asphalt concrete depending on characteristics of bitumen, its content in the mix and porosity of the mix (Heukelom and Klomp 1964; Bonnaure et al. 1977).

Van der Poel's nomograph was included into reference books (The SHELL Bitumen Handbook 2003), manuals for Civil Engineers (Roberts et al. 1996 etc.), monographs for pavement design (Huang 1993) etc.), as well as in a number of technical papers. Van der Poel did not publish empirical equations, which he used in construction of the nomograph, and therefore, stiffness modulus can be found only graphically, and the procedure is time consuming and inaccurate.

According to Van der Pole's evaluation, maximum inaccuracy for determining of stiffness modulus via the nomograph is up to 50% compared with experimental data, on which it is based. It is due to construction the curves that fit to a series of data points on logarithmic scale, variety of experimental points and replacement of wavy sections for the curves by smooth ones. If to have in mind, that a range for moduli, which are determined using the nomograph, covers 13 decades of time (from 10^{-4} to 2.5×10^{9} Pa), then maximum inaccuracy of 50% is quite reasonable. Average inaccuracy is much less. In addition, as Van der Poel mentioned (Van der Poel 1954a), double difference of asphalt moduli complies roughly with the difference of temperatures about 2 °C, and it is difficult to expect practically that information regarding actual temperature conditions of pavement will be much more accurate.

Later the staff of SHELL lab enlarged the Van der Poel's nomograph, scanned and digitized. Then Ullidtz and Peattie developed Fortran-program PONOS for determination of stiffness modulus by programmable calculators (Bats 1973; Ullidtz and Peattie 1980). G.M. Rowe and M.J. Sharrock (ABATECH, Inc.) developed a program BitProps for personal computers in 2000, based, like PONOS, on interpolation between the points of digitized Van der Poel's nomograph. It allows finding the stiffness of asphalt modulus of bitumen without graphical procedure.

2.2 Empirical Formulas Earlier Suggested for Stiffness Modulus

For practical and research purposes, mathematical equations are needed for the important viscoelastic characteristics of bitumen such as a stiffness modulus $S(t)$, the shear and longitudinal creep compliance $J(t)$ и $D(t)$, the shear and longitudinal relaxation moduli $G(t)$ and $E(t)$, and for the complex modulus $|G^*(\omega)|$ or $|E^*(\omega)|$.

Those equations should allow obtaining these characteristics depending on standard properties of asphalt (penetration P at 25 °C and the softening point T_{rb}), load duration and temperature.

Several researchers tried to develop mathematical equation for stiffness modulus of bitumen $S(t)$ depending on P,T_{rb} and T.

Saal (1955) proposed such a formula, based on the graphs in Figs. 11 and 12 of Van der Poel's article (1954a). It relates the asphalt stiffness modulus with load duration t = 0.4 s and its penetration without regard to the temperature susceptibility of asphalt:

$$S_{0.4} = \frac{10^{9.4}}{P^{1.9}} \tag{2.5}$$

where stiffness modulus is expressed in Pa.

This formula has a number of drawbacks. First, stiffness modulus can be determined only at one load duration (0.4 s). Second, to determine it at some temperature you should know the depth of needle penetration at this temperature, but it is usually known only for T = 25 °C. Third, according to formula (2.5), asphalt stiffness modulus with t = 0.4 s does not depend on softening point, i.e., penetration index. For example, with P = 100 dmm under formula (2.5) $S_{0.4}$ = 0.4 MPa. Actually, for P = 100 dmm and softening points T_{rb} = 38.8, 47.5, and 59.5 °C (penetration indexes PI = −3, 0, and +3), the Van der Poel's nomograph (or program BitProps) shows S = 0.26, 0.40 and 0.52 MPa respectively. It turns out that only asphalt stiffness modulus for PI = 0 agrees with the formula, and moduli with penetration indexes PI = −3 and +3 differ in two times, although according to formula (2.5) stiffness does not depend on PI.

Ullidtz and Larsen (1984) proposed the equation

$$S(t) = 1.157 \cdot 10^{-7} t^{-0.368} e^{-PI} \cdot (T_{rb} - T)^5 \tag{2.6}$$

Drawbacks of this simple formula are obvious. With load duration, tending to zero, stiffness modulus under formula (2.6) tends to infinity, and therefore it is doubtful that this formula is applicable for very small t. When $T = T_{rb}$, according to formula (2.6), stiffness modulus equals to zero, which does not comply with reality. For $T > T_{rb}$, it becomes negative, which does not have sense. Therefore, the Eq. (2.6) might return unrealistic values for stiffness modulus at temperature greater than softening point. Ullidtz and Larsen (1984), limited the applicability of Eq. (2.6) to the duration of loading $0.01 < t < 0.1$, range of penetration index $-1 <$ PI < 1, and temperature range 10 °C $< (T_{rb} - T) <$ 70 °C.

Nevertheless, even within the ranges, mentioned by them, it differs essentially from Van der Poel's data, on which it is based. Therefore, for asphalt with PI = −1, which has P = 54.5 dmm and T_{rb} = 50 °C, at T = 30 °C and t = 0.1 s formula (2.6) predicts S = 2.35 MPa while the Van der Poel's nomograph (or program BitProps) returns S = 1.27 MPa, i.e., modulus is two times higher. For asphalt with PI = + 1, which has P = 109.5 dmm and T_{rb} = 50 °C, at T = 30 °C and t = 0.01 s

formula (2.6) predicts $S = 0.742$ MPa, while the program BitProps returns $S = 2.021$ MPa, i.e., modulus is three times lower. Calculations show that the coefficient of variation of stiffness modulus calculated using Eq. (2.6) from the Van der Poel's data even in that quite narrow range of input parameters, is 40%.

Nevertheless, the Eq. (2.6) was used in a number of works, for example in (Collop and Cebon 1995), but the authors of the last paper reduced the temperature interval of its applicability to $20\ °C < (T_{rb} - T) < 60\ °C$. For example, at $T_{rb} = 50\ °C$ it means applicable for using only at T from −10 to 30 °C, but it does not allow using formula (2.6) for analysis of pavement behavior neither at low winter, nor for high summer temperatures.

Two formulas like (2.6), but more cumbersome, were proposed by Shahin (1977), who worked in predicting of low temperature cracks formation in asphalt concrete pavements. Shahin used three operational variables in his equations: the logarithm of time $\lg(t)$, a penetration index PI, and the temperature difference $(T - T_{rb})$. Based on Van der Poel's nomograph and using two hundred points, by regression analysis he found stiffness as a function of $\lg(t)$, PI, and $(T - T_{rb})$; the square and the cube of these variables, as well as their products. That is why the Shahin's two equations for log(S) are so lengthy.

Shahin did not specify the range of their applicability. He only mentioned that his first formula was intended for small stiffness modulus $S < 1$ MPa [formula (2.2) in (Shahin 1977)], and the second formula—for $S > 1$ MPa [formula (2.3) in (Shahin 1977)].

Meanwhile, it is unknown beforehand what value of stiffness modulus will be and which of these formulas should be used. Moreover, for example for asphalt with PI = −1, which has $P = 54.5$ dmm and $T_{rb} = 50\ °C$, at $T = 23\ °C$ and $t = 1$ s according to the formula for small moduli, the asphalt stiffness equals to $S = 0.826$ MPa while according to formula for large ones the asphalt stiffness equals $S = 13.34$ MPa, i.e., both formulas are applicable, but it is unknown which of the results is correct. The similar picture can be observed for the asphalt at all temperatures from 23 to 35 °C. Similar situation is valid for other asphalts as well.

Recently, Molenaar (2005) of Delft University, using Shahin's formulas (1977), tried to establish the range of their applicability for the binders of penetration index $-2 < \text{PI} < 2$. According to our evaluation, Shahin's equation for large stiffness is worse than for small stiffness. Particularly, for asphalt with PI = −1, at T = −15 °C and $t = 0.01$ s, Eq. (2.3) in (Shahin 1977) returns the bitumen stiffness of 16,000 MPa. This value is 6–7 times greater than asphalt stiffness modulus in glassy state and even exceeds asphalt concrete gassy modulus.

As one can see, many researches expressed their interest to the equations that relate the stiffness modulus of bitumen with its standard characteristics, time, and temperature. Attempts to find such relations in the papers (Ullidtz and Larsen 1984; Saal 1955 and Shahin 1977) were not successful. In our opinion, it can be explained by usage of purely statistical methods for their derivation without involving of the theoretical interrelationships describing the viscoelastic behavior of asphalt binder.

2.3 Development of Formula for Asphalt Stiffness

As viscoelastic material, asphalt combines the properties of perfectly elastic solid and perfectly viscous liquid. It is illustrated by Van der Poel's data on asphalt stiffness $S(t)$ (Fig. 2.1). Asphalt is characterized by penetration depth P = 80 dmm at 25 °C and softening point T_{rb} = 50 °C (penetration index PI = 0). Thirty-two values for stiffness modulus are taken with the help of program BitProps for temperature 15 °C and 32 values of load duration t within the range of 10^{-6} and 10^{3}s that are shown by points on the graph.

Under constant stress σ_c,at short loading time $t \to 0$ the asphalt deformation $\varepsilon(t)$ tends to its instantaneous elastic value $\varepsilon = \sigma_c/E_g$, and therefore, its stiffness modulus, according to Eq. (2.1), at $t \to 0$ tends to instantaneous longitudinal elastic modulus E_g(glassy modulus). Horizontal asymptote of the curve $S(t)$ corresponds to the value of E_g.

As load duration increases, input of viscous flow into deformation increases too. Deformation during tension of ideal viscous liquid, under Newtonian law Eq. (1.7), is equal to $\varepsilon(t) = \sigma_c t/3\eta$, and therefore, according to Eq. (2.1), at $t \to \infty$ stiffness modulus tends to $S(t) = 3\eta/t$. In logarithmic scale log(S) − log(t) last equation is shown by straight line with slope 45°.

Horizontal (elastic) and inclined (viscous) asymptotes of the curve $S(t)$ are shown in the Fig. 2.1. It is obvious that they are crossing in the point, where $E_g = 3\eta/t$, i.e., $t_0 = 3\eta/E_g$. For this example t_0 = 0.005 s. These two asymptotes limit the area of location for the curve $S(t)$. It is convenient to describe the curve of such geometry by the function like

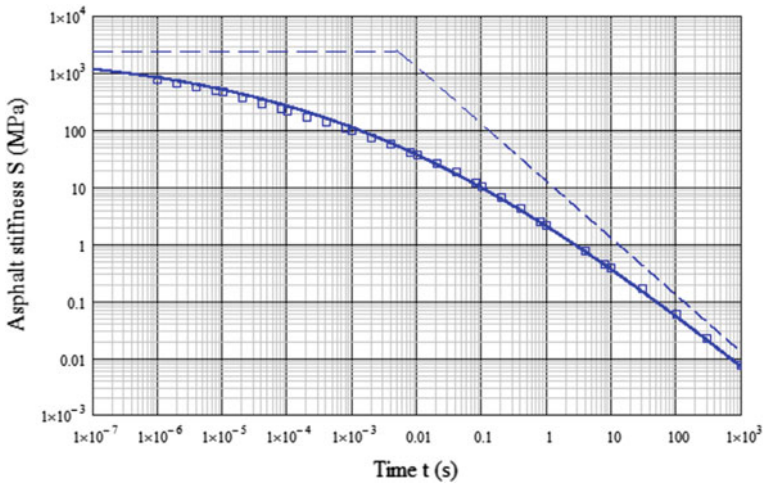

Fig. 2.1 Typical master curve of creep stiffness as a function of loading time at constant temperature

$$F(t) = E_g\left[1 + \left(\frac{t}{t_0}\right)^{v}\right]^{-1/w} \tag{2.7}$$

This expression was proposed by Havrilyak and Negami (1966) during their research of dielectric permittivity for polymers, which is mathematically similar to complex modulus of viscoelastic material. This function with the equal exponents v = w was adopted in 1992 for description of asphalt complex modulus $|G^*(\omega)|$ by Christensen and Anderson (1992), Christensen (1992), and in short it is called CA model (Christensen-Anderson model). Parameter t_0 of this model depends on temperature, but parameter v does not depend on it, and both parameters are determined from experimental data. Meanwhile, Christensen and Anderson did not find the relationship between parameter v and asphalt penetration index *PI* (Christensen and Anderson 1992). The authors of CA model limited its applicability by the values of asphalt complex modulus greater than 0.1 MPa (Christensen 1992, p. 198).

Later Anderson and Marasteanu considered the applicability of model (2.7) with unequal exponents of $v \neq w$ (Marasteanu and Anderson 1999) (CAM model) to asphalt. Lesuer with co-authors did the same (Lesuer et al. 1997), but they considered all three parameters t_0, w and v as the temperature dependent. It made very difficult to use the model, as it required calculating three parameters at each temperature of testing.

We assumed the following equation for asphalt stiffness modulus in this work

$$S = E_g\left[1 + \left(\frac{E_g t}{3\eta}\right)^{\beta}\right]^{-\frac{1}{\beta}} \tag{2.8}$$

where E_g is the uniaxial glassy modulus of binder (MPa); η is the steady-state Newtonian viscosity (MPa·s), which is dependent on asphalt type and its temperature; β is the exponent of power ($0 < \beta < 1$), which is supposed to be dependent only on asphalt type. Equation (2.8) is similar to CA model, which has been proposed in the paper Christensen and Anderson (1992) for complex modulus $|G^*(\omega)|$. Eq. (2.8) is shown by the curve in the Fig. 2.1.

Stiffness modulus (2.8) tends to instantaneous stiffness modulus E_g with the decrease of load duration. With unlimited increase of load duration, it tends to the equation describing viscous flow $S = 3\eta/t$. Exponent β is the shape parameter the curve $S(t)$. With the decrease of β at constant viscosity, the curve $S(t)$ becomes more flat, i.e., transformation from elastic to viscous asphalt behavior occurs more gradually.

We investigated the relations of E_g, η and β with the penetration P and the softening point T_{rb} for asphalt.

The instantaneous value for longitudinal modulus E_g was obtained by extrapolation of values for stiffness modulus $S(T, t)$ according to Van der Poel at low temperature T and small load duration t for $t \to 0$. With the purpose of

extrapolation, we used the model, developed by Drozdov for description of viscoelastic properties of amorphous glass forming polymers (Drozdov 2001). For a set of eight loading times t = 0.00005, 0.0001, 0.0002, 0.0005, 0.001, 0.002, 0.005 and 0.010 s, we selected the lowest temperature for the asphalt with certain penetration index, for which, using a program BitProps the value of stiffness S can be obtained fort = 0.00005 s. This lowest temperature was from −42 °C for PI =+2 to 9 °C for PI = −3. We obtained S at a very low temperature for those eight periods of time. Then using the formulas (18) and (37) of (Drozdov 2001) we found value of instantaneous modulus in such a way so that influence curve of modulus from temperature could pass through the points, corresponding to those eight periods of time.

We concluded that for asphalts with *PI* from −2 to +3 the average value of instantaneous longitudinal modulus equals to E_g = 2460 MPa with variation coefficient of 7%. Meanwhile, no regular variation of E_g was observed with variation of penetration index (Fig. 2.2).

Therefore, glassy modulus can be assumed to be E_g = 2460 MPa in extension or flexure. For reference, Van der Poel assumed E_g = 2500 MPa for all asphalts (1954a, b). Dobson accepted G_g = 1000 MPa, which is similar to E_g = 3000 MПa (Dobson 1969). Christensen and Anderson, according to the test results for eight types of asphalts with various levels of ageing, selected values for instantaneous shear modulus within the range of G_g = 720 MPa and G_g = 1120 MPa, which corresponds to E_g = 2160 − 3360 MPa, but they recommended to assume E_g = 3000 MPa (Christensen and Anderson 1992).

Obviously, asphalt stiffness is a function of time and temperature (Fig. 2.3). The steady-state viscosity η reflects a temperature dependency of stiffness S in the Eq. (2.8). To obtain the viscosity as a function of temperature, the equation for a time–temperature shift factor $a_{T_r}(T)$ should be formulated.

As it was specified in Sect. 1.5, it is convenient to think of $a_{T_r}(T)$ as of the coefficient, into which you should divide the loading time t during the testing at temperature T to obtain the same strain value for a loading time t_r during the testing

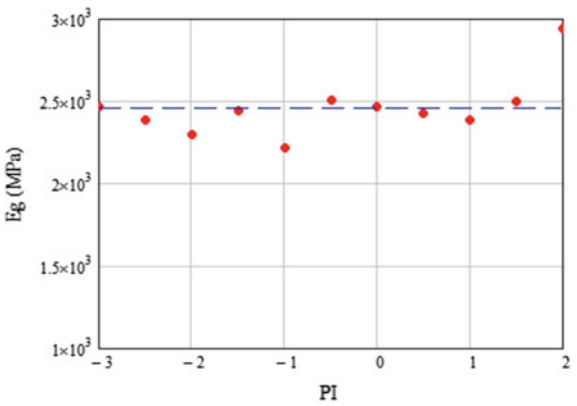

Fig. 2.2 Instantaneous glassy modulus of asphalt calculated by extrapolation of Van der Poel's data (horizontal line shows average value E_g = 2460 MPa)

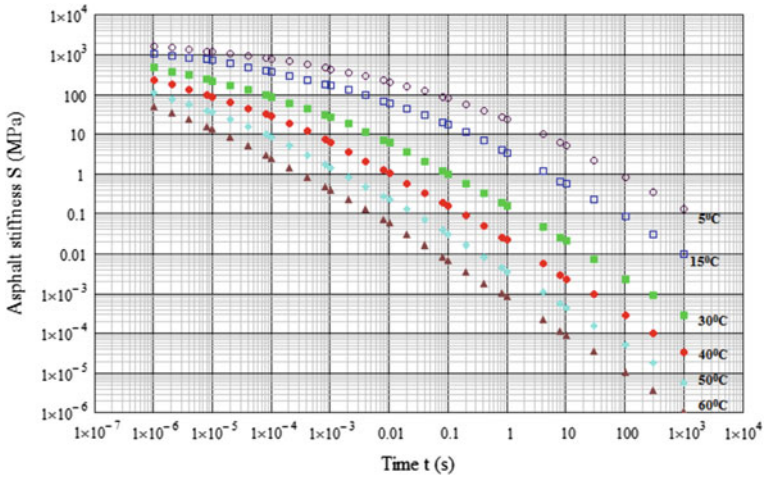

Fig. 2.3 Variation of asphalt stiffness with time and temperature: points correspond to Van der Poel's data for asphalts with PI = −0.5, T_{rb} = 50 °C

at reference temperature T_r, i.e., to perform time-temperature shift $t_r = t/a_T(T)$ for creep or relaxation curve along axis log(t) in order to join the curves, obtained at different temperatures. In other words,

$$a_{Tr}(T) = t/t_r, \tag{2.9}$$

where t and t_r are such loading times at the temperatures T и T_r that the moduli (or compliances) are equal.

For instance, for asphalt with PI = −0.5 and T_{rb} = 50 °C (Fig. 2.3) we will find a value of time-temperature shift function for test results at the temperature T = 15 °C to the reference temperature T_r = 40 °C. Using the program BitPros, we can find at T = 15 °C and t = 100 s the stiffness S = 0.0807 MPa. The same value of stiffness modulus for this type of asphalt is obtained at temperature T_r = 40 °C for the loading time t_r = 0.2205 s. Now from Eq. (2.9) one can obtain for this type of asphalt $a_{T_r}(T)$ = 100/0.2205 = 454. In other words, difference of temperatures 40 − 15 = 25 °C for this type of asphalt is equivalent to variation of t in 454 times. Let us check that this value does not depend on load duration. Let us take for T = 15 °C loading time t = 10 s (instead of 100 s as before). Then stiffness modulus for this type of asphalt is S = 0.5395 MPa. The same value of stiffness modulus for this type of asphalt at temperature T_r = 40 °C will be at the loading time t_r = 0.02153c, from which $a_{T_r}(T)$ = 10/0.02153 = 464. The difference between obtained values is only 2%. Thus, the curves $S(t, T = 15\ °C)$ and $S(t, T = 40\ °C)$ for this type of asphalt in Fig. 2.3 can be joined by displacement along the axis log(t) on a segment around log(460) = 2.663 in logarithmic scale.

In the same manner using Eq. (2.9), we found the values of $a_{T_r}(T)$ for asphalts with the various *PI*. Parameters of function $a_{T_r}(T)$ were fitted to those values.

Function $a_{T_r}(T)$ was composed from equations of Arrhenius and M. Williams, R. Landel, J. Ferry (WLF) (Ferry 1963), described above in Sect. 1.5:

$$a_{Tr\ Ahrr}(T) = \exp\left[\frac{E_a}{R}\left(\frac{1}{(273+T)} - \frac{1}{(273+T_r)}\right)\right] \tag{2.10}$$

$$a_{Tr\ WLF}(T) = \exp\left[\frac{In(10)C_1(T-T_r)}{C_2+(T-T_r)}\right] \tag{2.11}$$

Arrhenius's equation was chosen for temperatures lower than the reference temperature $T < T_r$ while the WLF equation was selected for $T > T_r$. As a reference temperature, we selected a temperature 10 °C lower than the softening point, determined by "ring and ball" method.

Assuming the reference temperature $T_r = (T_{rb} - 10)$, we took into consideration that the glass transition temperature for asphalt T_g is usually about 50–70 °C lower than the softening point T_{rb} (Schmidt and Santucci 1965; Bahia and Anderson 1993), and the WLF equation is intended for temperatures higher than the glass transition temperature. Moreover, the "standard values" of its constants $C_1 = 8.86$ and $C_2 = 101.6$ were determined for the reference temperature $T_r = (T_g + 50)$. Then the WLF equation is valid for the temperatures $(T_g + 100)$ and higher. Therefore, having selected $T_r = (T_{rb} - 10)$, we can with the help of the WLF equation cover the range of summer temperatures for asphalt concrete pavement. On the other hand, Arrhenius's equation should cover the range from $(T_{rb} - 10)$ to low winter temperatures. For penetration indexes from $PI = -3$ to $PI = +2$ with values of difference $(T - T_r)$ from −100 to +140 and a step 10 °C we determined values $a_{T_r}(T)$ based on Van der Poel's data using Eq. (2.9) and found the relationships $E_a(PI)$ and $C_1(PI)$, $C_2(PI)$.

The energy of activation in Arrhenius's equation was expressed as

$$E_a = 9.745 \times 10^4 \frac{3(30+PI)}{5(10+PI)}$$

It has appeared that energy of activation varies within $E_a = 1.56 \times 10^5$ J/mol for $PI = +2$ and $E_a = 2.25 \times 10^5$ J/mol for $PI = -3$. As a comparison, Van der Poel (1954a, b) accepted for asphalts at average $E_a = 50$ kcal/mol $= 2.09 \times 10^5$ J/mol, having selected as a reference temperature $T_r = T_{rb}$. Christensen and Anderson assumed $E_a = 2.5 \times 10^5$ J/mol (Christensen 1992) or $E_a = 2.61 \times 10^5$ J/mol (Christensen and Anderson 1992) at a reference temperature much lower than T_{rb}.

We obtained the following coefficients in WLF equation:

$$C_1 = \frac{1}{0.11 + 0.0077PI}, C_2 = 104.5$$

The first one varies from $C_1 = 7.97$ for $PI = +2$ to $C_1 = 11.5$ for $PI = -3$, and the second one was found to be independent on PI. As a comparison, standard

values, obtained WLF (Ferry 1963), C_1 = 8.86, C_2 = 101.6. Therefore, we obtained such equation for time–temperature shift factor $a_{T_r}(T)$:

– at T $\leq (T_{rb} - 10)$:

$$a_{Tr\,Ahrr}(T) = \exp\left[11720 \cdot \frac{3(30+PI)}{5(10+PI)}\left[\frac{1}{(T+273)} - \frac{1}{(T_{rb}+263)}\right]\right] \quad (2.12a)$$

– at T > $(T_{rb} - 10)$:

$$a_{Tr\,WLF}(T) = \exp\left[-\frac{2.303(T - T_{rb} + 10)}{(0.11 + 0.0077PI)(114.5 + T - T_{rb})}\right] \quad (2.12b)$$

Now the asphalt stiffness modulus as a function of temperature and loading time can be shown as a single curve, if instead of time t the stiffness is plotted versus the reduced time $t_r = t/a_{T_r}(T)$ in X-coordinate. As an example in Fig. 2.3, the points of six curves $S(t)$ for various temperatures T grouped together forming one master curve at reference temperature in Fig. 2.4. This curve coincides with the constructed one according to (2.12a, b). As the result, the time range that is for Fig. 2.3 from 10^{-6} to 10^3s, extended from 10^{-10} to 10^5 s, i.e., it is increased for six decimal orders.

Using Eq. (2.12a, b) for $a_{T_r}(T)$, one can obtain asphalt viscosity at any temperature $\eta(T)$ if it is known at a reference temperature $\eta(T_r)$:

$$\eta(T) = \eta(T_r) \cdot a_{Tr}(T) \quad (2.13)$$

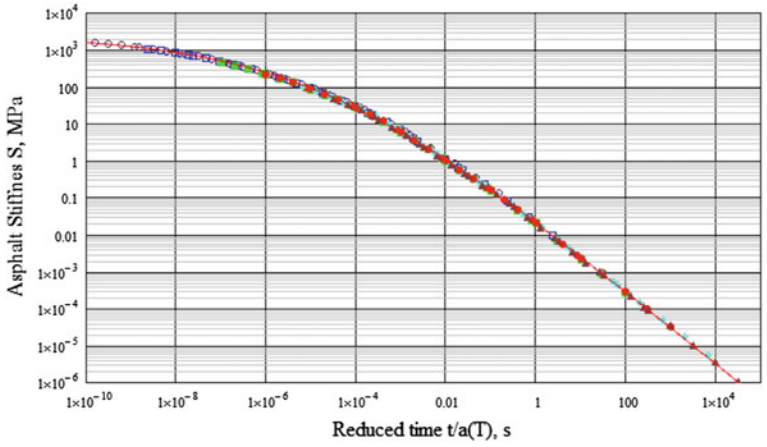

Fig. 2.4 Stiffness modulus of asphalt as a function of time and temperature after reducing to the reference temperature T = T_r: points Van der Poel's data (from Fig. 2.3), continuous curve–calculated from Eq. (2.12a, b) with T_r = 40 °C

Based on Van der Poel's data, we found the following approximate expression for asphalt viscosity at reference temperature

$$\eta(T_r) = 0.00124\left[1 + 71\exp\left[-\frac{12(20 - PI)}{5(10 + PI)}\right]\right] \cdot \exp\left(\frac{0.2011}{0.11 + 0.0077PI}\right) \quad (2.14)$$

Equations (2.13) and (2.12a, b) lead to the following formula for asphalt viscosity as a function of temperature:

$$\eta = a_{Tr\,Ahrr}(T) \cdot \eta(T_r)\,(T \le T_{rb} - 10);\ \eta = a_{Tr\,WLF}(T) \cdot \eta(T_r)\,(T > T_{rb} - 10) \quad (2.15)$$

where viscosity η is in MPa · s, and $a_{T_r\,Ahrr}(T)$, $a_{T_r\,WLF}(T)$, $\eta(T_r)$ are expressed by Eqs. (2.12a, b) and (2.14), respectively.

Asphalt viscosity calculated from Eq. (2.15) as a function of the penetration index and temperature is shown in Fig. 2.5. These curves are in agreement with the curves of SHELL (Molenaar 2005, p. 70) and (Claessen et al. 1977, p. 68).

In Eq. (2.8) for asphalt stiffness, the viscosity η as a function of time and temperature and the instantaneous longitudinal modulus E_g are already known. To obtain the exponent of power β, its value was considered as independent on temperature. In accordance with our assumption regarding applicability of time-temperature superposition principle, time and temperature should be included into formulas for mechanical characteristics of viscoelastic materials only using the ratio $(t/a_{T_r}(T))$. Equation for $\beta(PI)$ was fitted for each value of penetration index ranging from $PI = -3$ to $PI = +2$ within the temperature range $(T - T_{rb})$ from −45 to 10 °C to minimize the quadratic deviation of values $S(t)$, calculated using Eq. (2.8) from Van der Poel's data. The following approximate formula was obtained for the exponent of power as a function of penetration index:

$$\beta = \frac{0.1794}{1 + 0.2084PI - 0.00524PI^2} \quad (2.16)$$

It varies from $\beta = 0.1285$ for $PI = +2$ to $\beta = 0.5476$ for $PI = -3$.

Therefore, a stiffness modulus of asphalt S can be calculated as a function of penetration index, softening point, loading time and temperature using formula (2.8) where $E_g = 2460$ MPa, viscosity η is determined by formula (2.15), and β—by formula (2.16).

For example, for asphalt with the penetration depth $P = 80$ dmm at 25 °C and the softening point $T_{rb} = 50$ °C, penetration index PI = 0 we will obtain S at the temperature 15 °C and load duration 1 s. Using Eq. (2.12a), we calculate value of time–temperature shift factor $a_{T_r}(T)$ from the testing temperature T = 15 °C to the reference temperature $T_r = 40$ °C and obtain $a_{T_r\,Ahrr}(T) = 347.5$. Viscosity at the reference temperature, according to Eq. (2.14) is equal to $\eta(T_r) = 0.01222$ MPa · s. according to Eq. (2.15), viscosity at 15 °C is equal to their product $\eta = 4.25$ MPa · s. The exponent of power from formula (2.16)

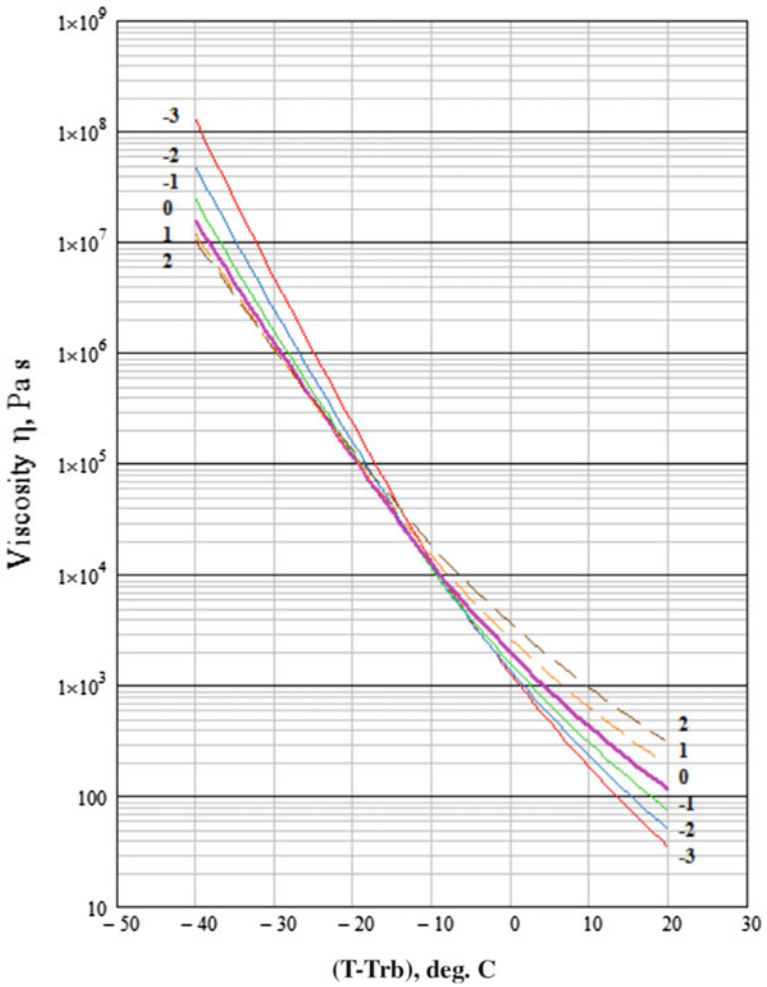

Fig. 2.5 Asphalt viscosity as a function of temperature and penetration index

$\beta = 0.1794$. Finally, the stiffness modulus of asphalt can be calculated from Eq. (2.8):

$$S = 2460\left[1 + \left(\frac{2460 \cdot 1}{3 \cdot 4.25}\right)^{0.1794}\right]^{-\frac{1}{0.1794}} = 2.042\ M\Pi a$$

Program BitProps gives the value $S = 2.107$ MPA, i.e., inaccuracy of our approximate formula is 3% in this example. Calculation results of stiffness modulus for this equation within large range of loading time are shown in Fig. 2.1 with continuous curve. As opposed to the nomograph or to the program BitProps, the operation with obtained equation using such standard programs as Mathcad or

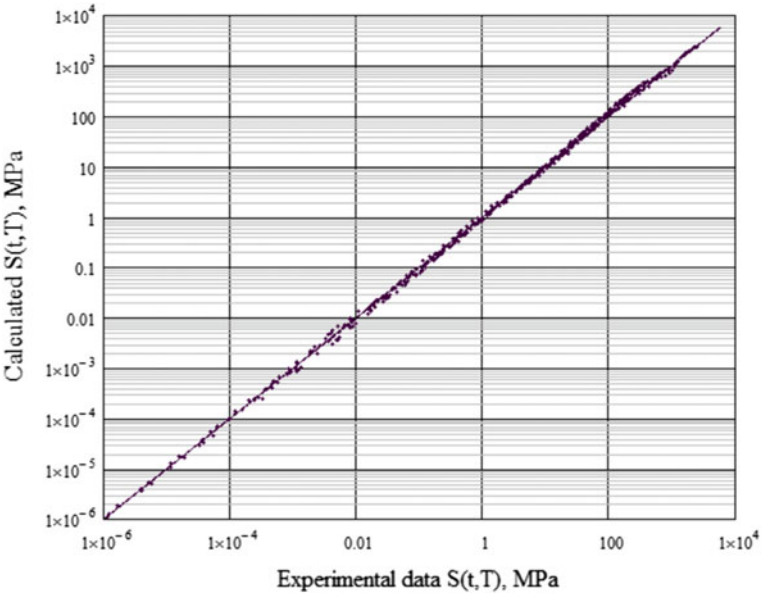

Fig. 2.6 Comparison of stiffness moduli from data of Van der Poel with stiffness moduli calculated using Eq. (2.8): $PI = -3$, 0 and $PI = 1$; T = 5, 15, 30, 40, 50, 60 °C; t = from 10^{-6} to 10^4 c

Excel, the construction of graph like in the Fig. 2.1takes just a few cent seconds. For 1910 points in the range of PI from −3 to +2,$(T - T_{rb})$ from −45 to 10 °C, and t from 10^{-4} to 10^4 s, the coefficient of variation of stiffness calculated using Eq. (2.8) from the Van der Poel's data (program BitPtops) was 14.6% and the coefficient of determination $R^2 = 0.978$. The comparison of stiffness moduli for 540 points calculated using Eq. (2.8) and those taken from Van der Poel's data is shown in Fig. 2.6.

One can analyze a number of practical problems using Eq. (2.8) for stiffness of asphalt. For instance, we can estimate the delayed elastic part of deformation for three types of bitumen having the same softening point T_{rb} = 50 °C, but different penetration: P = 54.5, 80 and 109.5 dmm (penetration indexes $PI = -1$, 0 and 1, respectively).

It is clear that total creep deformation under the constant stress σ at loading time t is $\varepsilon = \sigma/S(t)$. It consists of instantaneous elastic part $\varepsilon_g = \sigma/E_g$, deformation of viscous flow $\varepsilon_{visc} = \sigma t/3\eta$, and delayed elastic deformation ε_{del}. The latter occurs in time and is recoverable. It is not difficult to see that proportion of delayed elastic deformation is equal to

$$c_{del} = 1 - \frac{S(t)}{E_g} - \frac{S(t)t}{3\eta} \tag{2.17}$$

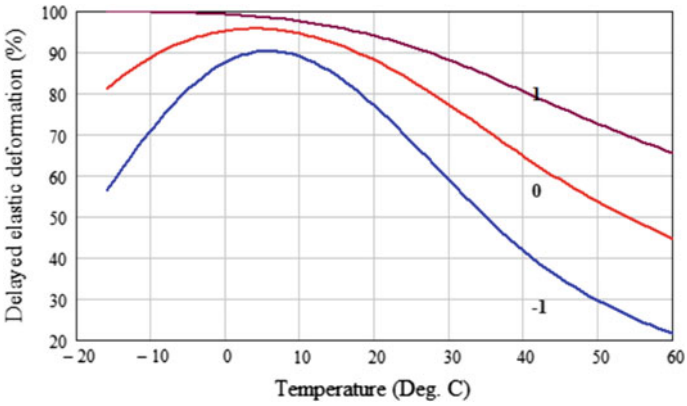

Fig. 2.7 Delayed elastic part of deformation for asphalt with various penetration indexes as the function of temperature: softening point T_{rb} = 50 °C, penetration index is shown on the curves, load duration t = 0.1 s

The results of calculation (Fig. 2.7) show that at loading time t = 0.1 s that is typical for asphalt concrete pavements under a moving load during passage of trucks, asphalts with penetration index −1 and 0 reveal maximum delayed elasticity at temperature about 5 °C—around 45 °C lower than softening point. Such temperature is typical for pavements in spring or late autumn during the periods of high water content in subgrade soil. Portion of delayed elastic deformation reduce with temperature decrease or increase, moreover, very dramatically for asphalt with PI = −1. As for asphalt of lower temperature susceptibility (PI = +1), the portion of its delayed elastic deformation slowly reduces with the increase of temperature and does not have maximum within service temperatures of pavement from −40 to 60 °C. It means that asphalt with high softening point T_{rb} = 50 °C and penetration 109.5 dmm (at 25 °C) keeps an ability to recover deformation at low winter temperatures, which might be important for resistance of asphalt concrete pavement to low temperature cracking.

Equation for stiffness modulus, obtained here will be used in final section of our work for calculation of relaxation modulus of asphalt, its dynamic modulus and asphalt concrete moduli depending on temperature and load duration.

References

Bahia HU, Anderson DA (1993) Glass transition behavior and physical hardening of asphalt binders. J AAPT 62:93–125

Bats FTh (1973) A computer simulation of Van der Poel nomograph. J Appl Chem Biotech 23:139–140

Bonnaure F, Gest G, Gervois A, Uge P (1977) A New method of predicting the stiffness of asphalt paving mixtures. In: Proceedings, Association of Asphalt Paving Technologists, vol 46, pp 64–100

Christensen DW (1992) Mathematical modeling of the linear viscoelastic behavior of asphalt cements. The Pennsylvania State University, Thesis
Christensen D, Anderson D (1992) Interpretation of dynamic mechanical test data for paving grade asphalt cements. J AAPT 61:67–116
Claessen AJM, Edwards JM, Sommer P, Uge P (1977) Asphalt pavement design—the shell method. In: Proceedings, 1977, 4th international conference on the structural design of asphalt pavements, vol 1, Ann Arbor, pp 39–74
Collop A, Cebon D (1995) A parametric study of factors affecting flexible pavement performance. ASCE J Trans Eng 121(6):485–494
Dobson GR (1969) The dynamic mechanical properties of bitumen. J AAPT 38:123–135
Drozdov AD (2001) A model for the viscoelastic and viscoplastic responses of glassy polymers. Int J Solids Struc 38:8285–8304
Ferry J (1963) Viscoelastic properties of polymers. Translation from English. IL, Moscow
Havriliak S, Negami S (1966) Complex plane analysis of α-dispersions in some polymer systems. J Polym Sci, Part C: Polymer Symposium 14:99
Heukelom W, Klomp AJ (1964) Road design and dynamic loading. In: Proceedings of the Association of Asphalt Paving Technologists, vol 33, pp 92–123
Huang Yang H (1993) Pavement analysis and design. Prentice Hall Inc, New Jersey
Lesuer D, Gerard J-F, Claudy P, Letoffe J-M, Planche J-P, Martin D (1997) Relationships between the structure and the mechanical properties of paving grade asphalt cements. J AAPT 66: 486–505
Marasteanu MO, Anderson DA (1999) Improved model for bitumen rheological characterization. Eurobitumen workshop on performance related properties for Bituminous Binders, vol 133, Luxembourg, May
Molenaar A (2005) Lecture notes road materials. Part III, Delft
Pfeiffer JPh, Van Doormal PM (1936) The rheological properties of asphaltic bitumens. J Inst Petr Tech USA:414–440
Roberts F, Kandhal P, Brown E, Lee D, Kennedy T (1996) Hot mix asphalt materials, mixtures, and construction. National Asphalt Pavement Association, Lanham, MD
Saal RN (1955) Mechanical testing of asphaltic bitumen. In: 4th world petroleum congress, Rome, Section VI/A, Paper 3, pp 1–17
Schmidt RJ, Santucci LE (1965) A practical method for determining the glass transition temperature of asphalts and calculation of their low temperature viscosities. J AAPT 35:61–85
Shahin MY (1977) Design system for minimizing asphalt concrete thermal cracking. In: Proceedings of 4th international conference on the structural design of asphalt pavements, Ann Arbor, University of Michigan, pp 920–932
The SHELL Bitumen Handbook (2003) 5th ed. Thomas Telford Ltd, London
Ullidtz P, Larsen BK (1984) Mathematical model for predicting pavement performance. Transportation Research Record, pp 45–54
Ullidtz P, Peattie KR (1980) Pavement analysis by programmable calculators. ASCE J Trans Eng 106:581–597
Van der Poel C (1954a) A general system describing the viscoelastic properties of bitumens and its relation to routine test data. J Appl Chem 4:221–236
Van der Poel C (1954b) Representation of rheological properties of bitumens over a wide range of temperature and loading times. In: Proceedings of 1st international congress of rheology, vol 2. Butterworth's Scientific Publications, London, pp 331–337

Chapter 3
Relaxation Modulus and Complex Modulus

Abstract The main purpose of this chapter is to relate the relaxation modulus of bitumen through its stiffness modulus with the penetration index and the softening point of asphalt. In this chapter, the equations are derived for numerical and analytical evaluation of relaxation modulus and complex modulus of asphalt based on its stiffness modulus. An enhanced Hopkins-Hamming algorithm was proposed and applied for numerical converting the creep compliance based on stiffness to relaxation modulus of binder. The recursive formula for converting the creep compliance to relaxation modulus was derived which is applicable not only for bitumen but also for polymer modified binders. This chapter also describes the derivation of approximate analytical equation to predict the relaxation modulus of bitumen as a function of its penetration index, softening point, time and temperature. This chapter discusses different equations obtained for evaluation of dynamic modulus and phase angle for asphalt as a function of frequency of loading and temperature based on its penetration and softening point. Good agreement of predicted dynamic modulus, phase angle, and relaxation spectrum of bitumen with test data is illustrated. Method of conversion from the measured dynamic modulus of bitumen to its relaxation modulus was proposed.

The first chapter discussed various rheological characteristics of viscoelastic properties of asphalt: creep compliance $J(t)$ or $D(t)$, relaxation modulus $G(t)$ or $E(t)$, complex (or dynamic) modulus $|G^*(\omega)|$ or $|E^*(\omega)|$, as well as stiffness modulus $S(t)$, and it was shown that they were interrelated. In the second chapter, asphalt stiffness modulus $S(t)$ was expressed as a function of loading time, temperature, its penetration and softening point based on Van der Poel's test data. Meanwhile one can process other similar test data by the proposed method.

Practically, it is a relaxation modulus $G(t)$ or $E(t)$, which is the most required characteristic of viscoelastic properties in practice. When we say, for example, that calculated modulus of elasticity for dense asphalt concrete is equal to 6000 MPa, we imply that asphalt concrete longitudinal relaxation modulus at a loading time of

B. Radovskiy and B. Teltayev, *Viscoelastic Properties of Asphalts Based on Penetration and Softening Point*, Structural Integrity 2,
https://doi.org/10.1007/978-3-319-67214-4_3

0.1 s and at the temperature of 0 °C $E(t) = E(t = 0.1) = 6000$ MPa. It depends mainly on asphalt relaxation modulus and asphalt concrete porosity. The main purpose of this chapter is to relate the asphalt relaxation modulus through its stiffness modulus with the penetration and the softening point of asphalt. In this chapter, we derive equations for numerical and analytical evaluation of relaxation modulus and complex modulus of asphalt based on its stiffness modulus. We will show how to obtain the relaxation modulus from experimental data for dynamic modulus by testing under cyclic load.

3.1 Asphalt Creep Compliance

We described above the asphalt stiffness modulus $S(t) = \sigma_c/\varepsilon(t)$ by formula of Gavrilyak-Negami (or Christensen-Anderson—CA model)

$$S = E_g\left[1 + \left(\frac{E_g t}{3\eta}\right)^{\beta}\right]^{-\frac{1}{\beta}} \tag{3.1}$$

and ascertained that the Van Der Poel's nomograph for determination of S can be described by using for η and β the following expressions:

$$\eta = a_{Tr\,Ahrr}(T)\cdot\eta(T_r) \quad (T \le T_{rb} - 10);\ \eta = a_{Tr\,WLF}(T)\cdot\eta(T_r) \quad (T > T_{rb} - 10) \tag{3.2}$$

$$\eta(T_r) = 0.00124\left[1 + 71\exp\left[-\frac{12(20 - PI)}{5(10 + PI)}\right]\right]\cdot\exp\left(\frac{0.2011}{0.11 + 0.0077PI}\right) \tag{3.3}$$

$$a_{Tr\,Ahrr}(T) = \exp\left[11720\cdot\frac{3(30 + PI)}{5(10 + PI)}\left[\frac{1}{(T + 273)} - \frac{1}{(T_{rb} + 263)}\right]\right] \tag{3.4}$$

$$a_{Tr\,WLF}(T) = \exp\left[-\frac{2.303(T - T_{rb} + 10)}{(0.11 + 0.0077PI)(114.5 + T - T_{rb})}\right] \tag{3.5}$$

$$\beta = \frac{0.1794}{1 + 0.2084PI - 0.00524PI^2} \tag{3.6}$$

In these formulas: is the asphalt stiffness modulus [MPa]; E_g is instantaneous elastic modulus, which can be assumed for all asphalts as $E_g = 2460$ МПа; η is a viscosity [MPa s]; $\eta\,(T_r)$ is the viscosity at the temperature $T_r = (T_{rb} - 10)$; $a_{T_r\,Ahrr}(T)$ is function of time-temperature shift at the temperature $T \le T_{rb} - 10$; $a_{T_r\,WLF}(T)$ is the same at $T > T_{rb} - 10$; T_{rb} is a softening point under "ring and

ball" method, [°C]; *PI*- penetration index for asphalt $PI = (20 - 500A)/(1 + 50A)$; $A = (\log(800/P))/(T_{rb} - 25)$ is a temperature susceptibility; P is a penetration depth at 25 °C [dmm]; t- load duration[s]; T- temperature [°C].

To compute from the formulas (3.1)–(3.6) the stiffness modulus of asphalt as a function of temperature and time, one needs two standard properties of asphalt: T_{rb} and P. Within the range of penetration index from $PI = -3$ to $PI = +2$, the temperature difference $(T - T_{rb})$ from −45 to 10 °C and time t from 0.0001 to 10,000 s the coefficient of variation of values S calculated using Eq. (3.1) from Van der Poel's data is at average 14.6%. Formulas (3.1)–(3.6) were determined for road asphalts, as they were based on Van der Poels' tests (1954). They are not intended for the polymer-modified asphalts, as standard properties of asphalt T_{rb} and P are not quite applicable to modified asphalts. The range of temperatures and load durations, for which we constructed Eqs. (3.2)–(3.6) for η and β, was limited by Van der Poel's nomograph and his data. For example, for asphalt with $PI = -3$ and $T_{rb} = 50$ °C at the temperature $T = -30$ °C, we have data for S only at $t > 300$ s.

By definition, creep compliance of viscoelastic material $D(t) = \varepsilon(t)/\sigma_c$, is the inverse of stiffness modulus: $D(t) = 1/S(t)$. Therefore, according to Eq. (3.1), the longitudinal creep compliance for asphalt is

$$D(t) = \frac{1}{E_g}\left[1 + \left(\frac{E_g t}{3\eta}\right)^{\beta}\right]^{\frac{1}{\beta}} \tag{3.7}$$

and shear creep compliance [considering expression (1.23)]–is three times greater

$$J(t) = \frac{3}{E_g}\left[1 + \left(\frac{E_g t}{3\eta}\right)^{\beta}\right]^{\frac{1}{\beta}} = \frac{1}{G_g}\left[1 + \left(\frac{G_g t}{\eta}\right)^{\beta}\right]^{\frac{1}{\beta}} \tag{3.8}$$

where $G_g = E_g/3$—instantaneous shear modulus $G_g = 820$ MPa.

For example, we will determine from formula (3.8) a shear creep compliance for asphalt, which has a penetration $P = 80$ dmm, and softening point $T_{rb} = 50$ °C (penetration index $PI = 0$), at the temperature 15 °C. From Eq. (3.6) $\beta = 0.1794$. From the first formula (3.2) asphalt viscosity at 15 °C is equal to η = 4.247 MPa s. From Eq. (3.8), we obtain creep compliance (Fig. 3.1):

$$J(t) = \frac{1}{820}\left[1 + \left(\frac{820 \cdot t}{4.247}\right)^{0.1794}\right]^{\frac{1}{0.1794}} \tag{3.9}$$

Asymptotes for the curve in Fig. 3.1 correspond to pure elastic deformation of asphalt and its viscous flow.

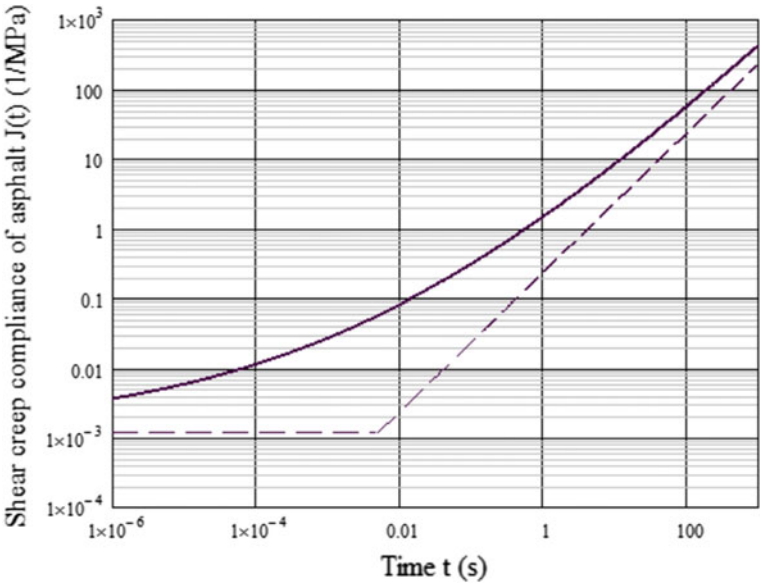

Fig. 3.1 Typical curve of the shear creep compliance as a function of the loading time at constant temperature

3.2 Asphalt Relaxation Modulus

Moduli of longitudinal $E(t)$ and shear $G(t)$ relaxation play the same key role for viscoelastic material, as they play for elastic one at the tension E or at the shear G. Particularly, speaking about dependence of asphalt concrete modulus on temperature and load duration, we usually have in mind exactly $E(t)$ at various T.

First, we will show how to calculate the relaxation modulus of asphalt, based on its creep compliance [for example, obtained under formulas (3.7) or (3.8)], and propose a recursive formula for its calculation with required accuracy. Second, we will derive an equation for predicting the relaxation modulus of asphalt based on its standard properties T_{rb} and P.

3.2.1 Recursive Formula for Relaxation Modulus

As it was described in the first chapter, the relationship between stresses, strains and time in tension or compression is expressed by Boltzmann relations (Ferry 1980; Tschoegl 1989):

$$\varepsilon(t) = \int_0^t D(t-\tau)\frac{\partial\sigma(\tau)}{\partial\tau}\partial\tau \tag{3.10}$$

$$\sigma(t) = \int_0^t E(t-\tau)\frac{d\varepsilon(\tau)}{d\tau}d\tau \tag{3.11}$$

For shear, these formulas look alike, but they contain angular deformation γ instead of longitudinal strain ε, shearing stress instead of normal stress, shearing creep compliance $J(t)$ instead of longitudinal creep compliance $D(t)$ and shearing relaxation modulus $G(t)$ instead of longitudinal relaxation modulus $E(t)$.

Therefore, if any relation was established between longitudinal creep compliance $D(t)$ and relaxation modulus $E(t)$, then a similar relation will be valid between shearing creep compliance $J(t)$ and relaxation modulus $G(t)$. Meanwhile, existence of relationship between $D(t)$ and $E(t)$ is obvious because the both parts of Eqs. (3.10) and (3.11) contain the same stresses and deformations. Traditionally, the relationship between $D(t)$ и $E(t)$ is derived by Laplace transformation (Tschoegl 1989; Hopkins and Hamming 1957), but we will determine it more illustratively. Let us consider deformation of material at constant strain rate. At constant strain rate r_e (where r_e is a specified rate of relative deformation), the strain is proportional to time $\varepsilon(t) = r_e t$. Substituting into Eqs. (3.10) and (3.11) leads to

$$r_e t = \int_0^t D(t-\tau)\frac{\partial\sigma(\tau)}{\partial\tau}d\tau, \quad \sigma(t) = r_e\int_0^t E(t-\tau)d\tau$$

After differentiation of the latter equation $d\sigma\ (t)/dt = r_e E(t)$ and substitution of the result into previous one, we obtain

$$\int_0^t D(t-\tau)E(\tau)d\tau = t \tag{3.12a}$$

$$\int_0^t D(\tau)E(t-\tau)d\tau = t \tag{3.12b}$$

The second Eq. (3.12a, b) immediately results from the previous one after change of variable $x = t - \tau$. Although we derived Eq. (3.12a, b), considering constant strain rate loading regime, it establishes common relation between the longitudinal creep compliance and the relaxation modulus independent on loading regime. So, if we know longitudinal creep compliance $D(t)$, then the values of relaxation modulus $E\ (t)$ can be obtained numerically by solving the Eq. (3.12a, b).

As we mentioned above, it is possible to obtain similar relation between the shearing creep compliance $J(t)$ and the shearing relaxation modulus $G(t)$:

$$\int_0^t J(t-\tau)G(\tau)d\tau = t \tag{3.13a}$$

$$\int_0^t J(\tau)G(t-\tau)d\tau = t \tag{3.13b}$$

If one knows the shearing creep compliance $J(t)$ in the form of the table or empiric formula, then the shearing relaxation modulus $G(t)$ can be obtained numerically by solving Eq. (3.13a, b).

The first recurrent formula for solving equations like (3.12a, b) was proposed by Hopkins and Hamming (1957), and some years later it was used by C. Monismith and K. Secor for analysis of rheological properties of asphalt (Secor and Monismith 1964). It was of essential interest, as the test with constant stress is simpler than the test with constant deformation, and one can calculate the relaxation modulus $E(t)$ from creep compliance $D(t)$ data.

As is known, the recursive formula expresses the next term of sequence using of the preceding terms. In this case, based on values of $D(t)$ at the specified moments of time t, sequence of $E(t)$ values was calculated in those moments.

Hopkins and Hamming (1957) divided the convolution integral in Eq. (3.12a) (3.12b) into a finite number of subintervals. In each subinterval, the target function is approximated to be constant. Hopkins and Hamming took the average value of the target function outside the integral sign (it complies with the rectangle method), supposing that those intervals were short, and obtained their recursive relation. Hopkins-Hamming's algorithm included a numerical calculation of integrals according to those intervals on each stage of calculation using a recursive relation. Calculation of integrals slowed down the calculations of the target function and required at that time using of main frame computer. Therefore, Monismith and Secor developed Fortran-program for calculations (1964). Tschoegl (1989) replaced the integrals in Hopkins-Hamming's formula by calculation with trapezium rule, which expedited calculation, but created an additional source for numerical error inherent in each conversion (Mead 1994).

The Hopkins-Hamming's algorithm is widely used in road literature for analysis the properties of bitumen binders (Bouldin et al. 2000; Marasteanu 2010; Bahia et al. 2000), etc. Moreover, the recursive Hopkins-Hamming formula is included into the standard specifications for asphalt binders: ASTM D 6816-02 and AASHTO PP 42-07. Therefore, if it is possible to improve this formula, then it makes sense.

We will derive a formula based on idea of Hopkins and Hamming, but more efficient in our opinion. We will start not from the Eq. (3.12a, b), but from the similar equation

$$D(0)E(t) + \int_0^t D'(t-\tau)E(\tau)d\tau = 1 \tag{3.14}$$

Equation (3.14) is easy to derive by differentiating the Eq. (3.12a, b) with respect to t, or directly from Boltzmann's relations (3.10), (3.11). The derivative of creep compliance is included into integrand of (3.14)

$$D'(t-\tau) = \frac{dD(t-\tau)}{d(t-\tau)}$$

We will also need the integral along the segment [a, b]:

$$\int_a^b D'(t-\tau)d\tau = D(t-a) - D(t-b) \tag{3.15}$$

Let us consider Eq. (3.14) from which we should obtain the target values $E(t)$ at the moments t_m according to the source values of $D(t)$ on segment $0 < t < t_m$. We divide it into intervals by points t_i (where $i = 0, 1, 2 \ldots m-1, m$). The integral in (3.14) we rewrite as a sum of integrals

$$D(0)E(t_m) + \int_0^{t_m} D'(t_m-\tau)E(\tau)d\tau = D(0)E(t_m) + \sum_{i=1}^{m} \int_{t_{i-1}}^{t_i} D'(t_m-\tau)E(\tau)d\tau = 1$$

Taking the average value of $E(\tau)$ from under the integral sign gives

$$D(0)E(t_m) + \sum_{i=1}^{m} \frac{1}{2}(E(t_{i-1}) + E(t_i)) \int_{t_{i-1}}^{t_i} D'(t_m-\tau)d\tau = 1$$

According to (3.15), the integrals in the last equation can be taken exactly:

$$D(0)E(t_m) + \sum_{i=1}^{m} \frac{1}{2}(E(t_{i-1}) + E(t_i))[D(t_m - t_{i-1}) - D(t_m - t_i)] = 1 \tag{3.16}$$

Separating the last (m-th) term of the sum in (3.16) and denoting for convenience $E(t_i) = E_i$:

$$D(0)E_m + \frac{1}{2}(E_{m-1} + E_m)[D(t_m - t_{m-1}) - D(0)] + \sum_{i=1}^{m-1} \frac{1}{2}(E_{i-1} + E_i)[D(t_m - t_{i-1}) - D(t_m - t_i)] = 1$$

Solving this equation for E_m, we obtain the recursive formula

$$E_m = \frac{2 - E_{m-1}[D(t_m - t_{m-1}) - D(0)] - \sum_{i=1}^{m-1} (E_{i-1} + E_i)[D(t_m - t_{i-1}) - D(t_m - t_i)]}{D(0) + D(t_m - t_{i-1})} \tag{3.17}$$

We did not specify the character of dividing the segment $0 < t < t_m$ into subintervals $[t_{i-1}, t_i]$. If the interval of integration spans over several logarithmic decades of time, it is convenient to equally space the points t_i on the $\log(t)$-axes.

Considering, that t_0 и t_1 occur under summation sign in (3.17) with $i = 1$, the values for relaxation function E are required in these moments to start the calculation procedure. First, it is required to set the value for instantaneous modulus, which is equal to reversible instantaneous creep compliance.

$$E_0 = 1/D(0) \tag{3.18}$$

Second, the value for relaxation modulus E_1 is required at the initial moment t_1. It can be obtained from the same recursive formula (3.17):

$$E_1 = \frac{3 - D(t_1)/D(0)}{D(0) + D(t_1)} \tag{3.19}$$

The Eqs. (3.18) and (3.19) are starting values for recursive formula (3.17). From (3.19), one can see that ratio $D\,(t_1)/D(0)$ should not exceed 3. It is advisable to select the first point t_1 so that it could not exceed 1.5. According to this and other reasons, it is more convenient to work not with the data table of creep compliance, but with approximate equation for $D(t)$ that smoothes the test data.

Note that functions $D(t)$ and $E(t)$ are included into the basic Eq. (3.12a, b) symmetrically, i.e. they are permuted. Therefore, although we obtained the formula (3.17) with the purpose of determination for relaxation modulus $E(t)$ from creep compliance $D(t)$, the same formula can be used by interchanging the two functions for determination of $D(t)$ from $E(t)$.

As it was mentioned above, if some dependence is established between creep compliance $D(t)$ and relaxation modulus $E(t)$ at tension, similar dependence can be formulated between creep compliance $J(t)$ and relaxation modulus $G(t)$ in shear.

Therefore, similar to (3.17) we have the same recursive formula for calculation of relaxation modulus in shear $G(t)$:

$$G_m = \frac{2 - G_{m-1}[J(t_m - t_{m-1}) - J(0)] - \sum_{i=1}^{m-1}(G_{i-1} + G_i)[J(t_m - t_{i-1}) - J(t_m - t_i)]}{J(0) + J(t_m - t_{i-1})} \tag{3.20}$$

with starting values

$$G_0 = 1/J(0), \quad G_1 = \frac{3 - J(t_1)/J(0)}{J(0) + J(t_1)} \tag{3.21}$$

Formulas (3.17), (3.20), in contrast to Hopkins-Hamming algorithm (1957), do not require the calculations of integrals, and a refusal from their calculation is not related with the error accumulation due to repeated applying the trapezoidal rule to compute the integrals as in formula of Tschoegl (1989, p. 405). We tested our formulas (3.17) and (3.20) on a very stiff example of Maxwell's model, where with on the time interval from 0.1 to 10 s the source creep compliance increased in 11 times while the target relaxation modulus reduced in 22,000 times. As the exact equations for the source function $J(t)$ and for the target function $G(t)$ are known for Maxwell's model, we could compare them with the results of calculation from our formula (3.20). Calculations showed that inaccuracy increases linearly with increase of t and is inversely proportional to the squared number of subintervals into which the interval of integration from 0 to t is divided. The calculation by formula (3.20) showed the highest inaccuracy of 0.09% with the number of subintervals of 100 in the each logarithmic decade of time variation.

To illustrate, we will calculate the shearing relaxation modulus $G(t)$ for asphalt with penetration of $P = 80$ dmm at 25 °C and softening temperature $T_{rb} = 50$ °C (penetration index $PI = 0$), at the temperature of 15 °C. Let us proceed from creep compliance, which is expressed by Eq. (3.9) and shown in Fig. 3.1.

We set $G_0 = 1/J(0) = 820$ MPa for zero moment $t_0 = 0$ under (3.21), that is we assumed the instantaneous elastic shearing modulus equal to one third of instantaneous longitudinal modulus of asphalt $E_g = 2460$ MPa. We selected $t_1 = 10^{-9}$s as an initial time, and $t_1 = 1000$ s as a final time. We selected only 5 points for logarithmic decade, because with larger number they run into one another and look like continuous curve in the graph. Time moments were defined by formula $t_i = t_{i-1} \cdot 10^{1/5}$, so that they are equally spaced on the $\log(t)$-axes. The results of calculations from Eq. (3.20) are shown in Fig. 3.2. Run time of calculations on the desktop of average capacity in MathCAD package was only 0.05 s.

As we obtain formulas (3.17) and (3.20) based on common relations of linear viscoelastic theory, they are applicable not only for asphalts, but for other viscoelastic materials, which may have the curves of creep compliance and the relaxation modulus not so smooth as in Figs. 3.1 and 3.2.

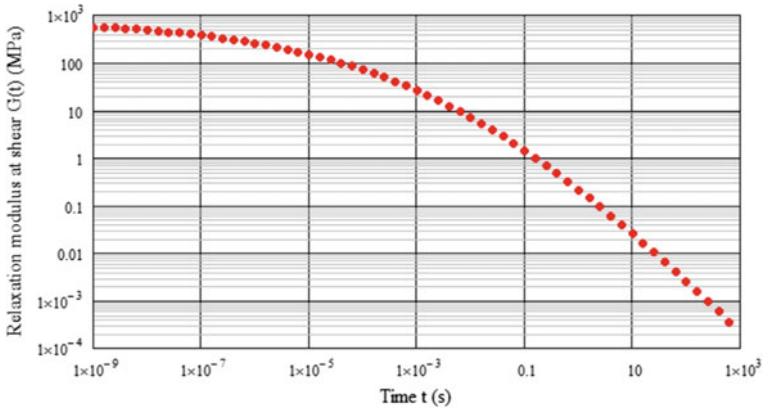

Fig. 3.2 Relaxation modulus of asphalt at shear calculated by formula (3.20) from the creep compliance shown in Fig. 3.1

For example, we took the experimental data from the work of Baumgaertel and Winter (1989) regarding the creep compliance of the mixture 1:1 of two polystyrenes with molecular weight of 125,000 and 750,000 at the temperature 180 °C (Schausberger 1986). Based on a certain creep compliance $J(t)$ (Table 1 in work Baumgaertel and Winter 1989), we calculated the shearing relaxation modulus $G(t)$ for the blend of those polystyrenes from Eq. (3.20). In the range from $t_1 = 10^{-4}$c to 100c, we accepted 50 points for each logarithmic decade—totally 300 time moments. All calculations took 0.5 s using MathCAD package. Obtained values of $G(t)$ at those moments are shown in Fig. 3.3 with red points (they run one into another), and authors' data (Baumgaertel and Winter 1989)—with continuous blue curve. Highest relative inaccuracy of calculated values of $G(t)$ within the range of 0.0001 s and 100 s did not exceed 0.4%.

Together with glass transition region onto horizontal plateau at small t (in the left part of blue curve), two rubber transition regions occur closer to its medium part, which is explained in (Schausberger 1986) by presence of two polymers with different length of molecule in the blend (Fig. 3.3). The wavy shape of the curve $G(t)$ is also typical for the polymer-modified asphalts. From the comparison of the calculated $G(t)$, and the curve shown in the work (Baumgaertel and Winter 1989), one can draw the conclusion that formulas (3.17) and (3.20) are applicable [in contrast to the formulas (3.1)–(3.6)] not only for asphalts, but also for polymer modified binders.

3.2.2 *Approximate Formulas for Relaxation Modulus*

Though recursive relations (3.17) and (3.20) are efficient for numerical calculation of relaxation modulus from creep compliance, it is practically more convenient to

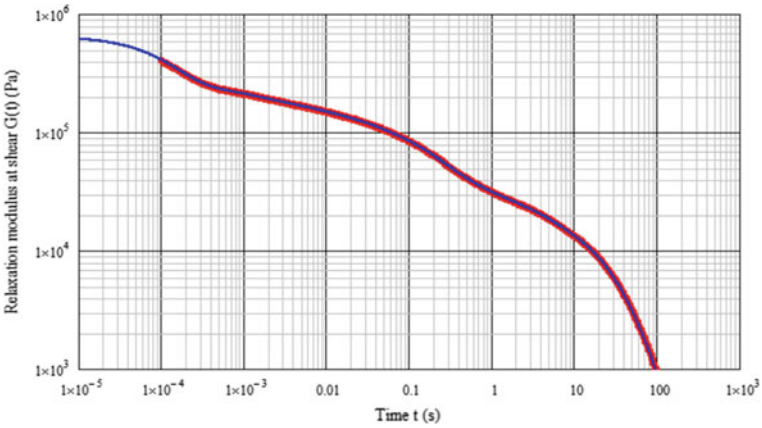

Fig. 3.3 Comparison of shear relaxation modulus calculated from formula (3.20) (*red points*) with shown in the work Baumgaertel and Winter 1989 (*blue line*)

have a formula for determination the relaxation modulus of asphalt directly based on its standard characteristics T_{rb} and P, which does not require carrying-out of test for creep compliance.

In particular, the equation for relaxation modulus $E(t)$ can be derived from creep compliance $D(t)$ of the power-law body

$$D(t) = \frac{1}{a}\left(\frac{t}{d}\right)^m \tag{3.22}$$

where a, d, m—constants, and $0 < m < 1$. We obtain relaxation modulus for such material based on the same Eq. (3.14) that we used above for derivation of recursive formula (3.17).

As a first approximation $E(t) \approx 1/D(t)$, and we can try to apply power-law relaxation modulus in (3.14)

$$E(t) = a\left(\frac{t}{d}\right)^{-m} \tag{3.23}$$

Differentiating

$$D'(t-\tau) = \frac{dD(t-\tau)}{d(t-\tau)} = \frac{m}{ad^m}t^{m-1}$$

And substituting the derivative in the Eq. (3.14), we will have its left part in the form of

$$D(0)E(t) + \int_0^t D'(t-\tau)E(\tau)d\tau = \int_0^t (t-\tau)^{m-1}\tau^{-m}d\tau = \frac{\pi m}{\sin(\pi m)},$$

Here we used the integral 855.51 from (Dwight G 1966), which is valid for—$1 < m < 1$. Instead of expression $\pi m/\sin(\pi m)$, we had to obtain the left part of equality (3.14) equal to one. Therefore, it is not the Eq. (3.23), which actually corresponds to creep compliance of (3.22) kind, but it is a relaxation modulus exactly in the form of expression (3.24):

$$E(t) = \frac{\sin(\pi m)}{\pi m}\, a \left(\frac{t}{d}\right)^{-m} \tag{3.24}$$

Obviously, expressions (3.22) and (3.24) transform equality (3.14) into identity.

Formula of G. Lederman (3.24) was given in (Leaderman 1958) without derivation, and it was re-derived many times using Laplace's transformation in the works (Schwarzl and Struik 1968; Schapery and Park 1999, etc.). Actually, there are not any materials with the power law creep compliance (3.22) and relaxation modulus expressed by (3.24) because the viscoelastic materials have a non-zero creep compliance and tend to finite value of relaxation modulus with tendency of time duration to zero. The Eqs. (3.22) and (3.24) are used to describe the so-called critical gel response close to sol-gel transformation point (Baumgaertel and Winter 1989; Winter and Chambon 1986).

However, it turns out that thanks to idea of Ferry and Williams (1952), the power-law functions for $D(t)$ and $E(t)$ open an opportunity for obtaining of approximate formulas for conversion of creep compliance into relaxation modulus and vice versa. Their idea is in the fact that the graphs of power-law function (3.22) and (3.24) in logarithmic coordinates $\log(D) - \log(t)$ or $\log(E) - \log(t)$ are straight lines with a slope m to $\log(t)$-axis, and any curve $D(t)$ and $E(t)$ can be approximated by set of segments with variable slope. The approximate formula of conversion from creep compliance into relaxation modulus results from (3.22) and (3.24):

$$E(t) = \frac{\sin(\pi m)}{\pi m}\frac{1}{D(t)} \tag{3.25}$$

and similarly at shear

$$G(t) = \frac{\sin(\pi m)}{\pi m}\frac{1}{J(t)} \tag{3.26}$$

where for optional curves $D(t)$ a slope m is determined as

$$m = \frac{d\,\log(D(t))}{d\,\log(t)} = \frac{t}{D(t)}\frac{d\,D(t)}{d\,t} \tag{3.27}$$

and similarly at shear

$$m = \frac{d\ \log(J(t))}{d\ \log(t)} = \frac{t}{J(t)}\frac{dJ(t)}{dt} \tag{3.28}$$

Equations (3.25) and (3.26) for an arbitrary source functions $D(t)$ or $J(t)$ are applicable when $0 < m < 1$, but already with $m > 0.5$ those equations lead to appreciable inaccuracy.

Now, based on the formula for the shearing creep compliance of asphalt (3.8) and on the Lederman's Eq. (3.26), it is possible to write the following approximate equation for the shearing relaxation modulus of asphalt:

$$G(t) = \frac{\sin(\pi m)}{\pi m} G_g \left[1 + \left(\frac{G_g t}{\eta}\right)^{\beta}\right]^{-\frac{1}{\beta}} \tag{3.29}$$

where m is determined by differentiation of the Eq. (3.8) by formula (3.28):

$$m = \frac{\left(G_g t/\eta\right)^{\beta}}{1 + \left(G_g t/\eta\right)^{\beta}} \tag{3.30}$$

Here η and β are already expressed using the standard penetration index and the softening point of asphalt by formulas (3.2) and (3.6).

For instance, let us calculate the relaxation modulus $G\ (t)$ by formula (3.29) for bitumen, which has a penetration $P = 80$ dmm and a softening point $T_{rb} = 50$ °C (penetration index $PI = 0$) at 25 °C, at the temperature 15 °C. Formula (3.6) gives $\beta = 0.1794$. Using Eq. (3.2) we obtain the viscosity $\eta = 4.247$ MPa s. Glassy modulus at shear is equal to $G_g = E_g/3 = 820$ MPa. The results of calculation by formula (3.29) are shown in Fig. 3.4 (continuous curve) and they are in agreement with relaxation modulus calculated using our recursive relation (3.20) (points).

A comparison demonstrates that the approximate Eq. (3.29) gives good results, though slightly overestimate the values of relaxation modulus: at $t = 0.01$ s—for 3.5%, at $t = 0.1$ s—for 5%, and at $t = 10$ s—for 12%, meanwhile in the last case the slope m is equal to $m = 0.795$, i.e. it is already close to 0.80.

We will derive one more formula for relaxation modulus, which is much more convenient in our opinion. We obtained that formula during analysis of empirical equation for shearing relaxation modulus of asphalt that was proposed by Marasteanu and Anderson (1999) (Christensen, Anderson, and Marasteanu—CAM model):

$$G(t) = G_g \left[1 + \left(\frac{G_g t}{\eta}\right)^{b}\right]^{-\frac{k}{b}} \tag{3.31}$$

Proposing it, the authors of Marasteanu and Anderson (1999) asserted that comparing with the formula like (3.7) or (3.8), which contained three parameters

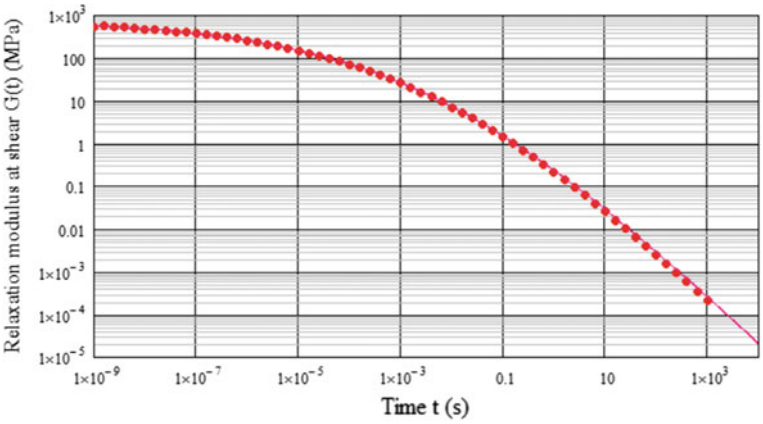

Fig. 3.4 Relaxation modulus of asphalt at shear calculated by formula (3.20) (points) and (3.29) (*red curve*) based on creep compliance shown in the Fig. 3.1

(G_g, η and β), Eq. (3.31) had one more additional parameter k, which was not dependent on others, and it will allow to fit the test data more accurately. In fact, as it is known, the integral over the relaxation modulus of a liquid is the zero shear Newtonian viscosity (Ferry 1980, p. 70, formula (51)):

$$\int_0^\infty G(t)dt = \eta \tag{3.32}$$

Substituting the expression (3.31) into (3.32) and replacing the variable of integration $t = \eta x/G_g$ leads to equality

$$\eta \int_0^\infty \left[1 + x^b\right]^{-\frac{k}{b}} dx = \eta,$$

from which it follows that the integral in the left part should be equal to one. This integral is known (Sayegh 1963, 3.241.4) and with $b > 0$, $k > 1$ it is equal to

$$\int_0^\infty \left[1 + x^b\right]^{-\frac{k}{b}} dx = \frac{1}{b} \cdot \frac{\Gamma\left(\frac{1}{b}\right)\Gamma\left(\frac{k-1}{b}\right)}{\Gamma\left(\frac{k}{b}\right)} \tag{3.33}$$

where $\Gamma(x)$ is gamma-function, for which the detailed tables are available. Right part of the Eq. (3.33) is equal to one if $k = 1 + b$. Thus, it follows that the parameter k of the Eq. (3.31), proposed in the work Marasteanu and Anderson

1999, actually is not independent fitting constant but it is related with the power exponent b by simple formula $k = 1 + b$.

This leads to the following formula for relaxation modulus at shear:

$$G(t) = G_g \left[1 + \left(\frac{G_g t}{\eta} \right)^b \right]^{-\left(1+\frac{1}{b}\right)} \tag{3.34a}$$

and similarly for longitudinal relaxation modulus

$$E(t) = E_g \left[1 + \left(\frac{E_g t}{3\eta} \right)^b \right]^{-\left(1+\frac{1}{b}\right)} \tag{3.34b}$$

To relate the parameter b and the penetration index of asphalt we will consider a moment $t_0 = \eta / G_g$ and will use an approximate formula (3.29). A slope of the curve for creep compliance from Eq. (3.30) equals to $m = 1/2$ and the formula (3.29) for this time moment has inaccuracy less than 3%. At $t = t_0$ formula (3.29) leads to relaxation modulus

$$G(t_0) = \frac{2}{\pi} G_g 2^{-\frac{1}{\beta}}$$

while from the formula (3.34a, b) it is equal to

$$G(t_0) = G_g 2^{-\left(1+\frac{1}{b}\right)}$$

Having compared the last two equations we obtain the relation between b and β:

$$b = \frac{1}{\frac{1}{\beta} + \frac{\ln(\pi)}{\ln(2)} - 2} \tag{3.35}$$

where β is already expressed in terms of penetration index by formula (3.6).The value of β varies from $\beta = 0.1285$ at PI = +2 to $\beta = 0.5476$ at $PI = -3$, and value b varies from $b = 0.1346$ at PI = +2 to $b = 0.6767$ at PI = −3.

For instance, let us calculate the relaxation modulus $G(t)$ by formula (3.34a, b) for bitumen, which has a penetration $P = 80$ dmm and a softening point $T_{rb} = 50$ °C (penetration index $PI = 0$) at 25 °C, at the temperature 15 °C. From Eq. (3.6) we have $\beta = 0.1794$ and from Eq. (3.36) $b = 0.1914$. Equation (3.2) yields the viscosity η = 4.247 MPa s. We have also $G_g = E_g/3 = 820$ MPa. The results of calculation by formula (3.34a, b) are shown in Fig. 3.5 (continuous curve) and they agree with relaxation modulus calculated from our recursive formula (3.20) (points).

The coefficient of variation of values obtained using Eq. (3.34a, b) from values, which were calculated numerically does not exceed 4%. To check it additionally,

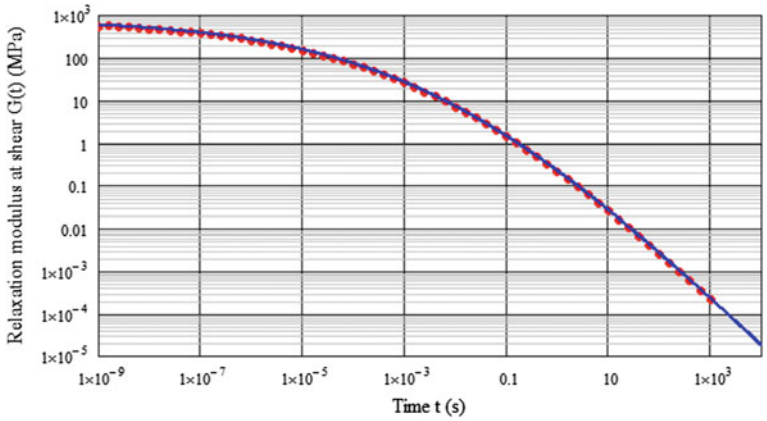

Fig. 3.5 Shear relaxation modulus of asphalt calculated from Eq. (3.20) (*points*) and (3.34a, b) (*blue curve*) based on creep compliance shown in the Fig. 3.1

we calculated the value of integral using formula (3.32), which should be equal to asphalt viscosity

$$\int_0^\infty G(t)dt = 820\int_0^\infty \left[1+\left(\frac{820t}{4.247}\right)^{0.1914}\right]^{-\left(1+\frac{1}{0.1914}\right)} dt = 4.23\ \text{MPa}\,s,$$

and it differs from η = 4.247 MPa s found from Eq. (3.2) only for 0.4%. Thus, we obtained two formulas for relaxation modulus of asphalt in this paragraph: Eqs. (3.29) and (3.34a, b).

3.3 Asphalt Complex Modulus

Complex modulus of asphalt binder, asphaltic mastic or asphalt concrete is determined by testing under a cycling load at various constant circular frequencies ω. Technology for performance of such tests is well-established, and they are used since 1960 for testing of asphalt and asphalt concrete (Van der Poel 1954; Marasteanu and Anderson 1999; Sayegh 1963; Zolotaryov 1977).

The determination of the dynamic shear modulus and phase angle of asphalt binder when tested in dynamic (oscillatory) shear using parallel plate test geometry is covered in AASHTO T315 and ASTM D7552. The test results are used in determination of performance grade of binder according to SUPREPAVE standard AASHTO M 320 (ASTM D 6373). Moreover, the asphalt concrete complex modulus is used in flexible pavement design according to a new Mechanistic-Empirical Pavement Design Guide (MEPDG) (AASHTO 2008).

Therefore, the opportunity to estimate the components of asphalt complex modulus based on its standard characteristics even approximately, is not only of scientific, but merely a practical interest.

3.3.1 Approximate Formulas for Dynamic Modulus

Complex modulus is a value, which is obtained during test with cyclic load at the frequency ω

$$G^*(\omega) = G'(\omega) + iG''(\omega),$$

where $i = \sqrt{-1}$—imaginary unit; G'—storage modulus; G''—loss modulus.

Test determines a ratio of shear stress magnitude to shear strain magnitude, which is called absolute value of complex modulus $|G^*|$ or in short dynamic modulus G_d, as well as phase angle $\delta(\omega)$, for which deformation is delayed in relation to stress. The dynamic modulus can be expressed in terms of the storage modulus and loss modulus, like a vector length in terms of the lengths of its components

$$G_d = |G^*| = \sqrt{G'^2 + G''^2} \tag{3.36}$$

Thus, the storage and loss moduli can be calculated based on the results of measurements of G_d and δ using the formulas

$$G' = G_d \cos(\delta), \quad G'' = G_d \sin(\delta) \tag{3.37}$$

Our purpose here is to express the dynamic modulus G_d and phase angle δ of asphalt as a functions of frequency and temperature in terms of penetration and softening point.

Exact formulas that express the storage modulus G' and loss modulus G'' in terms of the shearing relaxation modulus $G(t)$ are well known (Ferry 1980):

$$G'(\omega) = \omega \int_0^\infty G(s) \sin(\omega s) ds, \quad G''(\omega) = \omega \int_0^\infty G(s) \cos(\omega s) ds, \tag{3.38}$$

Unfortunately, the substitution of formulas (3.34a, b) into (3.38) results in integrals that cannot be expressed explicitly. A way out of a situation is the use of the same idea of Ferry and Williams (1952), based on which the formulas (3.25) и (3.26) were derived. The idea is in the fact that we can conceptually replace the actual curves $J(t)$ or $G(t)$ in logarithmic scale by piecewise linear function. In that case, the integrals (3.38) can be evaluated explicitly, and then proceed with actual curves, considering them as consisting of segments with variable slope to the axis

log(t). Therefore, we consider the creep compliance at shear as the power-law function

$$J(t) = \frac{1}{a}\left(\frac{t}{d}\right)^m \tag{3.39}$$

and obtain from the Eq. (3.13a, b), that similar to (3.24), the accurate expression for the relaxation modulus at shear is

$$G(t) = \frac{\sin(\pi m)}{\pi m}\, a\left(\frac{t}{d}\right)^{-m} \tag{3.40}$$

Substituting Eq. (3.40) into (3.38) and taking the integral (Dwight 1966, 858.812), we obtain the storage modulus

$$G'(\omega) = \frac{\omega\ \sin(\pi m)}{\pi m} a d^m \int_0^\infty \frac{\sin\ (\omega s)}{s^m} ds = a(d\omega)^m \frac{\cos(m\pi/2)}{\Gamma(1+m)} \tag{3.41}$$

It is easy to express the multiplier $a(d\omega)^m$ in terms of the creep compliance (3.39), having replaced the time in (3.39) by the inverse of frequency ($t \to 1/\omega$), and exactly $a(d\omega)^m = 1/J(1/\omega)$. Considering the above, we obtain the following formula for the storage modulus

$$G'(\omega) = \frac{\cos(m\pi/2)}{\Gamma(1+m)} \cdot \frac{1}{J(1/\omega)} \tag{3.42}$$

In the same way we derive formula for loss modulus

$$G''(\omega) = \frac{\sin(m\pi/2)}{\Gamma(1+m)} \cdot \frac{1}{J(1/\omega)} \tag{3.43}$$

Substituting the Eqs. (3.42) and (3.43) into Eqs. (3.36) and (3.37), we obtain the dynamic modulus and phase angle:

$$G_d(\omega) = \frac{1}{\Gamma(1+m)} \cdot \frac{1}{J(1/\omega)}, \quad \delta = m\pi/2 \tag{3.44}$$

Formulas (3.42)–(3.44) are known (Baumgaertel and Winter 1989; Schwarzl and Struik 1968; Schapery and Park 1999), but we showed our derivation, supposing that it can be of interest for the reader. They are accurate for exponential creep compliance like (3.39), graph of which in logarithmic scale is linear with constant slope m.

Based on Van der Poel's data, we already related the creep compliance that appears in Eq. (3.44) with the parameters η and β by formula (3.8). Those parameters are expressed in terms of penetration and softening point of asphalt by

formulas (3.2) and (3.6). Using the Eq. (3.44) for creep compliance like the expression (3.8) and considering a variable slope m, we arrive to approximate formulas for dynamic shear modulus and phase angle

$$G_d(\omega) = \frac{G_g}{\Gamma(1+m(\omega))}\left[1+\left(\frac{G_g}{\eta\omega}\right)^{\beta}\right]^{-\frac{1}{\beta}} \tag{3.45}$$

$$\delta = m(\omega)\pi/2 \tag{3.46}$$

where m is determined by differentiation of Eq. (3.8) by the formula (3.28):

$$m(\omega) = \frac{\left(G_g/\eta\omega\right)^{\beta}}{1+\left(G_g/\eta\omega\right)^{\beta}} \tag{3.47}$$

Similarly, we can derive the following equation for dynamic longitudinal modulus E_d

$$E_d(\omega) = \frac{E_g}{\Gamma(1+m(\omega))}\left[1+\left(\frac{E_g}{3\eta\omega}\right)^{\beta}\right]^{-\frac{1}{\beta}} \tag{3.48}$$

$$\delta = m(\omega)\pi/2 \tag{3.49}$$

$$m(\omega) = \frac{\left(E_g/3\eta\omega\right)^{\beta}}{1+\left(E_g/3\eta\omega\right)^{\beta}} \tag{3.50}$$

For instance, let us calculate the dynamic shear modulus of asphalt, which has the penetration $P = 80$ dmm at 25 °C and the softening temperature $T_{rb} = 50$ °C ($PI = 0$), at the temperature T = 15 °C. In the same way as before, we have in this example $\beta = 0.1794$, the viscosity $\eta = 4.247$ MPa s, and glassy modulus $G_g = 820$ MPa. The dynamic shear modulus calculated from Eq. (3.45) is presented in Fig. 3.6.

3.3.2 Comparison of Formulas for Dynamic Modulus and Phase Angle with Test Data

Test data of D. Christensen and D. Anderson (1992) were selected for comparison. The asphalt designated by the Strategic Highway Research Program (SHRP) as the AAB-1core asphalt was produced from Wyoming crude oil. Its viscosity grade is AC-10 (i.e. the viscosity at 60 °C is within 1000 ± 200 Poise = 100 ± 20 Pa s),

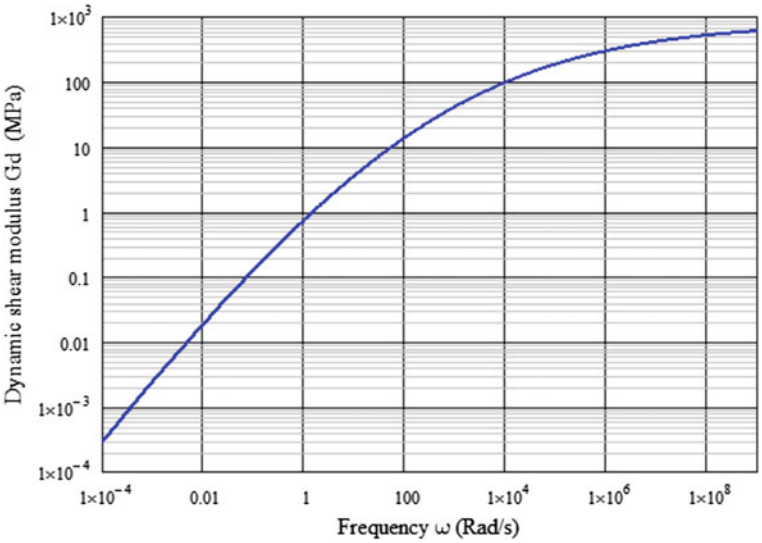

Fig. 3.6 Dynamic shear modulus of asphalt calculated from Eq. (3.45): penetration $P = 80$ dmm (25 °C) and the softening point $T_{rb} = 50$ °C ($PI = 0$) at T = 15 °C

and its Superpave grade is PG 58-22 (for a pavement with the design summer temperature 58 °C and winter temperature −22 °C). According to data of (SHRP Materials 1993) (Appendix A), this asphalt consists of 17.3% of asphaltenes dissolvable in n-heptane, 2% asphaltenes dissolvable in isooctane, 38.3% polar aromatic hydrocarbons, 33.8% naphtheno-aromatic hydrocarbons and 8.6% saturated hydrocarbons. Asphalt AAB-1 is characterized by penetration P = 98 dmm at 25 °C and the softening point $T_{rb} = 47.8$ °C, i.e. it has the penetration index $PI = 0$.

Tests were performed on dynamic shear rheometer with a range in frequency from 0.1 to 100 rad/s at the temperatures −35, −25, −15, −5, 5, 15, 25, 35, 45, and 60 °C. The data at all temperatures was then shifted with respect to time to construct the master curve at the reference temperature 25 °C (Fig. 3 in Christensen and Anderson 1992, and Fig. 3.3 in Christensen 1992). These curves are shown in Figs. 3.7 and 3.8 with points. The values of the dynamic modulus and the phase angle calculated from Eqs. (3.45) and (3.46) are presented by solid curves in Figs. 3.7 and 3.8. Notice that the agreement between the calculated and experimental results for the norm of complex modulus and the phase angle is good. The coefficient of variation of dynamic modulus G_d measured by Christensen and Anderson from the calculated curve is 16% in natural scale (i.e. not in logarithm of modulus, but for the value of modulus). The coefficient of variation of the measured phase angle from the curve calculated using Eq. (3.46) is 12.2%.

The coefficient of variation for the repeated measurements of dynamic modulus G_d varied from 10 to 25% with the average value of 15%, and for the phase angle the standard deviation ranges from about 0.4° to 0.9° (Christensen 1992, p. 100).

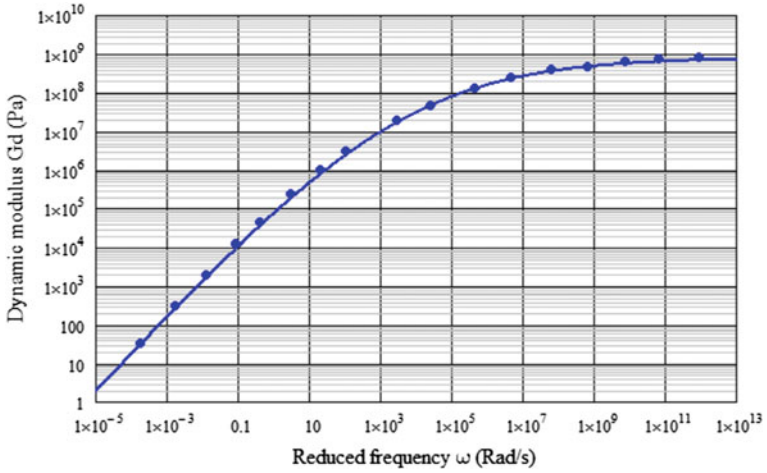

Fig. 3.7 Comparison of calculated and measured dynamic modulus G_d for asphalt AAB-1: *points*—measured (Christensen and Anderson 1992; Christensen 1992); *line*—calculated from Eq. (3.45)

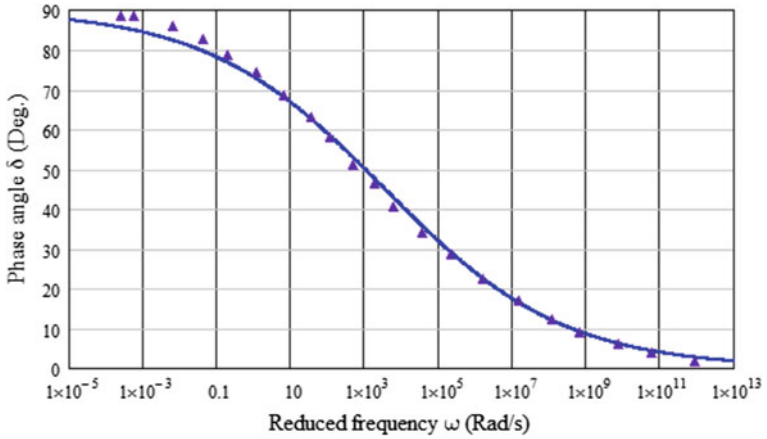

Fig. 3.8 Comparison of calculated and measured phase angle δ for asphalt AAB-1: *points*—measured (Christensen and Anderson 1992; Christensen 1992); *curve*—calculated from Eq. (3.46)

Therefore, the deviation of predicted values of G_d and δ from the test data complies with the accuracy of measurements.

The comparison confirmed not only the quality of approximate formulas (3.45) and (3.46) for the asphalt complex modulus, but also the validity of our Eqs. (3.1)–(3.7), which relate the asphalt stiffness modulus with the penetration and the softening temperature of asphalt.

3.3.3 Relaxation Spectrum of Asphalt Binder and Its Comparison with Test Data

The relaxation spectrum is a useful, fundamental way of characterizing the time dependent behavior of asphalt binders. Relaxation spectrum shows the distribution of the relaxation times and its study is the attribute of comprehensive rheological analysis. This spectrum can be interpreted as a graphic chart of relaxation process in the viscoelastic material. Relaxation spectrum $H(\tau)$ represents a density of modulus distribution as a continuous function of time. It has dimension of load per unit area like a stress or modulus of elasticity.

Thesis of Christensen (1992, p. 31, Fig. 3.4) presents the relaxation spectrum for asphalt AAB-1 at T = 25 °C. It is shown in Fig. 3.9. D. Christensen determined the spectrum based on measurements of dynamic modulus G_d and the phase angle δ shown above in Figs. 3.7 and 3.8 using method proposed by Ninomia and Ferry (1959). We will compute the spectrum using our Eq. (3.34a, b) for relaxation modulus of asphalt $G(t)$ and simplest rule of T. Alfrey. According to this rule (Ferry 1980, p. 81), the spectrum is determined approximately by differentiating the shear relaxation modulus $G(t)$:

$$H(\tau) = -\tau \frac{dG(\tau)}{d\tau} \tag{3.51}$$

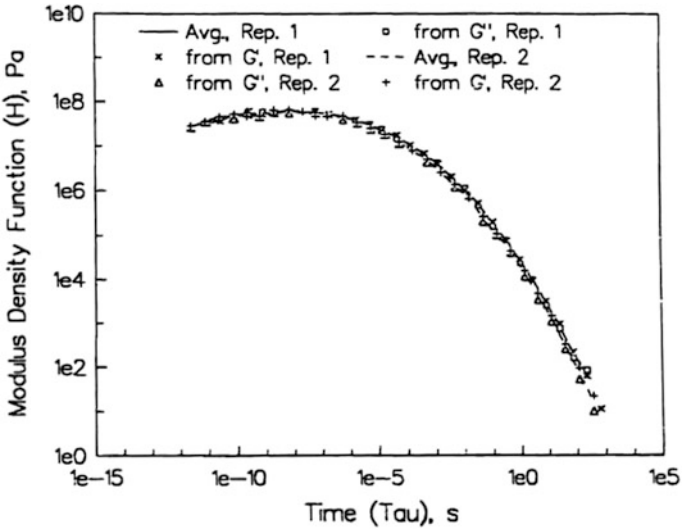

Fig. 3.9 Relaxation spectrum for asphalt AAB-1 at the temperature 25 °C based on experimental data (reproduced with permission from Christensen 1992): six groups of points correspond to calculations based on test data related to storage modulus G', loss modulus G'' and to an average value of $H(\tau)$ for two identical samples

Substituting Eq. (3.34a, b) into (3.51), we obtain the approximate formula for the relaxation spectrum of asphalt

$$H(\tau) = \frac{(1+b)G_g\left(\frac{G_g\tau}{\eta}\right)^b}{\left[1+\left(\frac{G_g\tau}{\eta}\right)^b\right]^{(2+1/b)}} \tag{3.52}$$

Using Eqs. (3.3), (3.6) and (3.35) for asphalt AAB-1 ($P = 98$ dmm at 25 °C and $T_{rb} = 47.8$ °C), we have $\eta = 4.247$ MPa s, $b = 0.1914$ and, as it was before, $G_g = 820$ MPa. Spectrum calculated from the Eq. (3.52) is shown in Fig. 3.10 and it is in a good agreement with spectrum presented in Fig. 3.9.

The maximum density of relaxation spectrum in this example is situated at the relaxation time $\tau = 1.9 \cdot 10^{-8}$ s. Relaxation time corresponding to maximum of spectrum can be obtained analytically from (3.52) and it is equal to

$$\tau_{\max} = \frac{\eta}{G_g}\left(\frac{b}{1+b}\right)^{\frac{1}{b}} \tag{3.53}$$

It follows from Eq. (3.53) that the peak position for distribution of asphalt relaxation times moves to the right with the increase of viscosity. The power

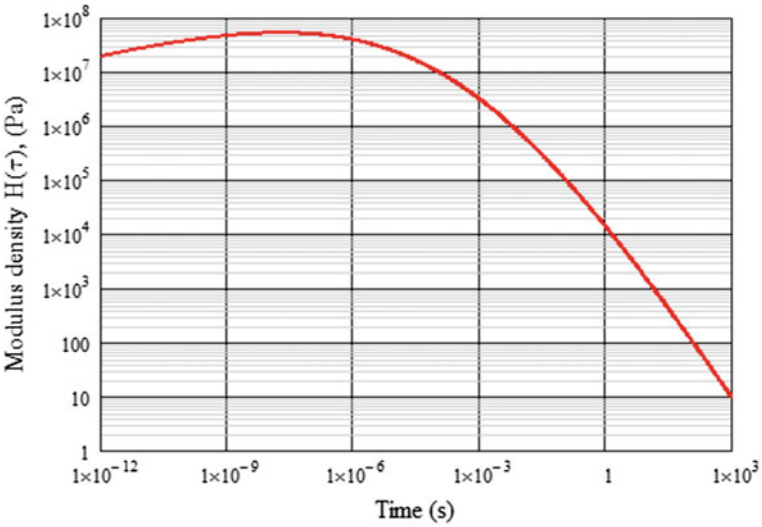

Fig. 3.10 Relaxation spectrum for asphalt AAB-1 at the temperature 25 °C, calculated from Eq. (3.52)

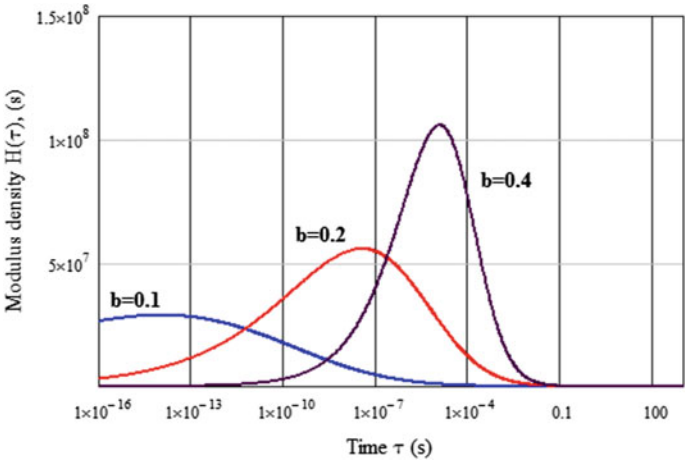

Fig. 3.11 Relaxation spectrum for asphalts with various values b

exponent b in the formula (3.34a, b) for relaxation modulus characterizes the width of spectrum and its height (Fig. 3.11). The value of b depends only on asphalt penetration index (Eq. 3.35). It varies from $b = 0.1346$ at $PI = +2$ to $b = 0.6767$ at $PI = -3$. The greater is b, the more restricted is the spectrum and the higher is its maximum.

Since the spectrum is the density of distribution of relaxation modulus, the area between the curve $H(\tau)$ and axis $\log(\tau)$ is equal to the instantaneous shear modulus, i.e. it is the same for the three spectra in Fig. 3.11 and equals to $G_g = 820$ MPa. At small load duration, the value of H tends to zero since the properties of asphalt at short load durations tend to the properties of perfectly elastic body. Maximum of spectrum corresponds to concentration of relaxation processes. At large load duration the viscoelastic material approaches a viscous flow and the value of H reduces fast—relaxation is almost completed by this time.

A good estimate for the maximum density of relaxation spectrum of bitumen is

$$H_{\max} = bG_g/3 \tag{3.53}$$

It follows that maximum density of spectrum is proportional to the parameter b of CAM model and is independent on temperature of bitumen. The maximum density of spectrum depends on the temperature susceptibility of bitumen. Greater is the temperature susceptibility, the higher is the peak of relaxation spectrum.

3.4 Calculation of Relaxation Modulus Based on Complex Modulus Test Data

3.4.1 Calculation Method

Complex modulus of viscoelastic material, particularly of asphalt or asphalt concrete (i.e. its absolute value—the dynamic modulus $E_d(\omega)$ coupled with the phase angle $\delta(\omega)$) is quite important property of the material because it allows obtaining its relaxation modulus $E(t)$. Furthermore, as it was mentioned before, the most convenient and commonly used method for determining the viscoelastic properties of asphalt and asphalt concrete is the periodical loading testing.

The complex modulus of asphalt concrete can be used directly in calculation of stresses and strains in pavement structure only under the harmonic time-varying loading—similar to sine curve. Load from the wheel of the moving vehicle on pavement is not a cyclic one: distances between the vehicles vary at random, their wheels do not run along one track, and their passages are distributed along the width of the lane. In addition, loads on the wheels have different values. Because the load conditions for pavement structure under the moving vehicles are not periodical ones, the complex modulus should not be applied directly in pavement design and analysis. The relaxation modulus or alternatively the creep compliance is required as the basic characteristics of viscoelastic properties for asphalt concrete in solving the problems of stress-strain state in the multilayer viscoelastic structure under a moving load (Elliot and Moavenzadeh 1971; Huang 1973; Privarnikov and Radovskiy 1981; Chen et al. 2011). Relaxation modulus $E(t)$ of asphalt concrete and asphalt is also an important property for calculation of the temperature-induced stresses in pavement from cooling action to estimate the low temperature crack resistance of asphalt pavement (Monismith et al. 1965; Radovskiy and Mozgovoy 1989; Bouldin et al. 2000).

Below we present the methods for determination of the asphalt relaxation modulus $E(t)$ based on tests results for its dynamic modulus $E_d(\omega)$. The idea of the methods is simple and it is as follows. The comparison of Eqs. (3.1) and (3.48) leads to the following relation between dynamic modulus and stiffness modulus of asphalt:

$$S(t) = \Gamma(1 + m(\omega))E_d(\omega)|_{\omega=1/t} \tag{3.54}$$

With the increase of frequency ω a slope $m(\omega)$ of the curve $\log(E_d(\omega))$ to the $\log(\omega)$-axis decreases from one to zero (see Fig. 3.12). Meanwhile, the multiplier $\Gamma(1+m)$ reduces from 1 at $m = 1$ to minimum, which is equal to 0.886 at $m = 0.46$, and then it increases up to 1 at $m = 0$. In other words, the multiplier $\Gamma(1+m)$ varies within the range of 0.886 and 1 for all possible range variation of circular frequency. We can assume $\Gamma(1+m) \approx 1$ within accuracy of less than 11.4% and then rewrite the Eq. (3.54) in the following form

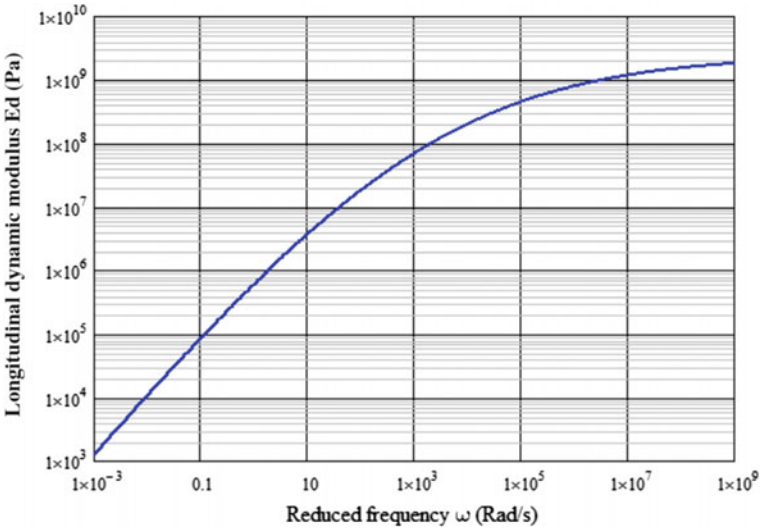

Fig. 3.12 Example of dynamic modulus as a function of frequency at the reference temperature $T_r = 20$ °C for asphalt with the softening point 46 °C and penetration 100 dmm at 25 °C

$$S(t) = E_d(\omega)\,|_{\omega=1/t} \tag{3.55}$$

Van der Poel (1954) used the same simple formula (3.55) determining the stiffness $S(t)$ at long times of loading from the creep tests while using the values $E_d(\omega)$ obtained at cyclic loading for $t < 1$ s. Thus combining the test results of these methods, he made an error less than 13% because 1/0.886 = 1.13, i.e. Van der Poel slightly overestimated the values of stiffness $S(t)$ obtained from the tests by cyclic load.

Thus, we arrived to the following methods of conversion from dynamic modulus $E_d(\omega)$ to relaxation modulus $E(t)$:

(1) Having measured values of $E_d(\omega_i)$ for asphalt and replacing a cyclic frequency ω_i with the value reciprocal to time of loading $1/t_i$, we obtain the approximate values for stiffness modulus of asphalt:

$$S(t_i) = E_d(1/t_i) \tag{3.56}$$

(2) We determine the parameters η_1 and β_1 of the formula like (3.1):

$$S_1(t) = E_g\left[1 + \left(\frac{E_g t}{3\eta_1}\right)^{\beta_1}\right]^{-\frac{1}{\beta_1}} \tag{3.57}$$

by fitting the curve $S_1(t)$ to the points $S(t_i)$.

(3) We calculate b_1 from equation like formula (3.35):

$$b_1 = \frac{1}{\frac{1}{\beta_1} + \frac{\ln(\pi)}{\ln(2)} - 2} \tag{3.58}$$

and then we obtain the target equation for the relaxation modulus of asphalt:

$$E(t) = E_g \left[1 + \left(\frac{E_g t}{3\eta_1} \right)^{b_1} \right]^{-\left(1 + \frac{1}{b_1}\right)} \tag{3.59}$$

Let us consider the example. The values of dynamic modulus $G_d(\omega)$ and phase angle $\delta(\omega)$ at various frequencies ω were measured by testing in dynamic shear rheometer for several temperatures. The master curve for dynamic shear modulus as a function of frequency $G_d(\omega)$ was constructed according to those data by method of time-temperature analogy that was described in Sect. 1.5 (see also Figs. 1.5 and 1.6) and Sect. 2.3 (see Figs. 2.3 and 2.4) for the reference temperature 20 °C. It is easy to convert it to the dependence of longitudinal dynamic modulus on frequency because $E_d(\omega) = 3G_d(\omega)$. Example is shown in Fig. 3.12.

Values for dynamic modulus of asphalt were copied into the Table 3.1 at 23 points taken from the curve in Fig. 3.12: two points per logarithmic decade in the range from $\omega = 10^{-3}$ to $\omega = 10^8$Rad./s.

According to the formula (3.56), the values of dynamic modulus $E_d(\omega_i)$ in Table 3.1 are approximately equal to the values of stiffness modulus $S(t_i)$ at $t_i = 1/\omega_i$ within the range from $t = 10^{-8}$ s to $t = 10^3$ s.

Table 3.1 Example of data for dynamic modulus of asphalt at 20 °C

Frequency ω, rad/s	Modulus $E_d(\omega)$, Pa	Frequency ω, rad/s	Modulus $E_d(\omega)$, Pa
0.001	1.26×10^3	10^3	6.98×10^7
0.004	4.64×10^3	4×10^3	1.37×10^8
0.01	1.08×10^4	10^4	2.03×10^8
0.04	3.83×10^4	4×10^4	3.38×10^8
0.1	8.64×10^4	10^5	4.52×10^8
0.4	2.86×10^5	4×10^5	6.54×10^8
1	6.14×10^5	10^6	8.01×10^8
4	1.86×10^6	4×10^6	1.03×10^9
10	3.72×10^6	10^7	1.19×10^9
40	9.97×10^6	4×10^7	1.40×10^9
100	1.83×10^7	10^8	1.54×10^9
400	4.23×10^7		

Now we should find the values of parameters η_1 and β_1 in Eq. (3.57). Since according to the data of the Table 3.1, the values for stiffness modulus cover a wide range from $S(10^{-8}) = 1.54 \cdot 10^9$Pa to $S(10^3) = 1.26 \cdot 10^3$Pa (they differ in million times), mathematically it is more convenient to work not with the moduli themselves, but with their logarithms. To avoid the negative values of logarithms, we presented the moduli in the Table 3.1 not in MPa, as in the rest of the text of this work, but in Pa. We compute the parameters η_1 and β_1 in the Eq. (3.57) for $S_1(t)$ by minimizing sum of squares for deviations of the curve from the points:

$$dev\ (\eta_1, \beta_1) = \sum_{i=1}^{i=23} [\log\ (S(t_i)) - \log(S_1(t_i))\ ]^2, \qquad \min[dev\ (\eta_1, \beta_1)],$$

We obtained $\eta_1 = 5.34 \cdot 10^5$Pa $\cdot$ s, $\beta_1 = 0.2071$. Thus, the equation for $S_1(t)$ is obtained in the following form

$$S_1(t) = E_g \left[1 + \left(\frac{E_g t}{3 \cdot 5.34 \cdot 10^5} \right)^{0.2071} \right]^{-\frac{1}{0.2071}} \tag{3.60}$$

The stiffness modulus is presented in Fig. 3.13, where the points correspond to the values of stiffness moduli $S(t_i)$, complying with the values of dynamic modulus $E_d(1/t_i)$ from the Table 3.1. The curve constructed using expression (3.60) is shown in the Fig. 3.13 and it deviates from these points at average only for 0.3% in

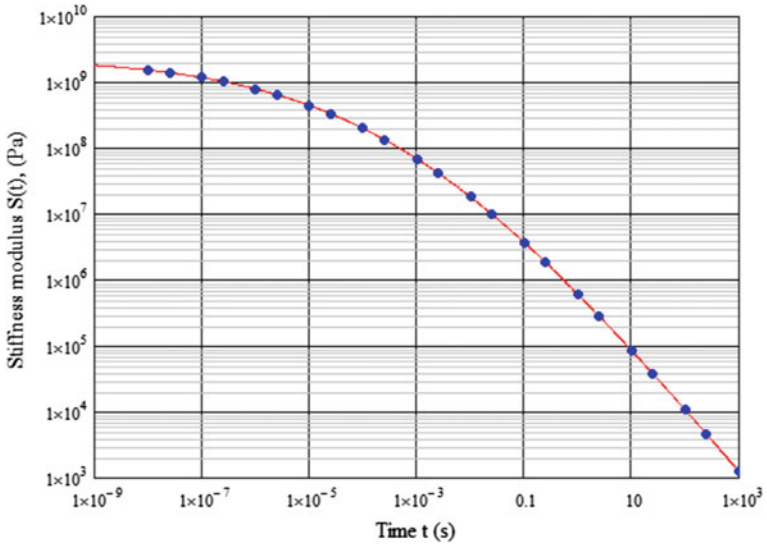

Fig. 3.13 The curve for asphalt stiffness modulus constructed based on data for dynamic modulus $E_d(\omega)$

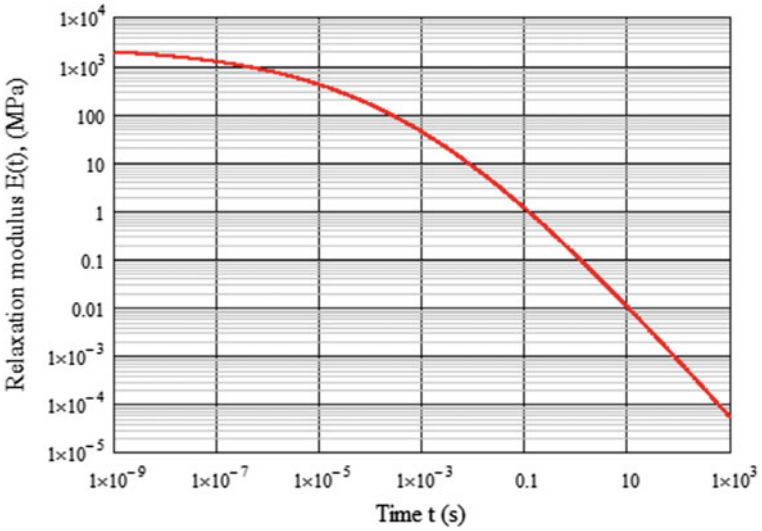

Fig. 3.14 Relaxation modulus of asphalt $E(t)$ calculated based on $E_d(\omega)$

the scale of stiffness moduli (not their logarithms). Now according to Eq. (3.58) we obtain $b_1 = 0.2232$ and using formula (3.59) we construct a graph for longitudinal relaxation modulus (Fig. 3.14), and that was our goal.

3.4.2 Comparison of Moduli

Let us compare the values of dynamic modulus $E_d(\omega)$ at $\omega = 1/t$, the stiffness modulus $S(t)$ and the relaxation modulus $E(t)$ of asphalt. For example, we calculate their values for asphalt which has at 25 °C penetration $P = 80$ dmm and the softening temperature $T_{rb} = 50$ °C (the penetration index $PI = 0$) at the temperature T = 10 °C and load duration 0.1 s using formulas (3.49) for $E_d(\omega)$, (3.1) for $S(t)$, and (3.34a, b) for $E(t)$. We obtain $E_d(10) = 23.7$ MPa, $S(0.1) = 21.1$ MPa and $E(0.1) = 11.3$ MPa.

As we already mentioned during analysis of Eq. (3.54) $S(t) \leq E_d(\omega = 1/t)$ they differ less than for 13%. Note that a maximum difference between them was evaluated as 18% in the paper (Christensen and Anderson 1992). Dynamic $E_d(\omega = 1/t)$ and relaxation $E(t)$ moduli differ much more (Fig. 3.15), and their ratio depends on temperature and load duration.

Thus, the dynamic modulus $E_d(\omega = 1/t)$ at load duration t = 0.1c, typical for pavement, is 1.6 times greater than relaxation modulus $E(t)$ at 0 °C, 2.1 times greater at 10 °C and 2.9 times greater at 20 °C.

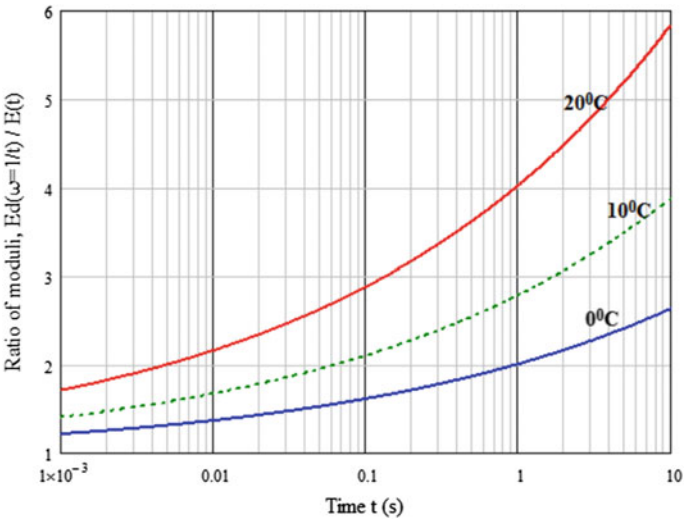

Fig. 3.15 The ratio between dynamic modulus and relaxation modulus for asphalt

Such difference between dynamic modulus and relaxation modulus for asphalt should be admitted as considerable, although these moduli for asphalt concrete are less different. It is important because the use of asphalt concrete dynamic modulus instead of its relaxation modulus for pavement design overestimates the ability of asphalt concrete layer to distribute the load.

The main results stated in this chapter are as follows:

(1) The enhanced recursive relation (3.17), (3.20) was derived for calculation of longitudinal $E(t)$ or shearing $G(t)$ relaxation modulus, based on creep compliance $D(t)$ or $J(t)$.
(2) Approximate formula (3.29) was proposed for determination of asphalt relaxation modulus as a function of its temperature and load duration based on the simplest standard properties of asphalt (penetration P at 25 °C and the softening point T_{rb}), and an alternative simple formula (3.34a, b) was proposed for determination of $E(t)$ or $G(t)$ depending on P and T_{rb}.
(3) Formulas (3.45)–(3.49) were obtained for evaluation of dynamic modulus G_d or E_d and phase angle for asphalt as a function of frequency of loading and temperature based on its standard properties P and T_{rb}. Agreement of predicted dynamic modulus, phase angle δ, and relaxation spectrum of asphalt with test data was illustrated.
(4) Method of conversion from the measured dynamic modulus of asphalt $E_d(\omega)$ to its relaxation modulus $E(t)$ was proposed.

References

AASHTO (2008) Mechanistic-Empirical Pavement Design Guide, Interim Edition: a manual of practice

AASHTO PP 42-07 Determination of low-temperature performance grade (PG) of asphalt binders

ASTM D 6816-02. Standard practice for determining low-temperature performance grade (PG) of asphalt binders

Bahia HU, Zeng M, Nam K (2000) Consideration of strain at failure and strength in prediction of pavement thermal cracking. J AAPT 69:497–535

Baumgaertel M, Winter HH (1989) Determination of discrete relaxation and retardation time spectra from dynamic mechanical data. Rheol Acta 28:511–519

Bouldin MG, Dongre RN, Rowe GM, Sharrock MJ, Anderson DA (2000) Predicting thermal cracking of pavements from binder properties: theoretical basis and field validation. J AAPT 69:455–496

Chen EY, Pan E, Norfolk TS, Wang Q (2011) Surface loading of a multilayered viscoelastic pavement. Road Mat Pav Des 12(4):849–874

Christensen DW (1992) Mathematical modeling of the linear viscoelastic behavior of asphalt cements. Thesis, The Pennsylvania State University

Christensen DW, Anderson DA (1992) Interpretation of dynamic mechanical test data for paving grade asphalt cements. J AAPT 61:67–116

Dwight G (1966) Tables of integrals and other mathematical formulas. Nauka, Moscow

Elliot JF, Moavenzadeh F (1971) Analysis of stresses and displacements in three-layer viscoelastic systems. Highway Res Rec 345:45–57

Ferry JD (1980) Viscoelstic properties of polymers, 3rd edn. John Willey & Sons Inc, New York

Ferry JD, Williams ML (1952) Second approximation methods for determining the relaxation time spectrum of viscoelastic material. J Colloid Sci 7:347–353

Hopkins IL, Hamming RW (1957) On creep and relaxation. J Appl Phys 28:906–909

Huang YH (1973) Stresses and strains in viscoelastic multilayer systems subjected to moving loads. Highw Res Rec 457:60–71

Leaderman H (1958) Viscoelasticity phenomena in amorphous high polymeric systems. In: Eirich FR (ed) Rheology, vol II. Academic Press, New York

Marasteanu M (2010) Low temperature testing and specifications. Transportation Research Circular E-C147. Development in Asphalt Binder Specifications, TRB, Washington, DC, pp 34–40

Marasteanu MO, Anderson DA (1999) Improved model for bitumen rheological characterization. Eurobitumen Workshop on Performance Related Properties for Bituminous Binders, Paper No. 133, Luxembourg

Mead DW (1994) Numerical interconversion of linear viscoelastic material function. J Rheol 38:1769–1795

Monismith CL, Secor GA, Secor KE (1965) Temperature induced stresses and deformations in asphalt concrete. J Assoc Asph Pav Tech 34:245–285

Ninomiya K, Ferry JD (1959) Some approximate equations useful in the phenomenological treatment of viscoelastic data. J Colloid Interface Sci 14:36–48

Privarnikov AK, Radovskiy BS (1981) Moving load impact on viscoelastic multilayer base. Appl Mech 17(6):45–52

Radovskiy B, Mozgovoy V (1989) Ways to reduce low temperature cracking in Asphalt Pavements. In: 4th Eurobitume Symposium, Madrid

Sayegh G (1963) Variation des modules de quelques bitumes purs et bétons bitumineux. Conférence au Groupe Français de Rhéologie, France

Schapery RA, Park SW (1999) Methods of interconversion between linear viscoelastic material functions. Part II—an approximate analytical method. Int J Sol Struc 36:1677–1699

Schausberger AA (1986) Simple method of evaluating the complex moduli of polystyrene blends. Rheol Acta 25:596–605

Schwarzl FR, Struik CE (1968) Analysis of relaxation measurements. In: Advances in molecular relaxation processes (1): pp 201–255
Secor KE, Monismith CL (1964) Analysis and interrelation of stress–strain–time data for asphalt concrete. Trans Soc Rheol 8:19–32
Standard Specification for Performance Graded Asphalt Binder: ASTM D 6373, AASHTO M 320
The SHRP Materials Reference Library, SHRP A-646 (1993). Washington, DC, pp 1–228, (Appendix A)
Tschoegl N (1989) The phenomenological theory of linear viscoelastic behavior. Springer-Verlag, Heidelberg
Van der Poel C (1954) A general system describing the viscoelastic properties of bitumens and its relation to routine test data. J Appl Chem 4:221–236
Winter HH, Chambon F (1986) Analysis of linear viscoelasticity of a cross linking polymer at the gel point. J Rheol 30:367–382
Zolotaryov V (1977) Durability of road asphalt concretes. Vysshaya shkola, Kharkov

Chapter 4
Practical Applications

Abstract The subject of this chapter is the practical application of proposed equations for prediction the viscoelastic properties of bitumen. This Chapter reviews the evolution of penetration and the softening temperature of bitumen during preparation of the asphalt mix at the hot mixing facility and their variation in time during the service life of pavement that causes the variation of viscoelastic properties of asphalt pavement. The requirements of Superpave binder specification to the properties of asphalt are discussed. Those properties can be determined by laboratory testing with the equipment developed by Superpave researchers or they can be estimated for bitumen binders from the relationships described in the monograph. Once the viscoelastic properties of asphalt have been predicted using the methodology described in Chap. 3, there is a need to determine the engineering properties of asphalt concrete as a function of temperature and loading duration for use in evaluating performance and in the mechanistic-empirical thickness design methods. This chapter describes determination of the asphalt concrete relaxation modulus and complex modulus using the mixture rule (Hirsh model). The moduli predictions might be almost as accurate as independent measurements of moduli. For many pavement design and analysis procedures, predicted modulus values of asphalt concrete mixtures can be effectively used.

In the previous chapters, the approximate equations were derived that allow obtaining one viscoelastic function for asphalt from the other, for example, relaxation modulus—from creep compliance or from stiffness modulus, dynamic modulus and phase angle—from relaxation modulus, relaxation modulus—from complex modulus, etc. It was shown that an empirical Eq. (3.1) could be used to fit the Van der Poel's test data regarding the stiffness modulus of asphalt as function of its penetration and softening point, time of loading, and temperature. This enables expressing of the other viscoelastic functions for asphalt in terms its penetration and softening point. In this final chapter, we consider some examples for practical use of the obtained relations for predicting the viscoelastic properties of asphalt and asphalt concrete.

B. Radovskiy and B. Teltayev, *Viscoelastic Properties of Asphalts Based on Penetration and Softening Point*, Structural Integrity 2,
https://doi.org/10.1007/978-3-319-67214-4_4

Certainly, penetration and softening point of asphalt are outdated characteristics that do not completely define its mechanical properties, which depend upon the chemistry of the crude oil source, and the method used to refine it; however, we do not know its new characteristics, which could adequately define these properties. Naturally, it could be more reliable to determine asphalt and asphalt concrete mechanical properties experimentally by testing at creep or cyclic regime of loading. We do not always have the opportunity to test, and even if we had, the range of temperature and frequency in which these time-consuming tests are carried out proves frequently to be rather too narrow. Due to the above, the opportunity to predict approximately the mechanical properties of asphalt and asphalt concrete based on its simple standard characteristics seems very attractive; especially as it was demonstrated above, our forecast for viscoelastic properties of asphalt is in a good agreement with test data.

4.1 Effect of Aging on Viscoelastic Properties of Asphalt

It is known that asphalt properties vary significantly during preparation of the asphalt mix at the hot mixing facility and continue to vary in time during the service life of pavement. This variation is called aging. In the short term, asphalt hardens after heating, mainly due to volatilization, and, in the long term, it hardens mainly due to oxidation. Aging causes the asphalt to become more brittle. Some of the performance-graded properties of asphalt binder are specified at the beginning of pavement service life while some properties of asphalt and asphalt concrete are specified to the pavement condition approximately in the middle of service life. In this connection, it is important to predict relative changes that occur in penetration and softening temperature during hot-plant mixing and the years after road construction during service life.

The study of asphalt aging started long ago (Hubbard and Gollomb 1937; Traxler 1961), and the literature is extensive (Welborn 1979; Bell 1989). In 1961, Traxler listed five following factors influencing hardening of asphalt in approximate order of importance: (1) Oxidation, (2) Volatilization, (3) Time (development of internal structure on aging), (4) Polymerization induced by actinic light (free radical reactions) and (5) Condensation polymerization (by heat). Aging occurs due to a number of processes, proceeding from the contact of thin asphalt film with the surface of aggregate material, mainly during oxidation of hydrocarbons, their polymerization and less due to fume of volatile components. These processes are followed by structural transformations that result eventually in the increase of asphalt and asphalt concrete stiffness.

Short-time mixing of asphalt and aggregate particles at the high temperature 140–160 °C at the mixing facility results in fast hardening of binder compared with its long-term aging in pavement at the temperature lower than 60–70 °C. Due to the different rate of these processes, they are considered separately as the technological and service-life aging. Meanwhile, the technological aging is the aging during

preparation of the mix, its transportation and compaction, when the temperature of the mix is much higher than the temperature of pavement. The Superpave binder specification relies upon testing asphalt binders in conditions that reproduce three stages of binder's life: original asphalt, mix production and pavement construction, and aging over a long period in pavement layer. Two devices for artificial aging were developed: (1) Rolling Thin Film Oven (RTFO), where asphalt is tested in the form of thin films imitating volatilization and oxidation during mixing and construction; (2) Pressure aging vessel (PAV), where asphalt is tested at the increased temperature and pressure (100 °C and 2 MPa) to reproduce the variation of its properties in pavement after 4–8 years of service in continental climate for northern-eastern part of the USA (Anderson et al. 1994). Many field and laboratory data were accumulated regarding variation of penetration and softening temperature during asphalt aging. We will be interested here only in general information on how much the penetration and softening point of asphalt binder vary during its technological and service-life aging.

First, we shall consider the impact of technological aging. Brown (1980) recommended assuming the asphalt penetration after preparation of the mix P_T on average equal to 65% from penetration P_O of the original asphalt $P_T = 0.65P_O$. For example, in the Thesis (Brunton 1983) developed under Prof. S. Brown's advisorship, the following typical data was presented for dense mix with 5.7% of asphalt: original penetration P_O = 50 dmm and the softening point T_{rbO} = 52.9 °C, and after mixing penetration P_T = 32.5 dmm, the softening point T_{rbT} = 59.3 °C. For porous mix containing 3.5% of asphalt, original penetration P_O = 100 dmm and T_{rbO} = 44.9 °C, and after mixing P_T = 65 dmm and T_{rbT} = 51.4 °C (Table 4.1) in (Brunton 1983). In the paper of Airy and Brown (1997) for asphalt from Middle East, Russian and Venezuela oil, the ratio of values after technological aging to its original value was equal to 0.70–0.75 for penetration (at 25 °C), 1.08 for softening point, and 2.08 for viscosity at 60 °C.

Culley (1969) tested the asphalt before mixing, asphalt extracted from the prepared mix, asphalt extracted from the compacted mix and then from the pavement after a year in-service. He obtained that penetration after technological aging was equal to 0.6–0.8 of the original one, and penetration after the first year of service was equal to 0.6–0.8 of penetration after compaction of the mix. As the result, one year later, the asphalt penetration was approximately a half of the original one. According to data of Benson (1976) obtained in the Western Texas, the penetration of asphalt extracted from the pavement cores after one month of service can be described by empirical equation $P_1 = 0.52\ P_O - 2$. From this formula, the asphalt with original penetration of 60 dmm will have in a month the penetration of 29.2 dmm, and with the original penetration of 90–44.8 dmm, i.e., approximately a half of the original penetration.

Authors (Christensen and Anderson 1992) tested eight asphalt binders in Rolling Thin Film Oven (RTFO) imitating technological aging. The penetration (at 25 °C) after aging was on average 0.59 from the original one (ranging from 0.53 to 0.70), the viscosity (at 60 °C) increased on average in 2.5 times (the range of 1.8–3.2), and the softening point increased on average in 1.13 times. Thus, we can assume

that during the technological aging, the asphalt penetration reduces approximately to 0.6 from its original value and the softening temperature increases approximately in 1.1 times.

Let us consider now the impact of service-life ageing. The researchers of Leningrad branch of SoyuzdorNII (Russia) obtained the bulk of the data from cored samples taken periodically from over the highways projects throughout the Leningrad region after 5–15 years of service without surface treatment. They extracted the asphalt binder by alcohol-benzene or carbon tetrachloride and determined its penetration at 25 °C (Sall 1989). The data was obtained for asphalts of various original viscosities. The asphalt penetration for dense asphalt concrete (porosity of 4%) after five years in service was about 0.7 of original penetration, and after ten years—approximately 0.5. For asphalt concrete with air porosity of 8%, those values were 0.6 and 0.4 respectively.

The bulk of similar data were accumulated. Corbett and Merz (1975) studied hardening of six binders used in a Michigan test road during eighteen years of service. One of them originally had the penetration of 60 dmm; penetration of extracted asphalt four years later was 31–34 dmm, and eleven years later—26–29 dmm, i.e., four years later it was about 0.55 of original value and eleven years later—about 0.45. Softening point during eleven years increased from 52 to 66 °C, i.e., for 27%. According to the data of Benson (1976) in Texas, the average variation of penetration in time for penetration of asphalt from cored samples taken periodically from highways projects of fourteen pavements, depending on their service period can be described by linear regression equation

$$P(t) = P_1 - b \cdot \log(t)$$

where t = time of service in months, P_1 = penetration of extracted asphalt, determined from the above formula $P_1 = 0.52\ P_O - 2$, b = fitting parameter characterizing the rate of ageing and depending on porosity of asphalt concrete, asphalt properties and natural conditions.

The above regression equation describes the variation of penetration for fourteen pavement projects during nine years with high correlation (R^2 is over than 0.95). One of the Benson's graphs with $b = 9.7$ for asphalt having the original penetration 69 dmm is presented in Fig. 4.1 (Benson 1976). The point shows original penetration at initial moment. The fast drop in penetration close to the initial moment can be explained by mixing and intensive aging during the first month after construction. Five years later, the penetration of asphalt was only a quarter of the original one, and ten years later—20% of it. Such an intensive aging can be explained by hot climate of Texas.

The work (Kandhal 1977) presents the data for variation of penetration, ductility and viscosity for four asphalts during ten years of service in pavement on ten experimental road sections in Pennsylvania. After five-ten years, the initial penetration 60–70 dmm dropped to 20–25 dmm and the cracks in pavements occurred. Therefore, penetration during five-seven years decreased approximately in three times and viscosity at 60 °C increased approximately for the order of magnitude.

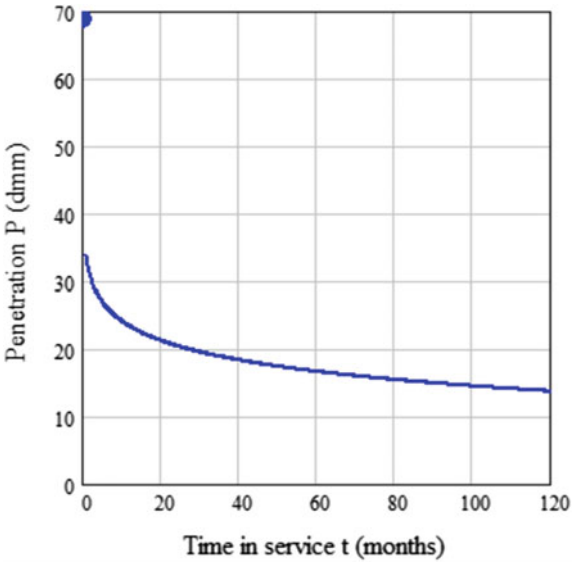

Fig. 4.1 Example of asphalt penetration variation (Benson 1976)

Christensen and Anderson (1992) tested eight asphalt binders in PAV (already aged in RTFO) imitating the service-life aging. The penetration (at 25 °C) after aging was on average 0.34 from the original one (ranging from 0.28 to 0.43), the viscosity (at 60 °C) increased on average in 7.5 times (the range of 4.2–10.5), and softening point increased on average in 1.25 times. Thus, we can assume that after the technological aging and hardening in pavement, the asphalt penetration reduces approximately to 0.3–0.4 of its original value and the softening temperature increases approximately in 1.25 times. Thus, we can assume that after mixing, construction, and hardening in pavement, the binder of dense asphalt concrete in conditions of continental climate during 5–7 years of service will have the penetration of about 0.3–0.4 of its original value, the softening temperature will increase approximately 20% comparing to its value before mixing, and viscosity at 60 °C will increase in 5–10 times.

Recent research has suggested that in many cases the premature pavement fatigue failure initiates at the surface of asphalt pavement and propagates downward, which is known as top-down cracking. In this connection, the impact of service-life aging was studied depending on the depth from pavement surface. The report (Harnsberger 2011) presents the dynamic shear test results for asphalt samples extracted after four years of service from the slices of thickness 13 mm cut from core of asphalt concrete pavement on the road US 93 in Arizona (Fig. 4.2). Due to a hot climate, asphalt binder PG 76-16 was selected for the mixture. As expected, the dynamic shear modulus of asphalt close to the surface is higher because the asphalt was subjected to more intensive aging than close to the bottom of layer.

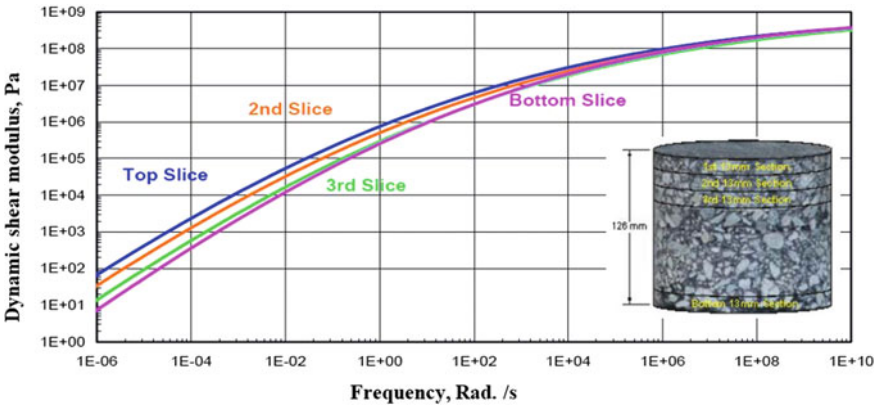

Fig. 4.2 Effect of pavement depth on dynamic modulus of asphalt recovered after four years of service: on the *right* the core sample is shown from which four discs were cut in 13 mm of thickness each; *top* (*blue*) curve shows $G_d(\omega)$ for asphalt extracted from the *top* disc, the next *curve*—from the disc second in depth, the next (*green*)—from the third one and low *curve*—from the disc close to the *bottom* of pavement. Master *curves* were constructed at reference temperature of 40 °C

4.2 Requirements to Asphalt in Terms of Pavement Low-Temperature Crack Resistance

During its cooling, the asphalt concrete pavement tends to reduce its length, but adjacent areas of pavement counteract to it, as well as the friction and bonding of pavement with the base. Due to incapability to shrink during its cooling, the pavement experiences the tension in longitudinal direction, and transversal cracks may develop. The higher asphalt concrete stiffness is and less its ability to relax the thermally induced stress, the more possible occurrence of cracks is. Cooling at seasonal and daily temperature variation also contributes to their appearing.

Observations of test roads in Canada are especially illustrative regarding occurrence of thermally induced cracks. They observed behavior of 29 sections with the length of 120 m (Deme and Young 1987) on Ste. Anne road with average daily traffic of 1250 (10% trucks) for 8 years (1967–75). The mixes were prepared with four different asphalts of three various contents (optimum under Marshall's method, for 1% less and for 0.5% more than optimum) meanwhile they used three different aggregates. Air temperature in summer reached 38 °C, and in winter dropped to −40 °C. Field trials indicated that the binder is mostly responsible for the low temperature cracking of asphalt pavements. Binder content and mix filler content, pavement thickness and subgrade type did not appear to have any significant effect on the frequency of transverse pavement cracking. It was concluded that use of binders, which do not get brittle at the prevailing low temperatures, was key to the prevention of thermal pavement cracking (Deme and Young 1987; Finn 1990). To develop performance-based specifications, the rheological parameters of

asphalt binder that affect thermal cracking were determined by Superpave researchers.

It was decided, first, to limit allowable stiffness modulus of binder S at low temperature, so that the binder was not too brittle. As S increases, the thermal stress developed in pavement due to thermal contraction also increase. Most researchers have correlated of in-service pavements with asphalt stiffness values at loading times of the order one or two hours. Initially, the maximal stiffness S = 200 MPa for two hour load duration t = 7200 s was accepted. The Bending Beam Rheometer (BBR) was designed to test the asphalt binder at low temperatures. The binder is tested on rheometer with bending beam, applying the concentrated load to the specimen of binder with dimensions 6.25 × 12.5 × 125 mm in the middle of span of 102 mm. Then, to shorten the laboratory test time, the time-temperature superposition principle was used. It was decided to perform test at the temperature of 10 °C above the lowest pavement temperature and to reduce the load duration to t = 60 s. The limiting stiffness was selected of $S(60)$ = 300 MPa in Superpave specification. The slope of master stiffness curve m is also used for specification purposes as a measure of the rate of stress relaxation at low temperature. As the m—value decreases, the ability of asphalt binder for relaxation of the thermal stresses also decreases.

The m—value is the slope of the log creep stiffness versus log time curve at any time t. The Superpave binder specification (AASHTO M 320-05) requires a maximum limit of stiffness $S(t = 60)$ = 300 MPa and m = 0.30 minimum, i.e.,

$$m_S = \frac{d\ \log(S(t))}{d\ \log(t)} > 0.30$$

at t = 60 s. The values $S(60)$ = 300 MPa and $m_S > 0.30$ are accepted in AASHTO M 320 standard.

Differentiating Eq. (3.1) for stiffness modulus of asphalt, we can find the slope

$$m_s = \frac{\left(E_g t/3\eta\right)^{\beta}}{1 + \left(E_g t/3\eta\right)^{\beta}} \tag{4.1}$$

Using Eqs. (3.1) and (4.1), we can estimate the temperature for which the Superpave requirements for this asphalt are satisfied without testing the asphalt on BBR.

For instance, we shall evaluate the minimum winter temperature, at which the bitumen of penetration 60 dmm (at 25 °C) and the softening point 48.8 °C (penetration index PI = −1.08) can be used. After artificial aging in RTFOT and PAV, which corresponds approximately to 5–7 years of service, the penetration is equal to 45 dmm and the softening point is 59.3 °C (penetration index PI = −0.68).

We calculated the values for stiffness modulus of this asphalt at t = 60 s for various temperatures from Eq. (3.1) for original and aged bitumen (Fig. 4.3). Maximum allowable stiffness modulus $S(60)$ = 300 MPa is shown by horizontal

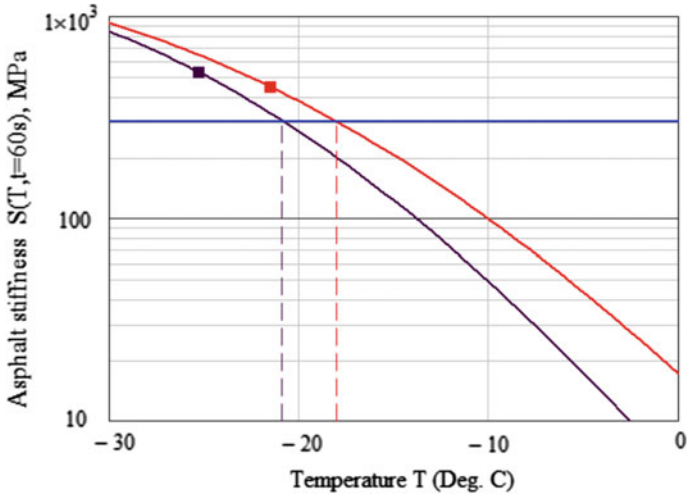

Fig. 4.3 The minimal winter temperature, at which the asphalt binder can be used based on Superpave requirements: *lower curve*—stiffness modulus of bitumen versus temperature (before aging); *upper curve*—the same after aging in RTFOT and PAV; *square* points correspond to the temperatures, at which $m_S = 0.30$; for aged bitumen at loading time t = 60c, the allowable value of stiffness S is obtained at minus 18 °C; thus, the bitumen can be used at T > −28 °C

(blue) line. Square points correspond to the temperature, at which the calculated from Eq. (4.1) slope equals to allowable $m_S = 0.30$.

One can see that the limiting stiffness modulus plays a crucial role in this example. It is achieved for original bitumen at T = −21 °C and for aged bitumen at T = −18 °C. At T = −18 °C for aged bitumen ($P = 45$ dmm, $T_{rb} = 59.3$ °C, $PI = -0.68$) at $t = 60$ s from Eq. (3.1) we obtain $S = 302$ MPa, and from Eq. (4.1) for this temperature $m_S = 0.356$. Thus, the stiffness modulus $S < 300$ MPa is the limiting requirement in this case.

Criteria ($S < 300$ МПа, $m_S > 0.30$) correspond to load duration 60 s and comply with the temperature, which is 10° higher than the design winter temperature for two hour loading duration. Therefore, according to Superpave, this bitumen can be used when the minimum air temperature expected for service life is not lower than minus 28 °C.

More recently, the Superpave approach (AASHTO M 320-05) using two separate low temperature controls was recognized as insufficiently substantiated. Bouldin et al. (2000) suggested to calculate the thermally induces stress on cooling and to find the critical temperature, at which the calculated stress from cooling reaches the tensile strength of the material. This critical temperature should not be higher than design winter temperature for pavement. Preliminary standard was issued, summarizing the experience for such calculations, and investigations are continued in this direction.

4.3 Asphalt Grade Defining in Accordance with Superpave Requirements

The Superpave binder specification is intended to limit the potential for asphalt to contribute toward permanent deformation (rutting), fatigue cracking and low temperature cracking in asphalt pavement by designating some rheological properties (AASHTO M 320-05; SP-1 2003). Those properties can be determined by laboratory testing with the equipment developed by Superpave researchers or they can be estimated for bitumen binders from the relationships described above.

The Superpave binder specification is focused on temperature and traffic conditions of pavement functioning (SP-1 2003). For example, the performance grade (PG) for the binder PG 64-34 means that requirements to high temperature properties should be followed for summer temperature not less than 64 °C, and requirements to low temperature properties—for winter temperature not higher than −34 °C. Grade varies with the step of 6 °C for high and for low temperature. Important feature of Superpave specification is that the values of specified criteria remain constant, but the temperature at which the criteria must be reached changes for the various grade depending on the climate in which the binder should be used.

The hottest period out of seven consecutive days during the design service life was chosen to characterize the climate conditions at high temperatures, and minimum daily air temperature during design service life was chosen to characterize the climate conditions at low temperatures. For surface layers, Superpave defines the high pavement design temperature at a depth 20 mm below the pavement surface, and the low pavement design temperature at the pavement surface (AASHTO R 29-15). The empirical equations were developed for the high and low design pavement temperatures taking in the account the geographical latitude of project, air temperature and standard deviation of the mean air temperature. Calculating the design temperature, it is possible to assume a level of reliability depending on importance of the object.

Technical requirements of Superpave system (AASHTO M 320-05) are developed for the pavement that subjected to fast, transient loads with lane traffic less than 10 million equivalent single axle loads (ESAL) of 80 kN. If the design traffic is between 10 and 30 million ESAL, then the engineer may select one high binder grade higher than based on climate. The Superpave specification is also intended to accommodate slow transient or standing loads, such as those near intersections, toll booths or bus stops. In cases of slow loading rate, the high temperature should be increased by one grade, for example, PG 64 instead of PG 58. For stationary loads, the high temperature should be increased by two grades, for example, PG 70 instead of PG 58. This approach is based on the principle of time-temperature analogy. As discussed in Chap. 1, because of its viscoelastic nature, bitumen behavior depends on temperature and time of loading. Its deformation and strength at high temperature and short duration of loading is equivalent to the deformation at lower temperature and longer time of loading.

Design temperatures of 76 or 82 °C do not comply with any climatic zone in North America where the highest mean seven-day temperature is about 70 °C. Additional grades of PG 76 and PG 82 were included specially to accommodate slow traffic loading rates and high numbers of heavy traffic loads.

The performance based Superpave binder specification (AASHTO M 320-05; SP-1 2003) addresses three primary performance problems of asphalt pavements: permanent deformation (rutting), fatigue cracking, and low temperature cracking:

1. *A rutting factor*, $|G^*|/\sin(\delta)$, represents the asphalt binder's rut resistance at high pavement temperature. It is determined by dividing the absolute value of complex modulus (dynamic modulus) by the sine of the phase angle that are both measured using the dynamic shear rheometer (DSR) at the circular frequency 10 rad/s. The rutting factor should be not less than 1 kPa for the original binder and not less than 2.2 kPa after aging using the RTFO, so that the pavement had low tendency to rutting.
2. *Low temperature cracking*. As it was described in the previous paragraph, the Superpave standard (AASHTO M 320-05) requires the creep stiffness (S) at the lowest pavement design temperature not to exceed 300 MPa and the m-value must be at least 0.300.
3. *Fatigue cracking factor*, $|G^*| \cdot \sin(\delta)$, is a measure of asphalt binder's resistance to fatigue under the action of repeated moving loads. It is determined after testing the binder using the dynamic shear rheometer (DSR) at the circular frequency 10 rad/s and at the moderate temperature, close to the average annual temperature in daytime, when fatigue damage is accumulated as the result of vehicle passages. The Superpave standard (AASHTO M 320-05) shows this temperature for each grade of binder. For example, it is equal to 19 °Cfor the grade PG 64-34. The binder, tested in this conditions, should satisfy the requirement $|G^*| \cdot \sin(\delta) < 5$ MПa after the RTFOT and PAV aging.

The works of researchers, who developed the Superpave system, do not state that rutting, thermal and fatigue cracks will not occur if the performance based grading requirements (AASHTO M 320-05) are met, however, the damage will be less, than for penetration or viscosity grading system of binders. The Superpave standards as if (AASHTO M 320-05) are considered now as provided for purchasing the binder for certain climate and traffic conditions (see discussion in the paper Bouldin et al. 2000).

In accordance with Superpave requirements, the binder should be tested in laboratory to determine its PG-grade. We shall try here to estimate the PG-grade of bitumen, based on its penetration and softening temperature from the formulas, obtained above. In our example, we shall use the data published in Materials Reference Library Report (Mortazavi and Moulthrop 1993).

The Materials Reference Library (MRL) is a storage facility used to house highway materials consisting of asphalt cement, Portland cement, natural aggregates, and a combination of these materials in both loose and core form. A total of 32 asphalt cements (4000 L for bitumen of each type in twenty-liter containers), 11

aggregates (30 t for each type) and 82 asphalt modifiers are stored at the MRL (Mortazavi and Moulthrop 1993). Of the thirty-two asphalt cements selected, eight were designated as "core" asphalts and were used by the Superpave researchers. Four aggregates were selected from 11 types for the use in Superpave research activities. The most important properties for all asphalts are described in (Mortazavi and Moulthrop 1993), and researchers can compare their results with MRL data.

We selected bitumen AAB-1 from Wyoming oil, test results of which are available in the library (Mortazavi and Moulthrop 1993) and, in addition, it was tested by the authors of (Christensen and Anderson 1992). Original bitumen had the softening point T_{rb} = 47.8 °C, penetration P = 98 dmm (at 25 °C), penetration index PI = 0. Characteristics after ageing were as follows:

- After aging in Thin Film Oven Test apparatus (TFOT): T_{rb} = 52 °C, P = 58 dmm, PI =-0.355.
- After aging in TFOT and in PAV apparatus: T_{rb} = 57 °C, P = 34 dmm, PI = −0.455.

1. PG-grade of bitumen under the criteria of resistance to rutting.

Let us check a rutting factor for the design summer temperature T = 58 °C. For original bitumen with T_{rb} = 47.8 °C, P = 98 dmm, PI = 0 from formula (3.6), we find β = 0.1794, and from formula (3.2) $\eta = 4.115 \times 10^{-4}$ MPa s. Considering that glassy shear modulus equals to $G_g = 820$ MPa, we calculate from Eq. (3.47) m = 0.8993, and from the formula (3.46) we obtain δ = 1.413. Absolute value of complex modulus (dynamic modulus) from Eq. (3.45) is $|G^*| = 2.368 \times 10^{-3}$ MPa = 2.368 kPa. Having calculated the ratio $|G^*|/\sin(\delta)$ = 2.398 kPa, we conclude it is greater than the required value of 1 kPa for the original binder.

For bitumen after ageing in TFOT, after the similar calculations we obtain $|G^*|/\sin(\delta)$ = 2.38 kPa, which is greater than the required value of 2.2 kPa for binder after the artificial technological aging.

Let us try to check a rutting factor of same bitumen at higher design summer temperature T = 64 °C. We obtain that for a basic bitumen the ratio $|G^*|/\sin(\delta)$ = 1.148 kPa, i.e., the Superpave requirement is satisfied, but for aged bitumen this ratio equals to $|G^*|/\sin(\delta)$ = 1.89 kPa, which is less than the required value of 2.2 kPa. Therefore, the high temperature PG-grade of this bitumen is evaluated as PG 58.

2. PG-grade of bitumen under the criteria of resistance to low temperature cracking.

The Superpave specification (AASHTO M 320-05) provides the following possible low temperature grades for bitumen of high-T grade PG 58: −16, −22, −28, −34 and −40 °C (for two-hour loading). As we discussed above, the low T requirements (S < 300 МПа, m_S > 0.30) correspond to loading duration 60 s and comply with the temperature, which is 10° higher than the design winter temperature for two hour loading duration. Thus, the low T requirements for bitumen (after its

technological aging) at the temperatures −6, −12, −18, −24, and −30 °C correspond to the values with load duration of 60 s.

Let us check the low T criteria for design temperature T = −28 °C under two-hour loading. We should check those criteria at T = −18 °C and at loading duration t = 60 s. For the aged bitumen with T_{rb} = 57 °C, P = 34 dmm, PI = −0.455 we obtain from Eq. (3.1) $\beta = 0.1984$ and from Eq. (3.2) $\eta = 3.928 \times 10^5$ MPa s. Then we obtain under formula (3.1) considering that glassy modulus E_g = 2460 MPa, the stiffness modulus of binder S = 190 MPa, which meets the requirement $S < 300$ MPa. From Eq. (4.1), we obtain $m_S = 0.398$, which exceeds the required value of m-value 0.300.

We shall try to reduce the low temperature grade of the AAB-1 bitumen to −34 °C. We should check the both criteria at T = −24 °C and at t = 60 s. As before, from Eq. (3.6) we have $\beta = 0.1984$, but from Eq. (3.2) $\eta = 3.928 \times 10^5$ MPa s, and formula (3.1) predicts the bitumen stiffness modulus S = 391 MPa which exceeds the allowable value of 300 MPa. Thus, low temperature remains equal to −28 °C

3. PG-grade of bitumen under the criteria of fatigue crack resistance.

According to the previous criteria, PG-grade for the bitumen AAB-1 complies with the requirements to PG 58-28. The Superpave requirements for resistance to fatigue for such a grade should be checked after the aging in PAV at T = 19 °C. From Eq. (3.6), we find $\beta = 0.1984$, from Eq. (3.2) η = 7.885 MPa s, from Eq. (3.47) $m = 0.6141$, and from Eq. (3.46) we obtain $\delta = 0.965$. Absolute value of complex modulus from Eq. (3.45) equals to $|G^*|$ = 7.547 MPa. Having calculated the product $|G^*|/\sin(\delta)$ = 6.20 MPa, we conclude that this index is more than maximum allowable value 5 MPa. Therefore, this bitumen AAB-1 failed the test for fatigue criteria for binders of grade PG 58-28.

Let us check, if this bitumen satisfies the requirements for binders of grade PG 58-22. The Superpave requirements for resistance to fatigue for such a grade should be checked after the aging in PAV at T = 22 °C. From Eq. (3.6), we have $\beta = 0.1984$, from Eq. (3.2) we obtain η = 3.695 MPa s, from Eq. (3.47) $m = 0.6491$, and from Eq. (3.46) we obtain $\delta = 1.02$. Absolute value of complex modulus from Eq. (3.45) equals to $|G^*|$ = 4.650 MPa. Calculating the product $|G^*|\sin(\delta)$ = 3.96 MPa, we conclude that is less than allowable value of 5 MPa. Therefore, the bitumen AAB-1 passed the test for criteria of fatigue for binders of grade PG 58-22 and passed the tests for other two criteria.

In this example, we determined the PG-grade of bitumen AAB-1 from MRL based on its traditional characteristics (penetration and softening point) using the proposed equations. The bitumen grade PG 58-22, which we determined, coincides with its grade shown in the library (Mortazavi and Moulthrop 1993) for the binder AAB-1, as well as with the grade determined by the authors of (Christensen and Anderson 1992) after measurements of the rheological properties of AAB-1 binder on DSR and BBR.

Nowadays, the Superpave approach is used for improvement of requirements to binders in Kazakhstan (Teltayev and Kaganovich 2011, 2012), where it was

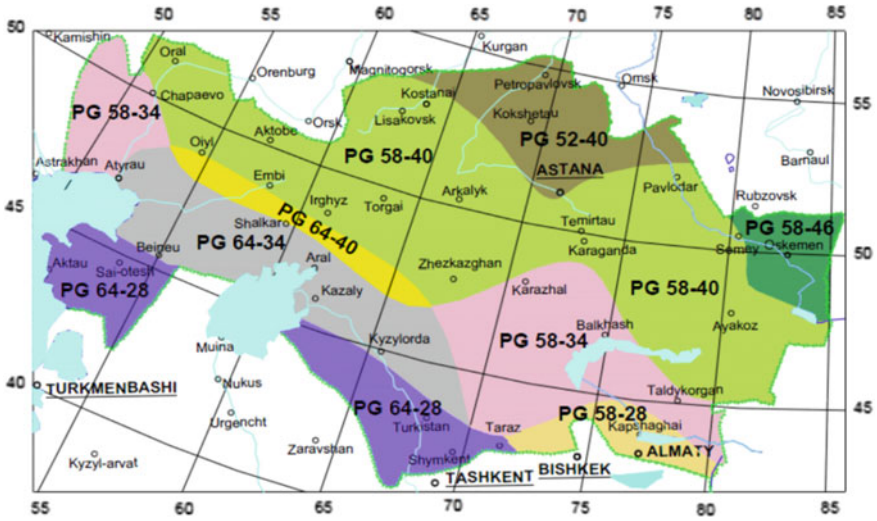

Fig. 4.4 Zoning map of Kazakhstan for selection of grade of the asphalt binder (Teltayev and Kaganovich 2011)

proposed to zone the country based on asphalt pavement performance criteria (Figs. 4.4).

4.4 Determining the Asphalt and Asphalt Concrete Relaxation Modulus as a Function of Temperature and Load Duration

Asphalt concrete is a typical composite material, and we can try to describe its mechanical behavior as a function of the properties of its individual constituents using the theory of composite materials (Broutman and Krock 1974). Below, we estimate the asphalt concrete relaxation modulus based on the approach suggested in (Christensen et al. 2003) using the mixture rule.

It is natural to assume the value of modulus of composite E_c consisting of two components with modulus E_1 and E_2, is within the range between moduli of constituents and depends on volume fractions c_1 and c_2 (meanwhile $c_1 + c_2 = 1$). There are two simplest rules of mixture. According to the Reuss's formula (Hill 1963), the effective modulus of composite E_R can be obtained by averaging the compliances of constituents from equation

$$\frac{1}{E_R} = \frac{c_1}{E_1} + \frac{c_2}{E_2} \tag{4.2}$$

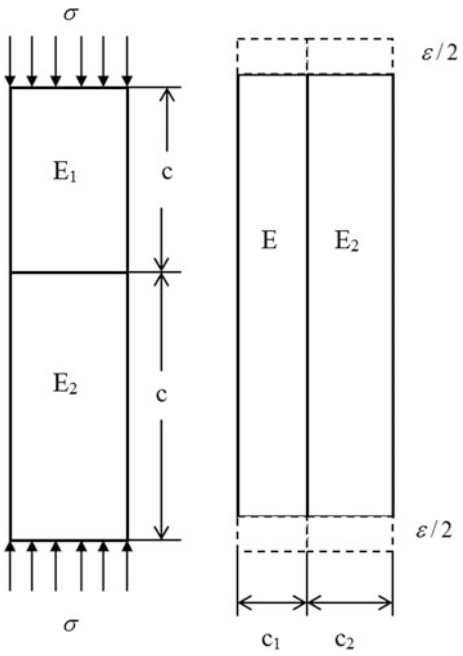

Fig. 4.5 Scheme of series and parallel connection for constituents of composite, resulting for composite stiffness modulus in evaluation of Reuss and Voigt respectively

that leads to

$$E_R = \frac{1}{c_1/E_1 + c_2/E_2} \tag{4.3}$$

According to the Voigt's formula (Hill 1963), the effective modulus of composite E_V can be obtained by averaging the moduli of constituents:

$$E_V = c_1 E_1 + c_2 E_2 \tag{4.4}$$

It has been proved that the effective modulus of composite E_c, consisting of two components with moduli E_1 and E_2, is always within Voigt and Reuss bounds (Hill 1963):

$$E_R \leq E_c \leq E_V \tag{4.5}$$

Simple interpretation can be given to the of Voigt's and Reuss's estimates. Let us start with the composite rod (Fig. 4.5 on the left) formed by the rods connected in series of similar width and thickness of the materials with stiffness modulus E_1 and E_2, and derive the effective modulus of this composite rod.

Obviously, a stress in the upper rod is equal to the stress of the bottom rod. The Absolute deformation of the composite rod with the length of $l = (l_1 + l_2)$ is equal to the sum of absolute deformations of its constituents

$$\Delta l = \frac{\sigma}{E_1} l_1 + \frac{\sigma}{E_2} l_2$$

and its strain is

$$\varepsilon = \frac{\sigma}{E_1} c_1 + \frac{\sigma}{E_2} c_2,$$

where $c_1 = l_1/l$, $c_2 = l_2/l$—volume fraction of materials with stiffness moduli E_1 and E_2 in composite rod, respectively. On the other hand, if to characterize the whole composite rod as produced from material with effective modulus E_c, then from the Hooke's law the strain is

$$\varepsilon = \frac{\sigma}{E_c}$$

Formula for modulus of composite from elastic elements connected in series results from two last equations:

$$\frac{1}{E_c} = \frac{c_1}{E_1} + \frac{c_2}{E_2}$$

and it coincides with Reuss's bound E_R (4.3).

Now we consider the composite rod formed by the two rods connected in parallel with the similar length of the thickness a and width l_1 and l_2 from the materials with moduli E_1 and E_2 (Fig. 4.5 on the right) and find the effective modulus of the composite rod. The strain ε of the composite rod is applied, and therefore the stresses in parallel rods are different:

$$\sigma_1 = E_1 \varepsilon,\ \sigma_2 = E_2 \varepsilon$$

To induce the strain ε, the longitudinal load Q should be applied to the end of composite rod

$$Q = \sigma_1 l_1 a + \sigma_2 l_2 a$$

The pressure on the end of the composite rod is

$$\sigma = \frac{Q}{(l_1 + l_2)a} = \sigma_1 c_1 + \sigma_2 c_2 = (E_1 c_1 + E_2 c_2)\varepsilon$$

where $c_1 = l_1/(l_1 + l_2)$, $c_2 = l_2/(l_1 + l_2)$—as before, they denote the volume fractions of materials with stiffness moduli E_1 and E_2 in a composite rod, respectively.

On the other hand, if to characterize a composite rod as produced from material with effective modulus E_c, then according to the Hooke's law, the stress equals to

$$\sigma = E_c \varepsilon.$$

Formula for modulus of composite from elastic elements connected in parallel results from two last equations:

$$E_c = E_1 c_1 + E_2 c_2$$

and it coincides with Voigt's bound E_V (4.4).

Therefore, the lower bound (Reuss) is found assuming that the stress is everywhere uniform formula (4.3) (connection in series) and the upper bound (Voigt) is found assuming that the strain is everywhere uniform formula (4.4).

In other words, according to Voigt-Reuss bounds, modulus of composite is between the harmonic mean modulus [formula (4.2)] and the arithmetic mean modulus [formula (4.4)] of its constituents. For a composite with equal volume fractions of constituents ($c_1 = c_2 = 0.5$) and twofold difference in moduli (E_1 = 1 МПа, E_2 = 2 МПА), we obtain that E_R = 1.33 MPa and E_V = 1.50 MPa, i.e., modulus of composite E_c should have the value within the narrow range 1.33–1.50 MPa. However, if the moduli of constituents differ in 100 times (E_1 = 1 МПа, E_2 = 100 МПА) then the Voigt-Reuss bounds show rather ambiguous range from 1.98 to 50.5 MPa for E_c.

The geometric details are the most difficult to know or measure. If we ignore (or do not know) the details of geometry, then the best we can do is estimate upper and lower bounds on the moduli. Lower and upper bounds for modulus of composite given by mixture rules (4.3) and (4.4) are known independently on geometry: which constituent is continuous (the matrix) and which constituent is the disperse phase (the inclusions); what is the shape of inclusions, etc. It opens up an opportunity for determining how close the actual modulus of composite is to the upper or lower Voigt-Reuss bounds. The bounds are powerful and robust tools. They give rigorous upper and lower limits on the moduli, given the composition. If you find that your measurements fall outside the bounds, then you have made a mistake.

In 1962, Hirsch proposed the model, combining formulas (4.2) and (4.4), for determining of E for cement concrete:

$$\frac{1}{E_c} = \frac{k}{E_1 c_1 + E_2 c_2} + (1 - k)\left(\frac{c_1}{E_1} + \frac{c_2}{E_2}\right) \tag{4.6}$$

where k is an empiric multiplier, showing how close concrete modulus is to the lower or upper bound and reflecting an impact of contact between inclusions and matrix. The parameter x can be interpreted as the ratio of phases in parallel arrangement to the total volume. When $x = 1$, the Hirsch model produces results identical to completely parallel phases [Eq. (4.4)], whereas when $x = 0$, it represents a pure series arrangement [Eq. (4.3)].

Christensen et al. (2003) used Hirsh's approach for predicting asphalt concrete modulus from binder modulus and volumetric properties of asphalt concrete. Consideration of air voids was an essential difficulty for that.

Christensen and his co-authors constructed the model of composite as the combination of elastic elements connected in parallel and series. Their contribution to the value of composite modulus is characterized by a "contact" function P_c. Equation for asphalt concrete modulus has the following form (Christensen et al. 2003):

$$E_{mix} = P_c\left[E_{agg} \cdot (1 - VMA) + E_b \cdot VMA \cdot VFA\right] + \frac{1 - P_c}{\frac{(1-VMA)}{E_{agg}} + \frac{VMA}{E_b \cdot VFA}} \tag{4.7}$$

where the empirical contact function is selected in the following form

$$P_c = \frac{\left(P_0 + E_b \cdot \frac{VFA}{VMA}\right)^{P_1}}{P_2 + \left(E_b \cdot \frac{VFA}{VMA}\right)^{P_1}} \tag{4.8}$$

and P_0, P_1 and P_2 are empirically determined constants.

In these formulas E_{agg} is the elasticity modulus of aggregate material; E_b is the modulus of binder; *VMA*—voids in of mineral aggregates (here—in unit fractions); *VFA* is fraction of air voids filled with binder. The difference $(1 - VMA)$ in Eq. (4.7) is the volume fraction of aggregate in asphalt concrete, and the product $VMA \cdot VFA$ is the volume fraction of binder. When $P_c = 1$, the formula (4.7) transforms into the mixture rule (4.4) (Voigt's formula). When $P_c = 0$ it is very close to the mixture rule (4.2) (Reuss's formula).

Equation (4.7) was proposed in (Christensen et al. 2003) as applied to the absolute value of asphalt concrete complex modulus, i.e., for dynamic modulus $E_d(\omega) = |E^*(\omega)|$. In other words, the authors (Christensen et al. 2003) considered modulus E_{mix} in formula (4.7) as equal to the $E_{mix\,d}(\omega)$. Average elasticity modulus for aggregate was assumed in (Christensen et al. 2003) equal to E_{agg} = 29,000 MPa, and then was reduced to 19,000 MPa in (Zofka et al. 2005). The modulus of binder in Eq. (4.7) was set equal to its dynamic modulus $E_b = E_{b\,d}(\omega)$ in (Christensen et al. 2003), which was measured at various temperatures and frequencies of cyclic loading.

Substantial set of data of modulus values for a wide range of mixtures was fitted to the model using non-linear least squares method. The database of mixture moduli from which the authors (Christensen et al. 2003) selected values of constants P_0, P_1 and P_2 in contact function (4.8), covered the range of voids in mineral aggregate from $VMA = 0.137$ to 0.216, fraction of air voids filled with asphalt from $VFA = 0.387$ to 0.68, air voids 5.6–11.2%. Dynamic modulus was measured at the frequencies 0.1 and 5 rad/s, and at the temperatures from −9 to +54 °C. Database included also the test results for asphalt concrete samples in shearing by cyclic loads on the device SSP (Superpave Shear Tester) and in compression on the device SPT (Simple Performance Tester). The aggregate was with grains of maximum size for 9.5, 19 or 37.5 mm. Dynamic modulus of binders was measured on DSR (Dynamic Shear Rheometer) at the same frequencies and temperatures as for asphalt concrete. According to these data, the authors of (Christensen et al. 2003) obtained the values of coefficients P_0, P_1 and P_2 in Eq. (4.8) for contact function.

Unfortunately, in expression for the contact function dimension of coefficients P_0 and P_2 depend on dimension of modulus E_b. After recalculation their values as applied to the modulus of binder in MPa, we obtained $P_0 = 0.138$, $P_1 = 0.58$ and $P_2 = 36.25$. Figure 4.6 shows the example of contact function P_c.

Suppose that empiric contact function P_c, which shows a relative contribution of parallel and series connected components of the mixture, can be applied for dynamic modulus $E_{mix\,d}(\omega)$ as well as for its relaxation modulus $E_{mix}(t)$. Then we can use the Eq. (4.7) for evaluation of asphalt concrete relaxation modulus as a function of the content and relaxation modulus $E(t)$ of bitumen. It is sufficient to replace in the formula (4.7) $E_{mix} = E_{mix}(t)$ and $E_b = E(t)$, where the relaxation modulus of bitumen is obtained using Eq. (3.34b):

$$E(t) = E_g \left[1 + \left(\frac{E_g t}{3\eta} \right)^b \right]^{-\left(1+\frac{1}{b}\right)} \tag{4.9}$$

Example 1 Let us give a detailed example of calculations. We shall compute the relaxation modulus of asphalt concrete, prepared with bitumen having the softening point $T_{rb} = 50$ °C and penetration 80 dmm (penetration index $PI = 0$), at the temperature $T = 20$ °C and load duration $t = 0.1$ s. Density of bitumen is 1.03 g/cm^3, average density of aggregates is 2.703 g/cm^3, average density of asphalt concrete is 2.442 g/cm^3. Bitumen content based on weight of aggregate is 5.60%, i.e., its content based on mix is $5.6 \times 100/(100 + 5.6) = 5.3\%$ of bitumen and 94.7% of stone material. Let us assume that the value for adsorption of bitumen is 0.8%. Then the portion of effective bitumen is $5.3 - 0.008 \times 94.7 = 4.54\%$ of the mixture weight. The volume fraction of effective bitumen in asphalt concrete equals to $4.54 \times 2.442/1.03 = 10.8\% = 0.108$. Volume fraction of aggregate is $94.7 \times 2.442/2.703 = 85.6\% = 0.856$. The volume fraction of voids in mineral aggregate is $VMA = 1 - 0.856 = 0.144$. The volume fraction of air voids in asphalt concrete is $0.144 - 0.108 = 0.036$ (i.e., 3.6%). A portion of voids, filled with

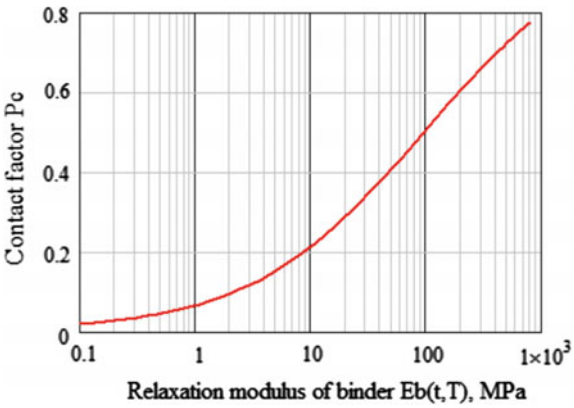

Fig. 4.6 Example of the contact factor for $VMA = 0.144$ and $VFA = 0.75$

bitumen, equals to VFA = 0.108/0.144 = 0.75. First, we find the exponent b using Eq. (3.34b) to obtain the relaxation modulus of bitumen. For PI = 0, we find from formula (3.6) β = 0.1794 and from (3.35) we obtain b = 0.1914. The viscosity of bitumen at T = 20 °C from formula (3.2) is equal to η = 1.217 MPa s. The relaxation modulus of bitumen at t = 0.1 s is determined by the formula (3.34b):

$$E = 2.46 \times 10^3 \left[1 + \left(\frac{2.46 \times 10^3 \cdot 0.1}{3 \cdot 1.217}\right)^{0.1914}\right]^{-\left((1+\frac{1}{0.1914}\right)} = 1.637 \text{ MPa}$$

A value of contact function from Eq. (4.8) equals to

$$P_c = \frac{\left(0.138 + 1.637 \cdot \frac{0.75}{0.144}\right)^{0.58}}{36.25 + \left(1.637 \cdot \frac{0.75}{0.144}\right)^{0.58}} = 0.088$$

Finally, we calculate the asphalt concrete relaxation modulus using Eq. (4.7):

$$E_{mix}(t) = 0.088\left[1.9 \times 10^4 (1 - 0.144) + 1.636 \cdot 0.144 \cdot 0.75\right] + \frac{(1 - 0.088)}{\frac{(1-0.144)}{1.9 \times 10^4} + \frac{0.144}{1.636 \cdot 0.75}}$$

$$= 1440 \text{ MPa}$$

Figure 4.7 shows dependence of asphalt concrete relaxation modulus on temperature, and Fig. 4.8 shows the relation of relaxation moduli of asphalt concrete and bitumen within the range of temperatures from −25 °C to +40 °C at the load duration of 0.1 s. It may seem that calculations are time-consuming, but it only took 0.09 s to calculate the relaxation modulus of asphalt concrete for 65 values of temperature together with the construction of graph in MATCAD-14, the package that the authors used (Fig. 4.8).

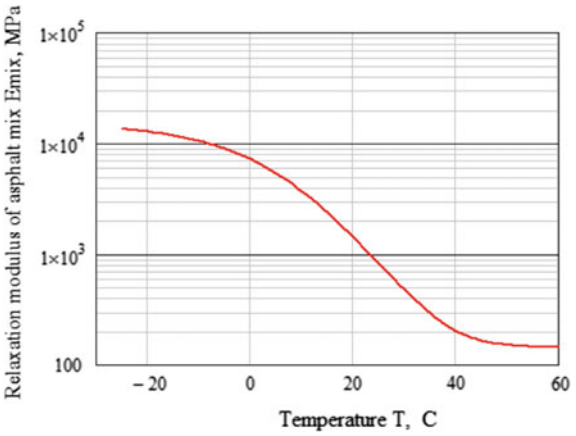

Fig. 4.7 Dependence of asphalt concrete relaxation modulus on temperature

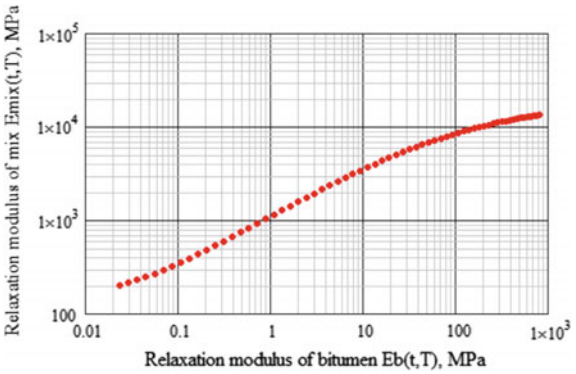

Fig. 4.8 Relation between relaxation moduli of asphalt concrete and bitumen

Let us evaluate the impact of aging on relaxation modulus of asphalt concrete, supposing that penetration of bitumen is 0.4 of its original value, and softening point is increased for 25% five-seven years later. Figure 4.9 shows the dependence of relaxation modulus on temperature calculated from Eq. (4.7) for the same asphalt concrete that was considered in the previous example, but for original bitumen with T_{rb} = 45 °C and *Pen* = 90 dmm. For example, modulus of original asphalt concrete is obtained as equal to 6600 MPa, and it equals to 8700 MPa after ageing for the typical spring temperature of pavement 5 °C at t = 0.1 s, with *VMA* = 0.144 and *VFA* = 0.75. At temperature of 20 °C, the asphalt concrete modulus after aging is 2.5 times greater than the original modulus.

It is a matter of interest to compare the values E_{mix} from Eq. (4.7) with experimental data. In Russia and Ukraine the researchers of SoyuzdorNII, Gosdor NII and KhADI tested the samples of asphalt concrete for bending and determined value of so-called "elasticity modulus" with load duration 0.1 s during development the Guide for pavement design VSN 46-83. For example, the technical report of GosdorNII (1979) "To complete the Guide for design of flexible pavement" shows the test results for asphalt concrete, prepared on the original bitumen of penetration

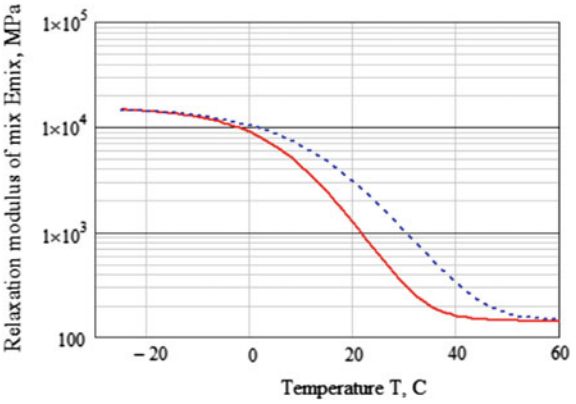

Fig. 4.9 Impact of aging on asphalt concrete relaxation modulus: *Lower curve*—for the original bitumen with T_{rb} = 45 °C and *Pen* = 90 dmm, *upper curve* for bitumen after ageing in 5–7 years with T_{rb} = 56 °C and *Pen* = 36 dmm; load duration 0.1 s

grade BND90/130 with T_{rb} = 47 °C and Pen = 114 dmm. The binder content was 5.5% based on aggregate weight. The mixture contained 40% of granite crushed stone, crushed sand and limestone mineral filler. Porosity was about 4%. Volume fraction of bitumen was around 12% (data on absorption are not available).

The following values for asphalt concrete were obtained by testing of samples with dimensions 4 × 4 × 16 cm at t = 0.1 s: 4130, 1830 and 1090 MPa at T = 0, 10 and 20 °C, respectively. Calculation using formula (4.7) with VMA = 0.16 and VFA = 0.75 shows at such temperatures the values of 5400, 2500 and 920 MPa. That is not to say that agreement is good, but you can consider it acceptable as the first approximation for 10–30% deviation.

Let us evaluate the impact of inaccuracy of information on penetration and the softening temperature on the predicted relaxation moduli of bitumen and asphalt concrete. According to ASTM D 36, the average experimental softening point should be rounded to the nearest values of 0.2 or 0.5 °C depending on the applied thermometer. The standard deviation for laboratory technician is 0.72 °C, and the standard deviation for different laboratories is 1.08 °C. For the penetration test, the standard deviation is σ = 0.8 dmm for penetration less than 60 dmm (ASTMD 5-06) for determination of penetration by the laboratory technician, and the standard deviation for different laboratories is $\sigma = 0.8 + 0.03(Pen - 60)$ dmm if penetration is greater than 60 dmm. For example, standard deviation is 1.4 dmm for penetration of 80 dmm for one laboratory technician. It is approximately three times more for different laboratories.

Let us consider the following example for evaluation of possible influence of these inaccuracies on the predicted viscoelastic properties. We have penetration index PI = 0 with Pen = 80 dmm and the softening point T_{rb} = 50 °C; from formula (3.34b) the relaxation modulus of bitumen equals to $E(t)$ = 11.2 MPa for t = 0.1c and T = 10 °C, and from formula (4.7) the asphalt concrete relaxation modulus is E_{mix} = 3730 MPa for the mixture with the same characteristics as in example on Figs. 4.5 and 4.6. If measured values were Pen = 78 dmm and T_{rb} = 49 °C (PI = −0.342), then the bitumen modulus would be $E(t)$ = 13.6 MPa, and from Eq. (4.7), the asphalt concrete relaxation modulus E_{mix} = 4050 MPa. It means that due to inaccuracies of measuring the penetration and the softening temperature of bitumen the error can account for approximately 20% for the predicted bitumen modulus and 9% for the predicted asphalt concrete relaxation modulus.

4.5 Determining of the Asphalt Concrete Complex Modulus

As we mentioned before, the most suitable method for determining of viscoelastic properties of bitumen and asphalt concrete is testing under sinusoidal loading conditions. It is useful to have an opportunity to predict the asphalt concrete complex modulus, i.e., its absolute value $E_{mix\,d}$ and its phase angle δ_{mix}.

We shall use the formula of Christensen and his co-authors (Christensen et al. 2003) like Hirsh model for this purpose, having added it with our formula (3.38) for determining of bitumen dynamic modulus E_{bd} depending on its penetration and the softening temperature.

Dynamic modulus and phase angle of asphalt concrete from equation proposed in (Christensen et al. 2003) are:

$$E_{mix\,d} = P_{c\,d}\left[E_{agg}\cdot(1-VMA)+E_{b\,d}\cdot VMA\cdot VFA\right]+\frac{1-P_{c\,d}}{\frac{(1-VMA)}{E_{agg}}+\frac{VMA}{E_{b\,d}\cdot VFA}} \tag{4.10}$$

$$\delta_{mix} = -21\cdot(\log(P_{c\,d}))^2 - 55\cdot\log(P_{c\,d}) \tag{4.11}$$

where the contact function (Christensen et al. 2003) is determined by the formula

$$P_{c\,d} = \frac{\left(P_0+E_{b\,d}\cdot\frac{VFA}{VMA}\right)^{P_1}}{P_2+\left(E_{b\,d}\cdot\frac{VFA}{VMA}\right)^{P_1}} \tag{4.12}$$

in which $P_0 = 0.138$, $P_1 = 0.58$ and $P_2 = 36.25$.

Dynamic modulus of bitumen in these formulas, we can obtain from our Eq. (3.38)

$$E_{b\,d}(\omega) = \frac{E_g}{\Gamma(1+m(\omega))}\left[1+\left(\frac{E_g}{3\eta\omega}\right)^{\beta}\right]^{-\frac{1}{\beta}},\ m(\omega) = \frac{\left(E_g/3\eta\omega\right)^{\beta}}{1+\left(E_g/3\eta\omega\right)^{\beta}},$$

Bitumen viscosity η can be obtained from Eq. (3.33) and exponent β—from Eq. (3.6).

Example 2 We shall compute the asphalt concrete dynamic modulus of the same mixture as in Example 1 above at the temperature $T = 20$ °C and load frequency $\omega = 10$ rad/s. Voids in mineral aggregate is $VMA = 0.144$; fraction of voids, filled with bitumen equals to $VFA = 0.75$. For penetration index $PI = 0$ from Eq. (3.6) it follows that $\beta = 0.1794$. Viscosity of bitumen equals to $\eta = 1.217$ MPa s at $T = 20$ °C from Eq. (3.2). The dynamic modulus of bitumen we calculate from Eq. (3.48):

$$m(\omega) = \frac{(2.46\times10^3/3\cdot1.217\times10)^{0.1794}}{1+(2.46\times10^3/3\cdot1.217\times10)^{0.1794}} = 0.68,$$

$$E_{b\,d}(\omega) = \frac{2.46\times10^3}{\Gamma(1+m(10))}\left[1+\left(\frac{2.46\times10^3}{3\cdot1.217\times10}\right)^{0.1794}\right]^{-\frac{1}{0.1794}} = 4.713\,\text{MPa}.$$

The value of contact function from Eq. (4.12) is

$$P_{cd} = \frac{\left(0.138 + 4.713 \cdot \frac{0.75}{0.144}\right)^{0.58}}{36.25 + \left(4.713 \cdot \frac{0.75}{0.144}\right)^{0.58}} = 0.15$$

The dynamic modulus of asphalt concrete from Eq. (4.10):

$$E_{mix\,d} = 0.15\left[1.9 \times 10^4(1 - 0.144) + 4.713 \cdot 0.144 \cdot 0.75\right] + \frac{1 - 0.15}{\frac{(1-0.144)}{1.9\times10^4} + \frac{0.144}{4.713\cdot0.75}} = 2461\ \text{MPa}.$$

Phase angle from Eq. (4.11) (Christensen et al. 2003) is:

$$\delta_{mix} = -21 \cdot (\log(0.15))^2 - 55 \cdot \log(0.15) = 31^0.$$

One can notice that asphalt concrete dynamic modulus for this example at the frequency ω = 10 rad/s is greater than relaxation modulus in the first example at load duration t = 0.1 s in 2461/1440 = 1.78 times. Figure 4.10 shows a comparison of relaxation modulus (at t = 0.1 s) and dynamic modulus (at ω = 10 rad/s) as the functions of temperature.

As Fig. 4.10 shows, the dynamic modulus exceeds asphalt concrete relaxation modulus at $t = 1/\omega$ for all temperatures, except for very low and very high. The ratio of $E_{mix\,d}$ and E_{mix} reaches 2.1 at 34 °C in this example.

Figure 4.11 shows the results of calculation for phase angle at different temperatures from formula (4.11) (Christensen et al. 2003). One can see that the phase angle for asphalt concrete as a function of temperature has a maximum.

It is interesting to compare the results of prediction with measurement data. However, not all publications that present the experimental results for determination of dynamic modulus report the required data for the properties of bitumen and its

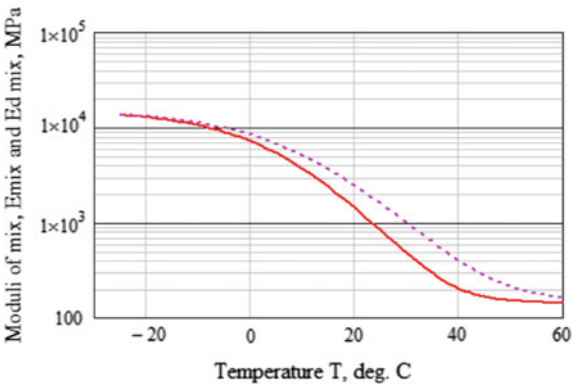

Fig. 4.10 The relaxation modulus (*lower curve*, t = 0.1 s) and the dynamic modulus (*upper curve*, ω = 10 rad/s) for asphalt concrete at T = 20 °C

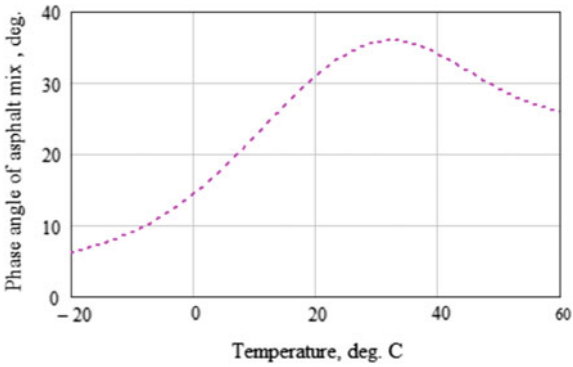

Fig. 4.11 Phase angle of asphalt concrete at frequency ω = 10 rad/s

content in asphalt mix. The paper of Pell and Cooper reports such data although it is devoted to the tests of asphalt concrete for fatigue (Pell and Cooper 1975). Pell and Cooper tested 48 mixes of asphalt concrete used in England for the surface course and base course. Mixes were prepared using bitumen with penetration from 40 to 200 dmm. Mineral aggregates were represented by crushed stone of maximum size 19 mm, sand of maximum size 3 mm, and mineral filler (or without it). Complex modulus of mixture was determined by applying the load to the cantilever sample with frequency of 16 Hz after 500 cycles of loading. For example, the dense mixture A8 for the base course contained 60% of crushed stone by weight, 34% of sand and 6% of bitumen with penetration of 39 dmm (at 25 °C) and the softening point 61 °C. The composition of asphalt concrete by volume is the following: aggregates—81.6%, bitumen—14.2%, air voids—4.2%. The measured asphalt concrete dynamic modulus was 8500 MPa at 10 °C and at frequency 16 Hz (Pell and Cooper 1975).

Let us calculate the dynamic modulus using our formulas. Penetration index for bitumen is equal to 0.63. Circular frequency is $\omega = 2\ \pi \cdot 16 = 100.5$ rad/s. Voids in mineral aggregate VMA = 18.4%. Fraction of voids filled with bitumen is VFA = 14.2/18.4 = 0.772. From Eq. (4.10), we obtain the dynamic modulus $E_{mix\,d}$ = 7996 MPa at the temperature 10 °C, which differs from the measured modulus for 6% only.

Mixture for the base course B1 was porous and contained by weight 95.3% of crushed stone and 4.7% of bitumen with penetration 197 dmm (at 25 °C) and the softening point 40 °C (penetration index $PI = -0.095$). The composition of asphalt concrete by volume is the following: aggregates—82.6%, bitumen—10.5%, air-voids—6.9%. The measured asphalt concrete dynamic modulus was of about 5100 MPa at 10 °C and frequency 16 Hz (Pell and Cooper 1975). From Eq. (4.10), we obtain the dynamic modulus $E_{mix\,d}$ = 4376 МПа at the temperature 10 °C and frequency $\omega = 2\ \pi \cdot 16 = 100.5$ rad/s, which differs from the measured one for 14.2%.

Although the Eqs. (4.7) and (4.10) based on Hirsh model (1962) are not perfect, the moduli predictions might be almost as accurate as independent measurements of moduli. For many pavement design and analysis procedures, predicted modulus values of asphalt concrete mixtures can be effectively used.

4.6 Low Temperature Cracking Problem for Asphalt Pavement

Thermal cracking in asphalt pavements has become a research focus in the asphalt materials community. Low temperature cracking is one of the major causes of failure of asphalt pavements in cold weather climates, including Canada, north of the United States, Russia, Ukraine, Kazakhstan and other countries at extreme northern and southern latitudes, however, pavement design methods do not directly address low temperature cracking. For instance, Kazakhstan is the ninth largest territory in the world with continental climate, warm summers and very cold winters. The minimum pavement design temperature in Kazakhstan is between −28 and −46 °C (Fig. 4.4). The oxidized bitumen from Western Siberian oil obtained in five oil refineries has been used for road construction. Typical thickness of new asphalt pavement is currently around 15 cm. After the first winter, 20–25 transverse cracks per kilometer appear, after the second or the third winter the number of cracks is 45–50.

Thermal cracking is believed to be associated with the volumetric change in the asphalt concrete layer. This phenomenon is due to the thermal stresses that develop in the restrained top layers of asphalt pavements when temperature drops. The stress increases as the temperature drops, and reaches the material strength at which point a crack initiates and eventually propagates. To better understand how to reduce the low temperature cracking, a comprehensive mechanistic model that includes rheological and fracture properties of asphalt mixture is needed.

Monismith et al. (1965) developed a theoretical calculation method for the thermally induced stress in asphalt pavement as in an infinite viscoelastic beam-based on Humphreys and Martin (1963) solution. This method is currently used for the estimation of critical cracking temperatureat which the mixture thermal stress curve and binder strength curve intersect. Christison et al. (1972) employed five different methods of stress computation and concluded that a potential of low temperature cracking can be evaluated if the mix stiffness and strength characteristics are known. Bouldin et al. (2000) considered the thermally induced stress in asphalt binder as in viscoelastic bar and reported that the midpoint of the binder's glass transition is close to the pavement critical cracking temperature. They also noted that mix with blown bitumen formed severe, wide cracks. The main objective of our study described in this paragraph was to develop relationships for prediction of critical low cracking temperature based on prediction of the rheological properties and tensile strength of asphalt concrete.

To analyze the temperature induced stresses, we need the uniaxial relaxation modulus of asphalt concrete $E_{mix}(t)$. Christensen and Bonaquist (2015) recently improved their model described in n. 4.4:

$$E_{mix}(t) = P_c\left[E_{agg} \cdot (1 - VMA) + E_b(t) \cdot VFA \cdot VMA\right] \tag{4.13}$$

$$P_c = 0.006 + 0.994\left[1 + \exp\left(-(0.663 + 0.586\ln(VFA \cdot E_b(t)/3) - 12.9VMA - 0.17\ln(\varepsilon_s \times 10^6))\right)\right]^{-1}$$

where: $E_b(t)$ is relaxation modulus of binder (MPa), E_{agg} is elastic modulus of aggregate (MPa), VMA are voids in mineral aggregate (volume fraction), VFA are voids filled with asphalt (volume fraction), ε_s = 0.0001 is the standard target strain, and P_c is the contact factor introduced in (Christensen and Bonaquist 2015). The same model can be used for the stiffness modulus of asphalt concrete $S_{mix}(t)$ if $E_b(t)$ is replaced by binder stiffness $S(t)$ defined according to Eq. (2.8).

To estimate a critical temperature, we need the tensile strength of asphalt concrete as a function of temperature and rate of loading. Heukelom (1966) demonstrated that the tensile strength of mix is related to the properties of bitumen contained herein. Based on tensile strength measurements of eight dense graded mixes at a variety of temperatures and speeds, Heukelom has showed that the relative tensile strength, i.e., the tensile strength divided by its maximum value, can be represented by one curve for all mixes tested as a function of the stiffness of bitumen recovered (Heukelom 1966, Fig. 22). We approximated the Heukelom's curve for relative strength by equation

$$R = \frac{0.774 + 0.039r + 0.141r^{4.547}}{1 + 0.026r^{3.608} \cdot \exp(1.245r)} \tag{4.14}$$

where $r = \log(E_g/S)$, E_g is the uniaxial glassy modulus of binder (MPa), S is the binder stiffness (MPa).

Molenaar and Li (2014) based on testing of seven nixes proposed an empirical equation to estimate the maximal tensile strength of asphalt concrete P_h as a function of mixture stiffness and the volumetric composition:

$$P_h = 0.505 \cdot S_{mix}^{0.308} \cdot VFA^{0.849} \tag{4.15}$$

The combination of our Eq. (4.14) based on the Heukelom's curve for relative strength of mix with empirical Eq. (4.15) for the maximal strength of mix leads to the following expression for tensile strength f as a function of temperature T and the loading time t:

$$f = 0.505 \cdot S_{mix}^{0.308} \cdot VFA^{0.849} \cdot \frac{0.774 + 0.039r + 0.141r^{4.547}}{1 + 0.026r^{3.608} \cdot \exp(1.245r)} \tag{4.16}$$

where: S is the binder stiffness (MPa) defined in Eq. (3.1) as a function of time and temperature, S_{mix} is the mix stiffness at T = 20 °C and at fixed loading time of 0.06 s, and f is the tensile strength under rectangular pulse loading of duration t.

Equation (4.16) relates the tensile strength of asphalt concrete f with temperature T and time to failure t_f in terms of the binder creep stiffness $S(t_f)$, as Heukelom suggested (1966). At constant strain rate V_ε, the tensile strength f_ε in the left hand side of Eq. (4.16) can be expressed as a product of time to failure, the strain rate, and the secant modulus at failure $H_{mix}(t_f)$. The secant modulus $H_{mix}(t)$ is related to the relaxation modulus $E_{mix}(t)$ by the following equation (Smith 1976):

$$H_{mix}(t) = \frac{1}{t}\int_0^t E_{mix}(t-\tau)d\tau \tag{4.17}$$

Thus using Eq. (4.17), one can find the time to failure t_f numerically as a root of the following equation:

$$t_f V_\varepsilon H_{mix}(t_f) = 0.505 \cdot S_{mix}^{0.308} \cdot VFA^{0.849} \cdot \frac{0.774 + 0.039r + 0.141r^{4.547}}{1 + 0.026r^{3.608} \cdot \exp(1.245r)} \tag{4.18}$$

where $r = \log\left(E_g / S\left(t_f\right)\right)$.

Then, the tensile strength of asphalt concrete f_ε at constant strain rate V_ε can be calculated as

$$f_\varepsilon = t_f V_\varepsilon H_{mix}(t_f) \tag{4.19}$$

In the Kazakhstan Highway Research Institute, the uniaxial tensile tests were performed on testing system TRAVIS (Infra Test GmbH) (Fig. 4.12). This testing system includes a compact test frame integrated in the temperature chamber. The load is applied to the specimen via heavy-duty screw jack and stepping motor. An electronic load cell is directly attached to the spindle. The equipment is controlled by a PC connected to the motor and the transducers. PC is used for measurement data logging, control of the test procedure and the temperature test chamber.

Dense graded asphalt mixture was prepared with the use of granite aggregate fractions of 5–10 mm (20%), 10–15 mm (13%), and 15–20 mm (10%) from the Novo-Alekseevsk rock pit (Almaty region); sand of fraction 0–5 mm (50%) from the plant Asphaltconcrete-1 (Almaty city) and activated filler (7%) from the Kordai rock pit (Zhambyl region). The air-blown bitumen was produced by the Pavlodar petrochemical plant from the crude oil of Western Siberia (Russia). After short-time aging, the bitumen penetration was 70 dmm (at 25 °C), softening temperature T_{rb} = 48 °C, and PI = −0.91. A mixture designated as K2 was prepared with 4.8% of bitumen by weight of aggregates. Mixture was compacted with the Cooper roller compactor (model CRT-RC2S) to the average void content of 3.6%. Rectangular specimens (50 × 50 × 160 mm) were then sawed from these slabs and glued with

Fig. 4.12 Testing system TRAVIS (InfraTest GmbH)

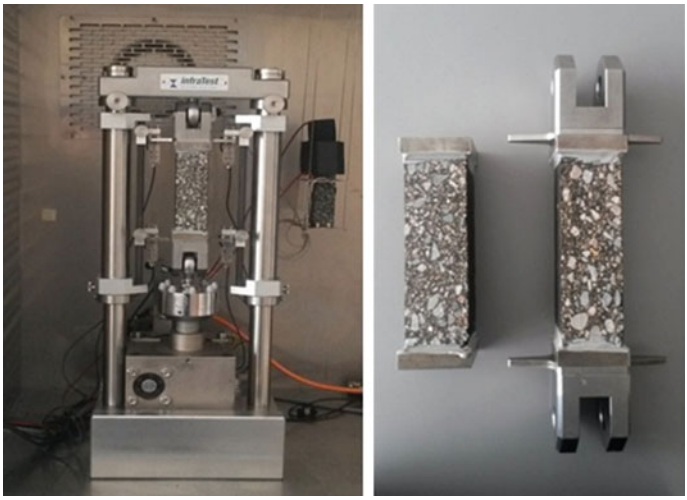

Fig. 4.13 Details of the direct tensile test setup

the epoxy resin to the mounts (Fig. 4.13). Specimens were tested with nominal deformation rate 1 mm/min ($V_\varepsilon = 1 \times 10^{-4}$/sec). Tests were performed at temperatures 20, 10, 0, −10, −20, and −30 °C. The strength values were obtained from five tensile tests for all temperatures (Fig. 4.14). The average coefficient of variation was of 15.6%.

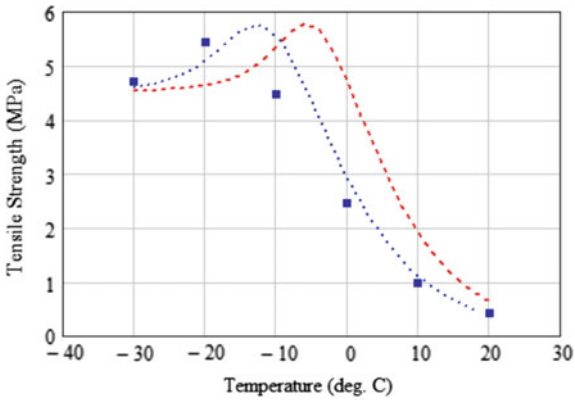

Fig. 4.14 Measured and calculated tensile strength values: *dashed red curve*—calculated from Eq. (4.18) and (4.19) at constant strain rate $V_\varepsilon = 1 \times 10^{-4}$/sec, *dotted blue curve*—calculated from Eq. (4.16) for average time to failure t_f = 40 s

Figure 4.14 presents the comparison of the measured tensile strength of asphalt concrete samples and the strength of asphalt concrete predicted form Eqs. (4.18) and (4.19) for $V_\varepsilon = 1 \times 10^{-4}$/s and the mix volumetric properties VMA = 0.144, and VFA = 0.75 (red curve). The modulus of aggregate of bulk specific gravity G_{sb} = 2.760 was estimated using the correlation recommended in (Christensen and Bonaquist 2015) as $E_{agg} = 7650 G_{sb}^{1.59} = 36{,}000$ MPa. In Fig. 4.14, the calculated maximal strength and the shape of the predicted curve (dashed red) agree with measured tensile strength but the predicted curve is constantly shifted along the temperature axis to higher temperatures.

The most probable reason of shift is the effect of machine compliance on specimen strain rates. To facilitate data acquisition, the system TRAVIS was designed to extend the testing time at cold temperatures. As a result, because of machine compliance, the on-specimen strain rate was not constant, given that the crosshead displacement rate 1 mm/min remains constant throughout the test, due to the high stiffness of the material at low temperatures. Actual time to failure was between 40 and 50 s at temperatures 20, 10, 0, −10,–20 °C and around 20–25 s at T = −30 °C. To check the validity of this reason, we calculated the tensile strength of the same asphalt mix K2 at loading time 40 s from Eq. (4.16) for PI = −0.91, T_{rb} = 48 °C, VMA = 0.144, and VFA = 0.75 (dotted blue curve in Fig. 4.14). Shift of calculated curve to cold temperatures closer to measured strengths confirms the significant effect of machine compliance on test results.

If a true constant-rate-of-deformation test is to be performed on asphalt concrete, feedback to loading unite must be from on-specimen LVDTs and not from the cross-head displacement as was the case in this experiment. This constant-strain loading requirement is difficult to achieve. Moreover, although used by some researchers (Bouldin et al. 2000; Christison et al. 1972; Stock and Arand 1993), the advantages of constant strain-rate test are doubtful of its value for low-temperature cracking problem because the longitudinal strain in asphalt pavement induced by cooling is unrealized, i.e., equals to zero up to appearance of the transverse crack.

For the single event low temperature cracking analysis, the stress-controlled strength test looks more important than strain-controlled test.

At constant stress rate V_σ, time to failure equals the tensile strength f_σ over the stress rate $t_f = f_\sigma / V_\sigma$. In that case, the binder stiffness in the right hand side of Eq. (4.16) depends on tensile strength and the stress rate. The tensile strength f_σ at constant stress rate V_σ can be found numerically from Eq. (4.20) as a function of T and V_σ:

$$f_\sigma = 0.505 \cdot S_{mix}^{0.308} \cdot VFA^{0.849} \cdot \frac{0.774 + 0.039r + 0.141r^{4.547}}{1 + 0.026r^{3.608} \cdot \exp(1.245r)} \tag{4.20}$$

where $r = \log\left(E_g / S\left(t_f = f_\sigma / V_\sigma\right)\right)$.

Fig. 4.15 depicts the tensile strength calculated from Eq. (4.20) for the same as before asphalt mix K2 at different constant stress rates.

To illustrate, the mix strength at T = −2 °C and V_σ = 0.05 MPa/s equals to 3.1 MPa (Fig. 4.15). In that case, time to failure is 62 s; stiffness of binder at T = 20 °C and t = 0.06 s according to Eq. (3.1) is S = 6.02 MPa; stiffness of mix at T = 20 °C and t = 0.06 s from Eq. (4.13) equals to S_{mix} = 6040 MPa. Parameter r is equal to $r = \log(2460/S(T = -2\,°\text{C}, t = 62s)) = 2.611$, and the right hand side of Eq. (4.20) returns the tensile strength of 3.1 MPa. A tenfold increase in stress rate shifts the strength versus temperature curve to higher temperatures as much as around 7 °C (Fig. 4.15).

The stress-rate dependent tensile strength f_σ was used to estimate the critical single-event cracking temperature. The critical cracking temperature (T_{cr}) is defined as the temperature at which the asphalt concrete tensile strength at constant stress rate crosses the thermal stress curve.

Low temperature induced stresses in asphalt pavement were calculated as in an infinite viscoelastic beam resting on frictionless foundation. The increment of temperature dT during the period $d\tau$ between τ and $\tau + d\tau$ is $dT = [\partial T(\tau)/\partial\tau]d\tau$. In case of unrestrained beam, the increment of associated thermal strain is $d\varepsilon(\tau) =$

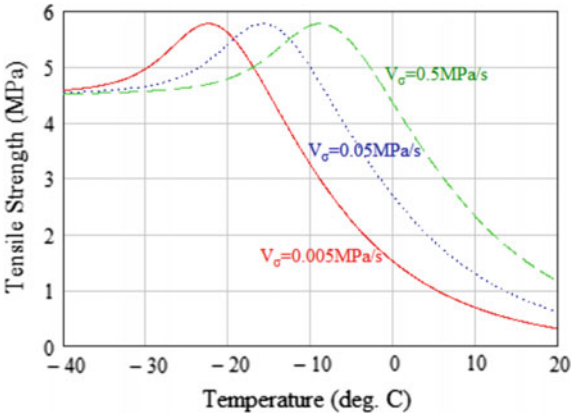

Fig. 4.15 Tensile strength of asphalt concrete as a function of temperature calculated from Eq. (4.20) at different stress rates

$\alpha_{mix}(T(\tau))dT$ where α_{mix} is the asphalt mixture coefficient of thermal contraction (/°C) which can be temperature dependent. When the temperature drops, the beam tends to contract its length but the thermal strains are unrealized in continuous infinite beam. That causes the thermal stresses in pavement. The incremental thermal strain $d\varepsilon(\tau)$ is unrealized due to counteraction of incremental stress $d\sigma(\tau) = -E_{mix}(\tau)d\varepsilon(\tau)$. The increment of thermal stress induced during the period $d\tau$ is

$$d\sigma(\tau) = -E_{mix}(\tau)\alpha_{mix}(T(\tau))[\partial T(\tau)/\partial\tau]d\tau \tag{4.21}$$

where $E_{mix}(t)$ is the relaxation modulus of asphalt concrete (MPa).

Summation of the increments (4.21) induced by action at the time points τ during the whole time elapsed t leads to the following expression for the longitudinal thermal stress in pavement as a function of time:

$$\sigma(t) = -\int_0^t \alpha_{mix}(T(\tau)) \cdot E_{mix}(\xi(t) - \xi(\tau)) \cdot (\partial T(\tau)/\partial\tau)d\tau \tag{4.22}$$

Here t is the present time (s), τ is the passed time (s), $T(\tau)$ is the temperature variation with time (°C), and $\xi(t)$ is the reduced time $\xi(t) = \int_0^t d\tau/a_T(T(\tau))$.

To illustrate the proposed methodology of critical temperature prediction we consider an example. Coefficient of thermal contraction was assumed constant $\alpha_{mix} = 2.5 \times 10^{-5}$/°C. The properties of binder and mix were taken as before: $T_{rb} = 48$ °C, $PI = -0.91$, $E_{agg} = 36000$ MPa, VMA = 0.144, VFA = 0.75. The relaxation modulus of asphalt concrete was determined from Christensen-Bonaquist model—Eq. (4.13).

A sinusoidal variation between the maximum and minimum temperatures during a day was assumed in our example (Fig. 4.16).

The temperature drops from 5 to −35 °C and returns to 5 °C over 24-hour period. Thermal stress build up was calculated according to Eq. (4.22). A tensile stress rate was estimated as $V_\sigma(t) = d\sigma(t)/dt$ and it varies from zero to 3.8×10^{-4} MPa/s with the average of about 2×10^{-4} MPa/s. Tensile strength of asphalt concrete f_σ at $V_\sigma = 2 \times 10^{-4}$ MPa/s according to Eq. (4.20) as a function of T is shown on the same graph (Fig. 4.16). The critical cracking temperature at which the thermal stress curve and asphalt concrete strength curve intersect is $T_{cr} = -33$ °C.

The proposed method to determine the critical single-event cracking temperature as the temperature at which the thermal stress curve intersect the constant-rate strength curve leads to reasonable results. Low-temperature cracking of asphalt pavements is a widespread and costly problem in cold regions. Ability to predict the temperature induced stress in asphalt pavement and asphalt concrete strength starting from the properties of binder and mix should be helpful for designing the more crack resistant mixes.

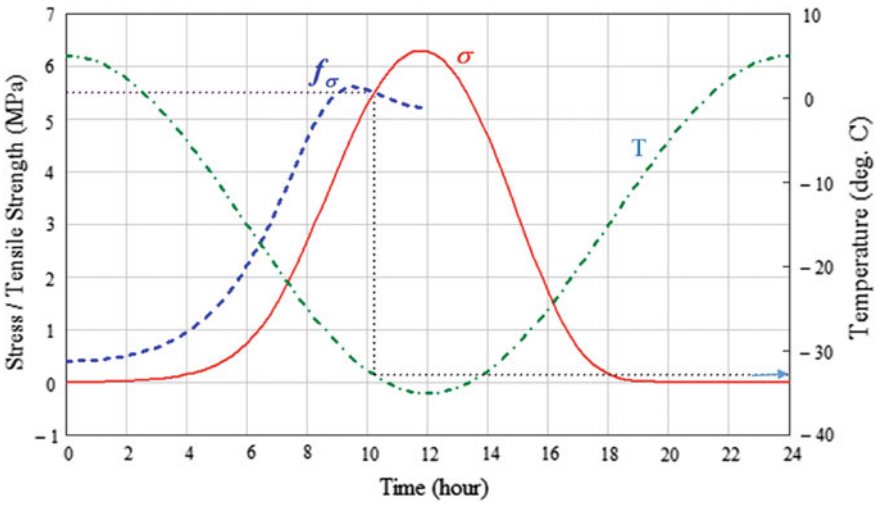

Fig. 4.16 Thermal stress and estimated fracture temperature for sinusoidal temperature variation during a day

4.7 Conclusion

In the last quarter of XX—first decade of XXI century, rheology as a science that deals with the deformation and flow of matter and a theory of the viscoelastic behavior of materials as a tool to describe mechanical properties of viscoelastic materials formed a scientific basis for understanding the properties of road construction materials and for their research and development.

One of the examples is the development and implementation of the Superpave asphalt mixture design and analysis system together with the progress in pavement design, construction and testing. Current performance graded system for specifying the properties of the asphalt binder and the Superpave mix design system have a number of drawbacks. However, the authors of this monograph can see the main advantage of Superpave in the fact that it turned the Civil Engineering community face to the fundamental sciences: rheology and viscoelasticity. Therefore, we consider the determination of relationships between various viscoelastic properties and different methods of their measurement very useful.

It is important in practice to have the relationship between "old" standard measures empirical properties of bitumen, such as penetration and softening point, and "new" characteristics of its mechanical properties: creep compliance, relaxation modulus and dynamic modulus. Those relationships were obtained and described above. We hope they will be useful for the forthcoming improvement of asphalt mix design standards and flexible pavement design methods in Russia, Belorussia, Ukraine and Kazakhstan.

First, the authors seek to outline the elements of linear viscoelasticity theory and describe the some methods for testing of viscoelastic materials in compact but accessible form (Chap. 1). Then, based on Van der Poel's experimental data, we determined relationship between the stiffness modulus of bitumen and its simplest properties (softening point and penetration), as well as the temperature and load duration (Chap. 2). The authors realize that measuring technique, which Van der Poel used sixty years ago, is not as good as the modern one, and his nomograph for some bitumens can exhibit an essential inaccuracy. Nevertheless, rather time-consuming job of obtaining the equation for stiffness modulus [formulas (3.1)–(3.6)] seems justified to us.

Probably, the main result of the book is determination of useful relationships between viscoelastic properties of binder (Chap. 3). The enhanced recursive relation was derived for calculation of longitudinal or shearing relaxation modulus, based on creep compliance [formula (3.17)]. Approximate formula (3.29) was proposed for determination of asphalt relaxation modulus as a function of its temperature and load duration based on the simplest standard properties of asphalt (penetration and the softening point). New alternative simple formula (3.34) was derived for determination of bitumen relaxation modulus. The formulas were obtained for evaluation of dynamic modulus and phase angle for asphalt as a function of frequency of loading and temperature. Agreement of predicted dynamic modulus, phase angle, and relaxation spectrum of asphalt with test data was illustrated. Equations (3.17), (3.34), (3.35), (3.52) and (3.53) are new.

As our academic interests have been focused mainly on pavement design and analysis, we tended to predict the viscoelastic properties of asphalt concrete (Chap. 4). The authors had to leave aside such important matters as demonstration of nonlinear nature, dependence of asphalt concrete relaxation modulus at low temperature on time of its storage at this temperature (physical aging), etc., so that to measure entire path from the simple standard properties of bitumen to asphalt concrete relaxation modulus. It was possible to widen a set of practical applications that were considered in the last chapter, but the authors decided to restrict themselves to the issues mentioned above.

The first approach to characterizing the stiffness of an asphalt cement was to chew on it. An engineer would take a small sample of asphalt, roll it into a ball, and place it between his teeth. The pressure required to deform the ball was considered an indication of the stiffness of the asphalt. If it crumbled, they considered it very stiff. If bitumen stuck to the teeth, they considered it very soft. Elastic bitumen was considered as a good one, which could be chewed like a chewing gum. They acted like that before penetrometer was invented in 1888, and even after that many years later the experienced road builders were proud that they could evaluate the bitumen not worse than the with penetrometer. We hope that after reading this monograph, the reader can learn about mechanical properties of bitumen more than just having chewed it.

References

Airy G, Brown SF (1997) Rheological performance of aged polymer modified bitumens. AAPT 67:66–100

Anderson DA, Christensen DW, Bahia HU, Dongre R et al (1994) Binder characterization and evaluation, vol 3: Physical Characterization, SHRP report A-369. National Research Council, Washington DC

Asphalt Institute Inc. (2003) Performance graded asphalt binder specification and testing. Superpave Series No. 1 (SP-1). 3rd ed. Asphalt Institute Inc.

Bell C (1989) Summary report on aging of asphalt-aggregate systems, SHRP Report A-305. National Research Council, Washington DC

Benson P (1976) Low temperature transverse cracking of asphalt concrete pavements in Central and West Texas. Texas Transportation Institute, Texas A&M University

Bouldin MG, Dongré R, Rowe GM, Sharrock MJ, Anderson DA (2000) Predicting thermal cracking of pavements from binder properties. AAPT 69:455–496

Composite Materials. Broutman LJ, Krock RH (ed) (1974) Mechanics of composite materials, vol 2. Sendeckyj GP (ed). Academic Press, New York and London

Brown S (1980) Introduction to analytical design of asphalt pavement, Nottingham

Brunton J (1983) Developments in the analytical design of asphalt pavements using computers. University of Nottingham

Christensen DW, Anderson DA (1992) Interpretation of dynamic mechanical test data for paving grade asphalt cements. J AAPT 61:67–116

Christensen DW, Bonaquist R (2015) Improved Hirsch model for estimating the modulus of hot mix asphalt. J Assoc Asph Pav Tech 84:527–557

Christensen DW, Bonaquist T, Pellinen RF (2003) Hirsch model for estimating the modulus of asphalt concrete. J Assoc Asph Pav Tech 72:97–121

Christison JT, Murray DW, Anderson KO (1972) Stress prediction and low temperature fracture susceptibility of asphaltic concrete pavements. J Assoc Asph Pav Tech 41:494–523

Corbett LW, Merz RE (1975) Asphalt binder hardening in the Michigan Test Road after 18 years of service. Transportation Research Record 544, Washington DC: 27–34

Culley R (1969) Relationships between hardening of asphalt cement and transverse cracking pavements in Saskatchewan. AAPT 38:629–645

Deme IJ, Young FD (1987) Ste. Anne Test Road revisited twenty years later. Proc Can Tech Asphalt Assoc 32:254–283

Finn F (1990) Asphalt properties and relationship to pavement performance. Literature Review, SHRP Task 1.4, ARE Inc

Harnsberger M (2011) Doing with WRI: an overview of FHWA research. Rocky Mountain Asphalt Conference, Denver, Colorado, February 23, 2011

Heukelom W (1966) Observations on the rheology and fracture of bitumens and asphalt mixes. J Assoc Asph Pav Tech 35:358–399

Hill R (1963) Elastic properties of reinforced solids: some theoretical principles. J Mech Phys Solid 11:357–372

Hirsch TJ (1962) Modulus of elasticity of concrete affected by elastic moduli of cement paste matrix and aggregate. J Am Conc Inst 59(3):427–452

Hubbard P, Gollomb H (1937) The hardening of asphalt with relation to development of cracks in asphalt pavements. Proc AAPT 9:165–194

Humphreys J, Martin C (1963) Determination of transient thermal stresses in a slab with temperature dependent viscoelastic properties. Trans Soc Rheol 7:155–170

Kandhal PS (1977) Low temperature ductility of asphalt in relation to pavement performance. American society for testing and materials. Special Technical Publication 628

Molenaar AA, Li N (2014) Prediction of compressive and tensile strength of asphalt concrete. Int J Pav Res Tech 7:324–331

Monismith CL, Secor GA, Secor KE (1965) Temperature induced stresses and deformations in asphalt concrete. J Assoc Asph Pav Tech 34:248–285
Mortazavi M, Moulthrop JS (1993) The SHRP materials reference library, SHRP-A-646, Washington DC
Pell PS, Cooper KE (1975) The effect of testing and mix variables on the fatigue performance of bituminous materials. J Assoc Asph Pav Tech 41:1–37
Sall AO (1989) Toward the problem for increase of long life for asphalt concrete pavements. Works of SoyuzdorNII, 128–133
Smith T (1976) Linear viscoelastic response to a deformation at constant rate: derivation of physical properties of a densely cross-linked elastomer. Trans Soc Rheol 1:103–117
Stock AF, Arand W (1993) Low temperature cracking in polymer modified binder. J Assoc Asph Pav Tech 62:23–53
Teltayev B, Kaganovich E (2011) Bitumen and asphalt concrete requirements improvement for the climatic conditions of the Republic of Kazakhstan. CD. Proceedings of the 24th World Road Congress, p 1–13
Teltayev B, Kaganovich E (2012) Evaluating the low temperature resistance of the asphalt pavement under the climatic conditions of Kazakhstan. In: 7th RILEM international conference on cracking in pavements, pp 211–221
Traxler RN (1961) Relation between asphalt composition and hardening by volatilization and oxidation. Proc AAPT 30:359–372
Welborn JY (1979) Relationship of asphalt cement properties to pavement durability. TRB, NCHRP Report, p 59
AASHTO M 320-05 (2005) Standard specification for performance-graded asphalt binder
AASHTO R 29-15 (2015) Grading or verifying the Performance Grade (PG) of an asphalt binder
ASTM D 6816—02 Standard practices for determining low-temperature Performance Grade (PG) of asphalt binders
Zofka A, Marasteanu M, Li X, Clyne T, McGraw J (2005) Simple method to obtain asphalt binders low temperature properties from asphalt mixtures properties. J Assoc Asph Pav Tech 74:255–282